Helmholtz-Zentrum Potsdam Deutsches GeoForschungsZentrum
Geomikrobiologie

Influence of CO_2 degassing on microbial community distribution and activity in the Hartoušov degassing system, western Eger Rift (Czech Republic)

Qi Liu

Kumulative Dissertation

zur Erlangung des akademischen Grades
"doctor rerum naturalium"
(Dr. rer. nat.)
in der Wissenschaftsdisziplin "Microbiologie"

Eingereicht an der
Mathematisch-Naturwissenschaftlichen Fakultät
der Universität Potsdam

Potsdam
Eingereicht am: 20.03.2020
Tag der Disputation: 18.08.2020

Prüfungskomission:

Betreuer: Prof. Dr. Dirk Wagner

Gutachter: Prof. Dr. Alexander Probst

Prof. Dr. Hans-Peter Grossart

Published online on the
Publication Server of the University of Potsdam:
https://doi.org/10.25932/publishup-47534
https://nbn-resolving.org/urn:nbn:de:kobv:517-opus4-475341

Statement of Original Authorship

Herewith, I assure that I have developed and written the enclosed PhD-thesis completely by myself, and have not used sources or means without declaration in the text. Any thoughts from others or literal quotations are clearly marked. The PhD-thesis was not used in the same or in a similar version to achieve an academic grading or is being published elsewhere.

Potsdam, 15,03,2020

Qi Liu

Preface

This study within the framework of the priority program 1006 “International Continental Drilling Program” (ICDP) by a grant to MA (AL 1898/1) and supported by the Deutsche Forschungsgemeinschaft (DFG). This thesis investigated the microbial composition, distribution and processes in CO_2 dominated soil and subsurface sediments in the active fault zone in the Cheb Basin, Western Eger Rift region (Czech Republic).

The first sampling campaign was conducted in September 2015. The expedition was organized by the section Geomicrobiology, Helmholtz Centre Potsdam, German Research Centre of Geosciences (GFZ) and with the operation assistance from Robert Bussert, two 3-m cores were retrieved. The deep drilling campaign was conducted from March to April 2016. The deep drilling campaign was organized by the section Geomicrobiology, Helmholtz Centre Potsdam, German Research Centre of Geosciences (GFZ). A 108.5 m core was retrieved from this deep drilling (HJB-1). The laboratory work described in this thesis was performed in section Geomicrobiology, Helmholtz Centre Potsdam, German Research Centre of Geosciences (GFZ).

This thesis is presented in English and submitted as a cumulative dissertation to the Faculty of Mathematics and Natural Science at the University of Potsdam. This thesis contains a general introduction to the particular research field including the deep biosphere, the description of the study sites and study objectives. The main part is composed of three manuscripts with the first authorship. A final synthesis and future outlook are summarized based on the manuscripts.

Acknowledgments

I would like to gratefully express my gratitude to Prof. Dr. Dirk Wagner for allowing me to study as a Ph.D. student in section Geomicrobiology in the GFZ Potsdam. My sincere thanks to Prof. Dr. Elke Dittmann from the University of Potsdam for continuous supervision. Special thanks to Dr. Mashal Alawi for his professional knowledge of environmental microbiology and comprehensive guidance regarding my study and my life in Germany.

I would like to thank my colleagues and friends from section Geomicrobiology, section Organic Geochemistry and the other section in GFZ Potsdam for the selfless help and nice working atmosphere in GFZ Potsdam.

I would like to thank all colleagues, partners and master students who participated in the project and the drilling campaign for the valuable joint work.

I gratefully acknowledge the financial support from the China Scholarship Council.

Finally, I would like to thank my parents and my wife for their love, understanding, and support. And I would like to thank all my friends in both Europe and China for the happiness we shared.

List of Publications

The following articles and conference contributions were published in the scope of this thesis:

Articles

Liu, Q., Kämpf, H., Bussert, R., Krauze, P., Horn, F., Nickschick, T., Plessen, B., Wagner, D., Alawi, M., (2018). Influence of CO_2 Degassing on the Microbial Community in a Dry Mofette Field in Hartoušov, Czech Republic (Western Eger Rift). Frontiers in Microbiology 9, 2787.

Liu, Q., Adler K. (co-first author), Kämpf, H., Bussert, R., Plessen, B., Schulz, H.-M., Krauze, P., Horn, F., Wagner, D., Mangelsdorf, K., Alawi, M.. Microbial signatures from a deep saline CO_2-saturated aquifer of the Hartoušov mofette system (Eger Rift, NW Czech Republic). **Submitted in** Frontiers in Microbiology.

Liu, Q., Hainzl, S., Kämpf, H., Bussert, R., Horn, F., Wagner, D., Alawi, M.. Direct link between earthquake and subsurface microbial methane production. **Final draft**

Conference Contributions

Liu, Q., Kämpf, H., Nickschick, T., Kyslik, P., Baldrian, P., Bussert, R., Plessen, B., Noah, M., Boteck, S., Wagner, D., Alawi, M., (2017). Microbial processes in the deep biosphere of the active CO_2-dominated fault zone in NW Bohemia. International Ocean Discovery Program (IODP) / International Continental Scientific Drilling Program (ICDP) Colloquium 2017, 14-16 March, Braunschweig, Germany. (Abstract, Oral Presentation)

Liu, Q., Kämpf, H., Bussert, R., Krauze, P., Horn, F., Plessen, B., Wagner, D., Alawi, M., (2018). Microbial diversity, abundance and activity in a dry CO_2 degassing mofette in Hartoušov, NW Bohemia. Annual Conference 2018 of the Association for General and Applied Microbiology (VAAM), 15-18 April, Wolfsburg, Germany. (Abstract, Poster)

Summary

The Cheb Basin (CZ) is a shallow Neogene intracontinental basin located in the western Eger Rift. The Cheb Basin is characterized by active seismicity and diffuse degassing of mantle-derived CO_2 in mofette fields. Within the Cheb Basin, the Hartoušov mofette field shows a daily CO_2 flux of 23–97 tons. More than 99% of CO_2 released over an area of 0.35 km^2. Seismic active periods have been observed in 2000 and 2014 in the Hartoušov mofette field. Due to the active geodynamic processes, the Cheb Basin is considered to be an ideal region for the continental deep biosphere research focussing on the interaction of biological processes with geological processes.

To study the influence of CO_2 degassing on microbial community in the surface and subsurface environments, two 3-m shallow drillings and a 108.5-m deep scientific drilling were conducted in 2015 and 2016 respectively. Additionally, the fluid retrieved from the deep drilling borehole was also recovered. The different ecosystems were compared regarding their geochemical properties, microbial abundances, and microbial community structures. The geochemistry of the mofette is characterized by low pH, high TOC, and sulfate contents while the subsurface environment shows a neutral pH, and various TOC and sulfate contents in different lithological settings. Striking differences in the microbial community highlight the substantial impact of elevated CO_2 concentrations and high saline groundwater on microbial processes. In general, the microorganisms had low abundance in the deep subsurface sediment compared with the shallow mofette. However, within the mofette and the deep subsurface sediment, the abundance of microbes does not show a typical decrease with depth, indicating that the uprising CO_2-rich groundwater has a strong influence on the microbial communities via providing sufficient substrate for anaerobic chemolithoautotrophic microorganisms. Illumina MiSeq sequencing of the 16S rRNA genes and multivariate statistics reveals that the pH strongly influences the microbial community composition in the mofette, while the subsurface microbial community is significantly influenced by the groundwater which motivated by the degassing CO_2. Acidophilic microorganisms show a much higher relative abundance in the mofette. Meanwhile, the OTUs assigned to family *Comamonadaceae* are the dominant taxa which characterize the subsurface

communities. Additionally, taxa involved in sulfur cycling characterizing the microbial communities in both mofette and CO_2 dominated subsurface environments.

Another investigated important geo–bio interaction is the influence of the seismic activity. During seismic events, released H_2 may serve as the electron donor for microbial hydrogenotrophic processes, such as methanogenesis. To determine whether the seismic events can potentially trigger methanogenesis by the elevated geogenic H_2 concentration, we performed laboratory simulation experiments with sediments retrieved from the drillings. The simulation results indicate that after the addition of hydrogen, substantial amounts of methane were produced in incubated mofette sediments and deep subsurface sediments. The methanogenic hydrogenotrophic genera *Methanobacterium* was highly enriched during the incubation. The modeling of the *in-situ* observation of the earthquake swarm period in 2000 at the Novy Kostel focal area/Czech Republic and our laboratory simulation experiments reveals a close relation between seismic activities and microbial methane production via earthquake-induced H_2 release. We thus conclude that H_2 – which is released during seismic activity – can potentially trigger methanogenic activity in the deep subsurface. Based on this conclusion, we further hypothesize that the hydrogenotrophic early life on Earth was boosted by the Late Heavy Bombardment induced seismic activity in approximately 4.2 to 3.8 Ga.

Zusammenfassung

Das Eger-Becken (CZ) ist ein flaches, intrakontinentales neogenes Becken im westlichen Eger-Graben. Das Eger-Becken zeichnet sich durch aktive Seismizität und die diffuse Entgasung von aus dem Mantel stammenden CO_2 in Mofettenfeldern aus. Das Mofettenfeld von Hartoušov weist einen täglichen CO_2-Fluss von 23-97 Tonnen auf. Mehr als 99% des CO_2 werden auf einer Fläche von 0,35 km^2 freigesetzt. Im Untersuchungsgebiet wurden in den Jahren 2000 und 2014 seismisch aktive Perioden beobachtet. Aufgrund der aktiven geodynamischen Prozesse gilt das Egerer Becken als ideale Region für die kontinentale Tiefenbiosphärenforschung, die sich auf die Wechselwirkung von biologischen Prozessen mit geologischen Prozessen konzentriert. Zur Untersuchung des Einflusses der CO_2-Entgasung auf die mikrobielle Gemeinschaft in der ober- und unterirdischen Umwelt wurden 2015 und 2016 zwei 3 m tiefe Flachbohrungen und eine 108,5 m tiefe wissenschaftliche Bohrung durchgeführt. Zusätzlich wurde auch aus dem Tiefbohrloch Flüssigkeit gewonnen. Die verschiedenen Ökosysteme wurden hinsichtlich ihrer geochemischen Eigenschaften, der mikrobiellen Abundanzen und der mikrobiellen Gemeinschaftsstrukturen verglichen. Die Geochemie der Mofetten zeichnet sich durch einen niedrigen pH-Wert und hohe TOC- und Sulfatgehalte aus, während das unterirdische Milieu einen neutralen pH-Wert und verschiedene TOC- und Sulfatgehalte in unterschiedlichen lithologischen Umgebungen aufweist. Auffällige Unterschiede in der mikrobiellen Gemeinschaft unterstreichen den erheblichen Einfluss erhöhter CO_2-Konzentrationen und stark salzhaltigen Grundwassers auf mikrobielle Prozesse. Generell waren die mikrobiellen Abundanzen in dem tiefen Untergrundsediment im Vergleich zur flachen Mofette gering. Innerhalb der Mofette und des tiefen unterirdischen Sediments zeigt die Häufigkeit der Mikroorganismen jedoch keine typische Abnahme mit der Tiefe, was darauf hinweist, dass das aufsteigende CO_2-reiche Grundwasser einen starken Einfluss auf die mikrobiellen Gemeinschaften hat, indem es genügend Substrat für anaerobe chemolithoautotrophe Mikroorganismen bietet. Die Illumina-MiSeq-Sequenzierung der 16S rRNA-Gene und die multivariate Statistik zeigen, dass der pH-Wert die Zusammensetzung der mikrobiellen Gemeinschaft in der Mofette signifikant bestimmt,

während die unterirdische mikrobielle Gemeinschaft signifikant vom Grundwasser beeinflusst wird, das durch das ausgasende CO_2 geprägt ist. Azidophile Mikroorganismen zeigen eine viel höhere relative Abundanz in der Mofette, wohingegen die der Familie Comamonadaceae zugeordneten OTUs die dominierenden Taxa der unterirdischen Gemeinschaften darstellen. Zusätzlich charakterisieren Taxa, die am Schwefelzyklus beteiligt sind, die mikrobiellen Gemeinschaften sowohl in der Mofette als auch in der CO_2-dominierten unterirdischen Umwelt.

Eine weitere wichtige Untersuchung der Geo-Bio-Interaktion ist der Einfluss der seismischen Aktivität. Während seismischer Ereignisse kann freigesetztes H_2 als Elektronendonator für mikrobielle hydrogenotrophe Prozesse, wie z.B. die Methanogenese, dienen. Um zu bestimmen, ob die seismischen Ereignisse durch die erhöhten geogenen H_2-Konzentrationen möglicherweise methanogene Prozesse auslösen können, führten wir Laborsimulationsexperimente mit Sedimenten durch, die aus den Bohrungen gewonnen wurden. Die Simulationsexperimente weisen darauf hin, dass nach der Zugabe von Wasserstoff beträchtliche Mengen an Methan in inkubierten Mofettensedimenten und tiefen unterirdischen Sedimenten produziert wurden. Die methanogene hydrogenotrophe Gattung Methanobacterium wurde während der Inkubation stark angereichert. Die Modellierung der in-situ-Beobachtung der Erdbeben-Schwarmzeit im Jahr 2000 im Schwerpunktgebiet Novy Kostel/Tschechische Republik und unsere Laborsimulationsexperimente zeigen einen engen Zusammenhang zwischen seismischen Aktivitäten und der biotischen Methanproduktion durch erdbebeninduzierte H2-Freisetzung. Wir kommen daher zu dem Schluss, dass H_2 - dass bei seismischer Aktivität freigesetzt wird - möglicherweise methanogene Aktivität im tiefen Untergrund auslösen kann. Basierend auf dieser Schlussfolgerung gehen wir weiter davon aus, dass das frühe hydrogenotrophe Leben, durch die durch Late Heavy Bombardment induzierte seismische Aktivität in etwa 4,2 bis 3,8 Ga verstärkt wurde.

Abbreviations

16S rRNA	ribosomal ribonucleic acid of the small subunit
ATP	Adenosine triphosphate
BLAST	Basic Local Alignment Search Tool
CMC	carboxymethyl cellulose
CZ	Czech Republic
$\delta^{13}C$	the ration of ^{13}C: ^{12}C
$\delta^{14}C$	the ration of ^{14}C: ^{12}C
DCM	dichlormethane
DDS	diffuse degassing structure
DFG	German Research Foundation (Deutsche Forschungsgemeinschaft)
DNA	desoxyribouncleic acid
DNA-SIP	DNA stable-isotope probing
dNTP	deoxynucleotide triphosphates
DOC	dissolved organic carbon
EI	electron impact
ENE	east-north-east
et al.	et alii (and others)
GDGTs	glycerol dialkyl glycerol tetraethers
GEOFOND	Czech Geological Survey
GFZ	German Research Center for Geoscience
HMF	Hartoušov mofette field
IC	ion chromatography
IODP	International Ocean Drilling Program
IPL	intact polar lipid
IRMS	isotope ratio mass spectrometer
mbs	meter below surface
MLF	Marianske Lazne Fault
MPLC	Medium Pressure Liquid Chromatography
MS	mass spectrometer

NCBI	National Center for Biotechnology Information
NGS	next generation high-throughput sequencing
NMDS	non-metric multidimensional scaling analysis
ODP	Ocean Drilling Program
OTU	operational taxonomic unit
PCR	polymerase chain reaction
PLFAs	polar lipid fatty acids
PPZ	Pocatky-Plesna Fault Zone
qPCR	real-time quantatitive polymerase chain reaction
RuBisCO	Ribulose-1,5-bisphosphate carboxylase/oxygenase
SOM	soil organic matter
SRB	sulfate reducing bacteria
TIC	total inorganic carbon
TN	total nitrogen
TOC	total organic carbon
UHPLC	Ultra high performance liquid chromatograph
VPDB	Vienna PeeDee Belemnite

Contents

List of Figure

List of Tables

1 Introduction

1.1 The deep biosphere

The concept of the biosphere was extended over the past three decades since the discovery of the deep biosphere (Gold, 1992). Global subseafloor sedimentary microbial abundance was estimated to be 4.1 x 10^{15} g C (Kallmeyer et al., 2012) whereas global continental subsurface biomass was estimated to be 10^{16} - 10^{17} g C (McMahon and Parnell, 2014). The microorganisms in the deep biosphere are involved in many fundamental processes, e.g. dissolution, alteration and precipitation of minerals, and changes in redox conditions (D'Hondt et al., 2002; Alt and Shanks, 2011; Vaughan and Lloyd, 2012). Although the deep biosphere was considered to be one of the hardest ecosystems to study due to the inherent difficulties (e.g. cost of the sampling campaign, contamination issue and sample handling), more and more studies focused on the deep biosphere so far. Until now, most deep biosphere studies focus on marine sediments are in the frame of the International Ocean Drilling Program (IODP) (Blazejak and Schippers, 2011; Mangelsdorf et al., 2011; Lomstein et al., 2012; Breuker et al., 2013; Yanagawa et al., 2013; Inagaki et al., 2015). However, the studies focus on the terrestrial deep biosphere are much less compared with that on the marine deep biosphere. The studies of terrestrial deep biosphere related to the investigations of oil reservoirs (Youssef et al., 2009), aquifers (Alawi et al., 2011; Lerm et al., 2013; Luef et al., 2015; Wu et al., 2016; Probst et al., 2017; Probst et al., 2018), deep mines (Takai et al., 2001b; Trimarco et al., 2006; Deflaun et al., 2007; Strapoc et al., 2008; Borgonie et al., 2011), and crust rock and sediment through deep drilling (> 20 m) were reported recently (Sass and Cypionka, 2004; Zhang et al., 2005; Breuker et al., 2011; Vuillemin and Ariztegui, 2013; Nyyssönen et al., 2014; Thomas et al., 2014). Microbial communities in the deep biosphere were site-specific due to the different environmental influences (Ariztegui et al., 2015). Compared with the large unexplored terrestrial subsurface environment, the studies so far only revealed a relatively small fraction of terrestrial deep biosphere and the knowledge is still lacking.

Unlike the surface environment, not only the light for the photosynthesis is not available in the deep biosphere but also the flux of energy and nutrients are extremely low (Morono et al., 2011). Microbial growth in the deep biosphere is also restricted by many extreme factors in comparison with the surface biosphere e.g. high temperature and pressure, anaerobic or hypoxic conditions, and less availability of water and organic carbon (Kallmeyer and Wagner, 2014). Furthermore, the substrates essential to deep subsurface microorganisms are getting depleted with the increase of depth (Froelich et al., 1979; Middelburg, 1989). Additionally, the nutrient flux is usually extremely low due to the limitations of sediment chemistry and hydrology (Stevens and McKinley, 1995). Hence, deep subsurface sediments were considered as the most oligotrophic environments on Earth (Phelps et al., 1994). The microbial processes in the deep subsurface are much slower and the turnover time of organic matters is much longer than the surface biosphere (Lomstein et al., 2012) as well. Although the microorganisms in the deep biosphere revealed relatively low abundance and low activity compare with that in the respective surface environment (Breuker et al., 2011; Yanagawa et al., 2014; Walsh et al., 2016), microbiological studies on hydrothermal systems, mineral water, and aquifers indicated that these deep subsurface habitats harbor diverse and active microorganisms (Anantharaman et al., 2016; Hernsdorf et al., 2017) as "hotspots" for the microorganisms in the deep biosphere. The chemolithoautotrophic microorganisms – which obtain energy from the oxidation of inorganic compounds and obtain carbon via CO_2 fixation – such as sulfate reducing bacteria (SRB; e.g. *Desulfobacca* and *Desulfotomaculum*), nitrifying bacteria (e.g. *Nitrospira* and *Nitrosomonas*) and iron-oxidizing bacteria (e.g. *Gallionella* and *Ferrovum*) are favored in these "hotspots".

With the decrease of the other substrates availability, H_2 becomes the major controlling and limiting factor for microbial activity in the terrestrial microbial deep biosphere (Stevens and McKinley, 1995; Nealson, 2005; Spear et al., 2005; Hinrichs et al., 2006). H_2 can be generated through fermentative processes within the subsurface ecosystem as well as the radiolysis of water, the water-rock interactions, and tectonic activity (Vovk, 1987; Stevens and McKinley, 1995; Savary and Pagel, 1997; Chapelle et al., 2002; Lin et al., 2005). Additionally, H_2 released in connection with tectonic stress was

observed (Sugisaki and Sugiura, 1985) and H_2 can be generated by a mechano-chemical reaction between groundwater and fresh surfaces of crushed rock material during earthquakes (Kita et al., 1982). Hydrogenotrophic microorganisms – e.g. hydrogenotrophic methanogens (e.g. *Methanobacterium*) (Zeikus, 1977) and hydrogenotrophic sulfate reducing bacteria (e.g. *Desulfovibrio*) (Jørgensen BoBarker, 1978) – which depend on biogenic and abiogenic processes provided H_2, become another important component of the deep subsurface microorganisms.

1.2 The Cheb Basin: the western Eger Rift region

The Cheb Basin (NW Bohemia, Czech Republic) is a shallow Neogene intracontinental basin filled with fluvial and lacustrine sediments (≤ 350 m thick; **Figure 1A**). The basin formed at the intersection of the Eger Rift (Kopecký, 1979) and the Regensburg–Leipzig–Rostock fault zone (Bankwitz et al., 2003b; Geissler et al., 2004). The Regensburg–Leipzig–Rostock fault zone is represented as the Marianske Lazne Fault (MLF, Variscian) and the Pocatky-Plesna Fault Zone (PPZ, Late Pleistocene) in the Cheb Basin (Bankwitz et al., 2003a; Bankwitz et al., 2003b). Four Quaternary volcanoes existed in this area (Mrlina et al., 2009; Rohrmüller et al., 2018). This intersection region is characterized by active seismicity in form of "earthquake swarms", which are typically clustered small earthquakes induced by fluid pressure at upper crustal depths (Weise et al., 2001; Bräuer et al., 2003; Fischer, 2003).

Due to magmatic activity beneath the crust, large-scale degassing of mantle-derived CO_2 (> 99%) – combined with traces of gases such as He, N_2, Ar, and CH_4 – occurs in Cheb Basin (Weinlich et al., 1999; Kämpf et al., 2013; Hrubcová et al., 2017; Bräuer et al., 2018). The emanating gas originates from magma chambers at the boundary between the Earth lithosphere and crust. The gas migrates through the upper lithospheric mantle and the crust to the surface and mixes with water in both deep thermal and shallow groundwater aquifers (Weise et al., 2001; Bräuer et al., 2008; Bussert et al., 2017). After the earthquake swarm 2000, Bräuer et al. (2005) reported the concentration of biogenically produced methane had increased in the emanating gas

at a wellhead in Wettinquelle (**Figure 1A**). The shift of the $\delta^{13}CH_4$ values indicated a microbial origin of the emanating methane, which had presumably been produced by hydrogenotrophic methanogens. Thus, Bräuer et al. (2005) established the hypothesis that seismic events may trigger methanogenesis. This finding hints us that the geological activities (e.g. emanating gas, ascending fluid and seismic activities) significantly influence the deep biosphere and motivates us to study the influenced surface and subsurface microbial processes in this CO_2-dominated active fault zone.

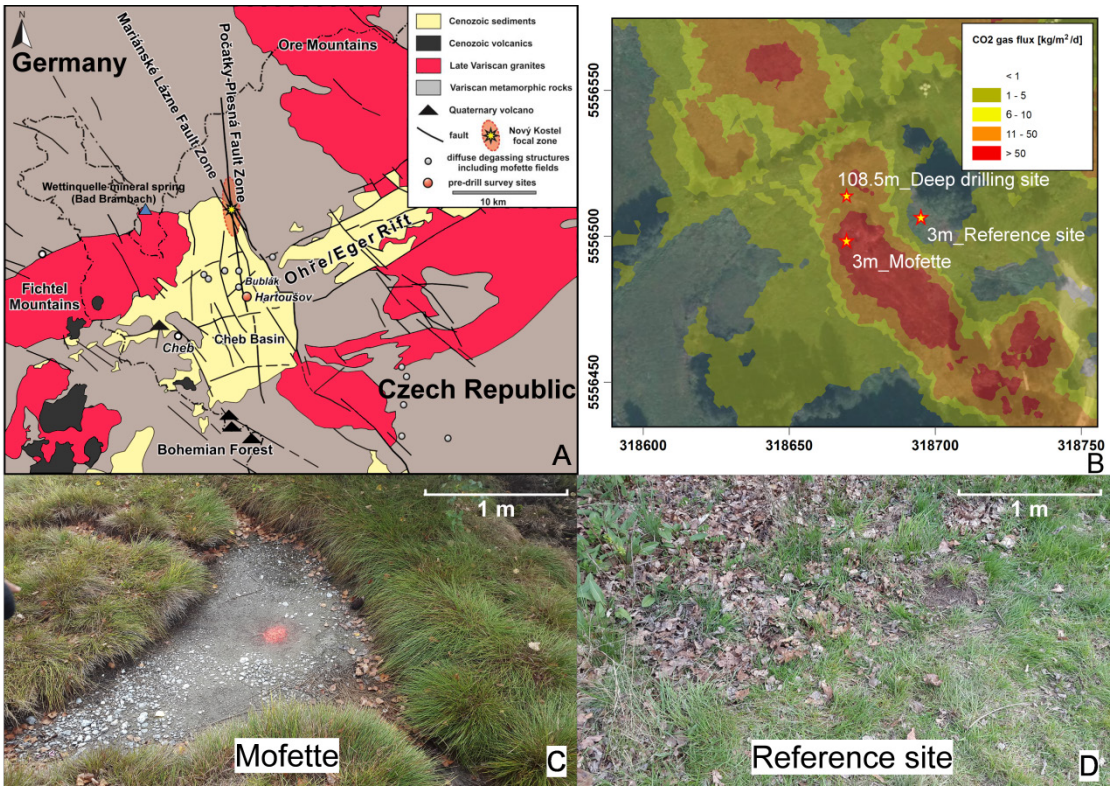

Figure 1 The description figures of the Hartoušov mofette field modified from Qi et al., 2018). Geological map of the Cheb Basin, Hartoušov mofette field and Wettinquelle mineral spring (modified from Flechsig et al., 2008) (A), CO_2 gas flux in the Hartoušov mofette field (modified from Nickschick et al., 2015, coordinates in UTM 33N) (B), the surface at the mofette (C) and the reference site (D). The 3 m drillings and 108.5 m deep drilling locations are marked by stars in the CO_2 gas flux map (B).

1.3 Mofettes in the Eger Rift

The mantle-derived emanating CO_2 created the diffuse degassing structure (DDS) – so-called mofette – on the surface, which apart from the surrounding normal soil. In general, mofette (**Figure 1C**) can be spotted and speculated by the much smaller, more chlorotic or totally extinct vegetation (Pfanz et al., 2004; Vodnik et al., 2007), the corpses of dead animals, and atmospheric abnormalities (Kies et al., 2015). The mofette occurs worldwide due to its co-existence with active seismic areas and volcanic areas (Rennert and Pfanz, 2016).

The elevated CO_2 concentration is the characteristic of the mofette: (i) the ascending CO_2 accumulates in the soil and excludes the oxygen, which creates a hypoxic even anaerobic environment in the mofette, and (ii) the CO_2 causes soil acidification (Beaubien et al., 2008; Blume and Felix-Henningsen, 2009; Rennert and Pfanz, 2016). The hypoxic and acidic environment in the mofette causes striking differences in the aspects of geology and biology. The acceleration of silicate weathering (Stephens and Hering, 2002; Beaubien et al., 2008; Blume and Felix-Henningsen, 2009; Videmšek et al., 2009; Mehlhorn et al., 2014), losses of base cations (Beaubien et al., 2008; Videmšek et al., 2009), and increase in metal mobilization (Mehlhorn et al., 2014; Mehlhorn et al., 2016) were reported within the mofette. The investigation on vegetations indicated a decelerated growth, an increased plant C/N ratio, and physiological adaptations to the acidic, hypoxic or even anoxic environments (Pfanz et al., 2004; Vodnik et al., 2007; Rennert and Pfanz, 2016). A common feature of the biota in the mofette is that a substantial amount of mantle-derived geological CO_2 is incorporated. It was first reported by Oppermann et al. (2010) in a CO_2 vent in the Latera Caldera (Central Italy) by $\delta^{13}C$ analyses of plant and microbial lipids. Around 8-27% of the bulk soil organic matter (SOM) derived from microorganisms was estimated by Nowak et al. (2015) through combined $\delta^{14}C$ and $\delta^{13}C$ isotope mass balances. Beulig et al. (2016) showed that up to 67% of mofette soil carbon content originated from the assimilation of geogenic CO_2 via plant primary production through radiocarbon analyses. This phenomenon was explained by the inhibited macro- and microbiological degradation of organic substances (Beulig et al., 2016).

Furthermore, a few studies revealed highly specialized microbial communities harboring in the mofette, which were considered to be significantly influenced by the elevated CO_2 concentration. A shift to anaerobic/microaerophilic and acidophilic community compositions has been reported in mofettes located near the Laacher See (Germany) (Krüger et al., 2009; Krüger et al., 2011), the Cheb Basin (Czech Republic) (Beulig et al., 2015), and in Stavešinci (Slovenia) (Videmšek et al., 2009). A high abundance of SRBs and high activity of sulfate reducing were demonstrated in mofettes (Beaubien et al., 2008; Frerichs et al., 2013) as well as the high activity of methanogenic archaea (Frerichs et al., 2013). The high-throughput sequencing was applied in a few mofette studies so far. Sáenz de Miera et al. (2014) reported a decrease of mofette microbial community richness, evenness, and diversity with an increase of CO_2 flux and an increase of the OTUs related to the *Chloroflexi* phylum in central-southern Spain. Beulig et al. (2015) studied a mofette located in the Cheb Basin and indicated the community was dominated by methanogens (e.g. *Methanosarcinales* and *Methanomicrobiales*) and subdivision 1 *Acidobacteria*, which likely adapted to the hypoxic and acidic environment. The metatranscriptomic and metagenomic approaches were also recently introduced into the study of the microbial composition and activity under the influence of CO_2 by Beulig et al. (2016). The metatranscriptomic data highlighted the enhancement of sulfate reduction, methanogenesis, and the CO_2 assimilation together with the disturbance of aerobic/anaerobic respiration. Futhermore, Krauze et al. (2017) revealed that the microbial communities in springs and wet mofettes are shaped by chemolithotrophic, anaerobic, and microaerophilic microorganisms. The authors further hypothesized a largely interconnected deep-trenching CO_2 conduits in the Cheb Basin.

However, microbiological studies of the mofette only focused on the springs, wells or near-surface soil layers (< 70 cm) so far. The sediments beneath the mofette and the CO_2-influenced deep biosphere have not yet been analyzed.

1.4 Study site: The Hartoušov mofette field (HMF)

The study site is located within the Hartoušov mofette field (HMF or DDS Hartoušov). The HMF covers an area of approximately 350,000 m^2 of grassland with two small ponds (2–6 m^2) and close to the river Plesná (Kämpf et al., 2013). Nickschick et al. (2015) estimated 23–97 tons of CO_2 released daily in the HMF and mapped the CO_2 flux in very high resolution (5 m between each measurement; **Figure 1B**). This relatively accurate CO_2 flux map hinted the potential CO_2 conduits and therefore contributed to the selection of the drilling site. The gas flux in the HMF has the highest ratio of mantle-derived gasses (Bräuer et al., 2008; Kämpf et al., 2013), which indicated much easier and more direct migration paths in the HMF. Thus, the drilling in the HMF would have a high possibility of reaching active CO_2 conduits. A 93-m-deep drilling was conducted by the GEOFOND Prague (well SA-30 /ID 103141) in 1957 (Flechsig et al., 2008), which is 200 m away from our planned drilling site. Hence, the stratigraphy and petrography of the sediments near the planned drilling site were provided and can be used to estimate and coordinate the drilling processes. The lithology of HMF is composed of distinct units. From the lowermost to the surface are Palaeozoic basement consists of weathered mica schist, Miocene terrestrial sediment deposited in a swamp environment, Miocene lacustrine sediment deposited in a relatively deep lake, and the last unit is the uppermost sediments deposited as floodplain due to the nearby Plesná river (Bussert et al., 2017).

A few studies investigated the local microbial compositions and processes within the Cheb Basin. As described before, the microbial CO_2 assimilation, microbial composition, and distribution were well studied from a nearby mofette located in the Cheb Basin (Beulig et al., 2015; Nowak et al., 2015; Beulig et al., 2016). These results indicated a significant influence from the elevated CO_2 concentration. Interestingly, Krauze et al. (2017) investigated wet mofettes in the Cheb Basin and found the microbial community highly adapted to the anoxic conditions in the mineral and thermal waters. The authors highlighted the connection between the wet mofettes and the deep biosphere according to the unique taxa which are usually found in the deep biosphere (e.g. *Hadesarchaea* and taxa related to *Bathyarchaeota*). The occurrence of

such taxa in the wet mofette was explained by the uprising mantle-derived CO_2. These studies provided us insights into the microorganisms in a CO_2 dominated environment and suggested a possible microbial background in the CO_2 dominated deep biosphere.

1.5 Methodology

The drilling core can be easily contaminated because of the exposure to the surface environment and the usage of drill mud during the drilling campaign. The contamination control approaches have been taken into consideration since the very beginning of the subsurface microbiological research (Phelps et al., 1988). The drill mud is used to provide hydrostatic pressure to prevent fluids from entering the borehole as well as lubricate, cool, and clean the drill bit. In conventional drilling, the risk of contamination from the microorganisms in the drill mud would be very high. The common approach to analyze the contamination in microbiological related drilling programs was adding dissolved tracers – which mimic the microorganisms and can be identified afterward – into the drill mud. In this case, fluorescein was used as the contamination tracer. Fluorescein is manufactured fluorescent dye. Its water-soluble disodium salt is widely used in hydrology and hydrogeology investigation (Goldscheider et al., 2008). Fluorescein was added into the KCl /$CaCO_3$ /carboxymethyl cellulose (CMC)-based drill mud during the drilling in Ketzin, Germany (Wandrey et al., 2010) and successfully revealed that the drill mud penetrated 20 mm into the core. Pellizzari et al. (2013) indicated that fluorescein was the simplest, cheapest, and most accurate tracing method among fluorescein, microspheres, and 40,6-diamidino-2-phenylindole stained bacteria. Although Wandrey et al. (2010) revealed that fluorescein concentration in the drill mud tank was stable within 3 days, fluorescein was added and mixed with drill mud freshly before the drill started as well as the addition of new drill mud during the drilling in HMF. Meanwhile, the drill mud tank was covered to avoid the photodecomposition of fluorescein. The laboratory fluorescence measurement detected several cores in the drilling HJB-1 that were highly contaminated and therefore would not be used for downstream analyses (Bussert et al., 2017).

To understand the long-term influence of elevated CO_2 concentration on the microbial communities in the Eger Rift fault zone, a combination of molecular microbiological methods and traditional cultivation-based approaches were introduced in this thesis. The molecular ecological methods based on the polymerase chain reaction (PCR), including real-time quantitative polymerase chain reaction (qPCR) and next-generation high-throughput sequencing (NGS). The qPCR is sensitive enough to detect the low amount of gene copies and can quantify microorganisms which contain a specific gene. The qPCR was widely introduced in the studies related to the deep biosphere studies (Nunoura et al., 2009; Webster et al., 2009; Biddle et al., 2011; Jorgensen et al., 2012; Schippers et al., 2012; Breuker et al., 2013; He et al., 2016) and mofette studies (Beaubien et al., 2008; Krüger et al., 2009; Krüger et al., 2011; McFarland et al., 2013; Krauze et al., 2017). Here in this thesis the bacterial 16S rRNA gene, the *dsrB* gene and the *mcrA* gene were quantified to reveal the abundance of bacteria (Lane, 1991), SRBs (Ben-Dov et al., 2007) and methanogens (Steinberg and Regan, 2009). Next-generation high-throughput sequencing significantly increases efficiency compared with Sanger sequencing. By parallel sequencing enormous highly variable regions of 16S rRNA gene fragments synchronously, the NGS provides much deeper insights into the microbial composition and distribution of the communities (Sogin et al., 2006). Another great advantage of NGS is that the NGS provides the possibility to identify taxa independent from the traditional culturing-based methods and the taxa in low abundance but essential to the whole microbial communities (Kysela et al., 2005; Sogin et al., 2006).

1.6 Objectives

The main objective of this thesis is to improve our understanding of the bio-geo interactions between microbial processes and the geological processes, namely CO_2 ascending and seismic active environment in the Cheb Basin, western Eger Rift region. For this purpose, two 3-m drillings were conducted in a mofette and an undisturbed reference site for comparison. Followed by a 108.5-m-deep drilling intended to drill into the active CO_2 conduits. Geochemical, microbiological, and molecular ecological

methods were performed on the retrieved core material to determine the influence of elevated CO_2 concentration. To clarify the interconnection between seismic and methanogenic activity, cultivation-based activity tests were provided in this thesis. To achieve the main objective, the following specific questions will be answered:

- How does the elevated CO_2 concentration alter the abundance and diversity of the mofette microbial community in the Hartoušov mofette field?
- What is the characterization of the deep subsurface microbial community (based on abundance, diversity, and distribution) in the Hartoušov mofette field with CO_2-saturated degassing conduit system?
- Is methanogenesis in the deep subsurface of the study area triggered by the seismic activities in the Eger Rift region? What is the mechanism behind it?

1.7 Thesis Organization

The material and method description, results and corresponding discussion of this cumulative dissertation are based on three manuscripts which have been published or in the process to be published as original research articles.

Manuscript I (published in Frontiers in Microbiology, 2018)
Influence of CO_2 Degassing on the Microbial Community in a Dry Mofette Field in Hartoušov, Czech Republic (Western Eger Rift)
DOI: https://doi.org/10.3389/fmicb.2018.02787

Authors
Qi Liu[1], Horst Kämpf[2], Robert Bussert[3], Patryk Krauze[1], Fabian Horn[1], Tobias Nickschick[4], Birgit Plessen[5], Dirk Wagner[1, 6] and Mashal Alawi[7]

Summary
This study aims to characterize the influence of elevated CO_2 concentration on the geochemistry, microbial abundance, community composition, and determination of the

significant community-shaping environmental factors in a mofette. To study the influence of mantle-derived CO_2, two 3-m drillings were performed, one of which was located in the center of a mofette and the other located at the undisturbed border of the mofette field. To unravel the community structures, a high-resolution sampling (every 5 to 10 cm) was conducted. Molecular microbiological approaches, namely qPCR and Illumina 16S rRNA gene amplicon sequencing were performed to reveal microbial abundance and community composition/distribution. Downstream statistical analyses indicated that the elevated CO_2 concentration significantly influenced the microbial community.

Author Contributions

Q. Liu wrote the manuscript, performed sampling, pore water analyses, DNA extractions and purification, gene quantification, and bioinformatical based statistical analyses. H. Kämpf and T. Nickschick performed CO_2 soil gas flux measurements. R. Bussert led the drilling campaign and performed sedimentological analyses. F. Horn and P Krauze were involved in statistical analyses. B. Plessen performed TOC and isotopic analyses. D. Wagner contributed to the interpretation of the results and valuable discussion. M. Alawi designed and supervised the study and led the writing of the present manuscript.

Manuscript II (submitted to Frontiers in Microbiology)

Microbial signatures from a deep saline CO_2-saturated aquifer of the Hartoušov mofette system (Eger Rift, NW Czech Republic)

Authors

Qi Liu[1, 6] & Karsten Adler[2, 6]*, Horst Kämpf, Robert Bussert[3], Birgit Plessen[5], Hans-Martin Schulz[2], Patryk Krauze[1], Fabian Horn[1], Dirk Wagner[1, 6], Kai Mangelsdorf[2], Mashal Alawi[7]

Summary

The objectives of this study are to investigate CO_2-influenced deep subsurface sediments in the Hartoušov mofette system and identify the impact of geogenic CO_2 on the deep microbial community. A 108.5-m-deep borehole was drilled and the core interval between 65 m and 95 m was selected for further investigations. The microbial signatures were obtained via molecular biological analyses (e.g. qPCR and Illumina 16S rRNA gene amplicon sequencing) and biomarker analyses. The deep biosphere is characterized by a similar abundance and diversity independent from the lithology over the entire investigated depth profile. These results suggesting an overall impact of the ascending CO_2-saturated groundwater on the microbial community structure.

Author Contributions

All authors have taken part in the interpretation of the results and writing of the manuscript. Q. Liu and K. Alder wrote the manuscript and performed subsampling and initial descriptions of the core material in an equal manner. Q. Liu processed the geomicrobiological analysis, i.e. DNA extractions and purification, gene quantification and bioinformatical based statistical analyses. K. Alder performed the analysis of the intact and past lipid membrane biomarkers and applied together with BP the bulk elemental analysis. F. Horn was involved in 16S rRNA sequencing data processing. P. Krauze was involved in statistical analyses. D. Wagner, K. Mangelsdorf, M. Alawi, H. Kämpf, R. Bussert and H.-M. Schulz gave essential technical advice and contributed to the interpretation of the results and valuable discussion. M. Alawi and K. Mangelsdorf supervised the study and led the writing of the present manuscript. All authors have taken part in the manuscript revisions and agreed with its scientific content.

Manuscript III (final draft)

Direct link between earthquake and subsurface microbial methane production

Authors

Qi Liu[1], Sebastian Hainzl[8], Horst Kämpf[2], Robert Bussert[3], Fabian Horn[1], Dirk Wagner[1, 6], Mashal Alawi[7]

Summary

This study aims to strengthen the hypothesis that seismic events can trigger methanogenesis by conducting laboratory simulation experiments with sediments down to 94.7 m at the Hartoušov mofette system. A simulation of an earthquake event was conducted by changing the headspace gas phase in the anaerobic vessels from N_2/CO_2 to H_2/CO_2 to investigate whether H_2 is the key molecule for microbial processes in the mofette system and essential to the methanogenesis in the Cheb Basin. The relation between the *in-situ* observation of the earthquake swarm period in 2000 at the Novy Kostel focal area/Czech Republic and our laboratory simulation experiments was revealed via a modeling procedure. The seismic events triggered methanogenesis was proved and based on this finding, we further hypothesize that the hydrogenotrophic early life on Earth was boosted by the Late Heavy Bombardment induced seismic activity in approximately 4.2 to 3.8 Ga.

Author Contributions

All authors took part in interpreting the results and writing the manuscript. Q. Liu involved in sampling, cultivations, DNA extractions, and sequencing. S. Hainzl provided the modeling and calibration of the cultivation results and the seismic data. H. Kämpf provided ideas and geological background. R. Bussert led the drilling campaign of the shallow mofette core. F. Horn was involved in Illumina sequencing data processes. D. Wagner provided valuable input in the interpretation of the results and the discussion. M. Alawi designed and supervised the study, led the 108.5 m deep drilling campaign and directed the writing of the present manuscript. All authors took part in manuscript revisions and agree with its scientific content.

Author affiliations

[1]GFZ German Research Centre for Geosciences, Section Geomicrobiology, Potsdam, Germany

[2]GFZ German Research Centre for Geosciences, Section Organic Geochemistry, Potsdam, Germany

[3]Institute of Applied Geosciences, Technische Universität Berlin, Berlin, Germany

[4]Institute for Geophysics and Geology, University of Leipzig, Leipzig, Germany
[5]GFZ German Research Centre for Geosciences, Section Climate Dynamics and Landscape Evolution, Potsdam, Germany
[6]Institute of Geosciences, University of Potsdam, Potsdam, Germany
[7]IMGM Laboratories GmbH, Martinsried, Germany
[8]GFZ German Research Centre for Geosciences, Section Earthquake and Volcanic Physics, Potsdam, Germany

2 Influence of CO_2 Degassing on the Microbial community in a Dry Mofette Field in Hartoušov, Czech Republic (Western Eger Rift)

2.1 Abstract

The Cheb Basin (Czech Republic) is a shallow Neogene intracontinental basin filled with fluvial and lacustrine sediments that is located in the western part of the Eger Rift. The basin is situated in a seismically active area and is characterized by diffuse degassing of mantlederived CO_2 in mofette fields. The Hartoušov mofette field shows a daily CO_2 flux of 23–97 tons of CO_2 released over an area of 0.35 km^2 and a soil gas concentration of up to 100% CO_2. The present study aims to explore the geo–bio interactions provoked by the influence of elevated CO_2 concentrations on the geochemistry and microbial community of soils and sediments. To sample the strata, two 3-m cores were recovered. One core stems from the center of the degassing structure, whereas the other core was taken 8 m from the ENE and served as an undisturbed reference site. The sites were compared regarding their geochemical features, microbial abundances, and microbial community structures. The mofette site is characterized by a low pH and high TOC/sulfate contents. Striking differences in the microbial community highlight the substantial impact of elevated CO_2 concentrations and their associated side effects on microbial processes. The abundance of microbes did not show a typical decrease with depth, indicating that the uprising CO_2-rich fluid provides sufficient substrate for chemolithoautotrophic anaerobic microorganisms. Illumina MiSeq sequencing of the 16S rRNA genes and multivariate statistics reveals that the pH strongly influences microbial composition and explains around 38.7% of the variance at the mofette site and 22.4% of the variance between the mofette site and the undisturbed reference site. Accordingly, acidophilic microorganisms (e.g., OTUs assigned to Acidobacteriaceae and Acidithiobacillus) displayed a much higher relative abundance at the mofette site than at the reference site. The microbial community at the

mofette site is characterized by a high relative abundance of methanogens and taxa involved in sulfur cycling. The present study provides intriguing insights into microbial life and geo–bio interactions in an active seismic region dominated by emanating mantle-derived CO_2-rich fluids, and thereby builds the basis for further studies, e.g., focusing on the functional repertoire of the communities. However, it remains open if the observed patterns can be generalized for different time-points or sites.

2.2 Introduction

Due to magmatic activity beneath the Cheb Basin, large-scale degassing of mantle-derived CO_2 (>99%) occurs. The diffuse cold gas emanations at the surface (diffuse degassing structures, DDS) can be distinguished as dry and wet mofettes (Kämpf et al., 2013). Mofettes provide insights into life under elevated CO_2 concentrations, low pH, and anoxic conditions comparable to the Earth's ancient atmosphere (Emiliani, 1992; Raven, 1995; Young et al., 2012). Moreover, mofettes are used as model ecosystems for studying the response of soil microorganisms to a potential CO_2 leakage of underground carbon capture and storage systems (Krüger et al., 2009; Krüger et al., 2011; Frerichs et al., 2013; Morales and Holben, 2013).

CO_2 degassing leads to hypoxia and acidification of the soil (Beaubien et al., 2008; Blume and Felix-Henningsen, 2009; Rennert and Pfanz, 2016). Additionally, an increase in metal mobilization was observed, which may affect the availability of soil nutrients (Mehlhorn et al., 2014; Mehlhorn et al., 2016). As shown by several studies, these direct influences of elevated CO_2 concentrations on the environment are affecting the mofette biota and its biological matter cycling.

First studies on the effects of CO_2 on the soil biota were focused on the plant vegetation. These studies point to a decelerated growth, an increased plant C/N ratio but also physiological adaptations that provide advantages in hypoxic or even anoxic environments (Pfanz et al., 2004; Vodnik et al., 2007; Rennert and Pfanz, 2016). A common feature of mofette soils are increased carbon and nitrogen contents (Ross et

al., 2000; Rennert et al., 2011). By $\delta^{13}C$ analyses of plant and microbial lipids, Oppermann et al. (2010) demonstrated that within a CO_2 vent in the Latera Caldera (Central Italy) a substantial amount of geothermal CO_2 is incorporated into the microbial, plant, and soil carbon pools. Recently, Beulig et al. (2016) performed radiocarbon analyses and showed that up to 67% of mofette soil carbon content originated from the assimilation of geogenic CO_2 via plant primary production and microbial CO_2 fixation. The authors pointed out that the almost undegraded organic material found in the mofette soil is facilitated by the permanent exclusion of meso- to macroscopic eukaryotes rather than an impaired biochemical potential for soil organic matter decomposition. Complementary, Nowak et al. (2015) estimated through combined $\delta^{14}C$ and $\delta^{13}C$ isotope mass balances that around 8–27% of the bulk soil organic matter (SOM) derived from microorganisms. DNA stable isotope probing allowed the identification of chemolithoautotrophic microorganisms such as methanogenic archaea and acetogens as well as sulfate reducing bacteria (SRB) to be involved in the assimilation of CO_2 (Oppermann et al., 2010; Beulig et al., 2015). However, a quantification of *cbbL* genes, encoding for the large subunit of RuBisCO, a carboxylase which is of crucial importance for carbon assimilation in chemolithoautotrophic microbes, revealed that only a part of the autotrophic CO_2-fixing microorganisms could adapt to the very high CO_2 concentrations found in a mofette in Slovenia (Videmšek et al., 2009).

In the last decade, several studies have focused on the impact of elevated CO_2 concentrations on the microbial community structure in mofettes. A shift to anaerobic/microaerophilic and acidophilic community compositions has been reported in CO_2 mofette soils located near the Laacher See (Germany) (Krüger et al., 2009; Krüger et al., 2011), the Cheb Basin (Czech Republic) (Beulig et al., 2015), and in Stavešinci (Slovenia) (Videmšek et al., 2009). Furthermore, at the Laacher See site, the abundance of several functional and group-specific gene markers revealed a decrease in *Geobacteraceae* and an increase in SRBs in the vent center and biomarker analysis revealed a predominance of *Thaumarchaeota* as possible indicator organisms for elevated CO_2 concentrations in soils (Frerichs et al., 2013). Also for a mofette in Latera,

Italy, it was shown that strictly anaerobic SRBs are abundant in mofettes, whereby the ATP biomass and total bacterial cell counts decreased (Beaubien et al., 2008). The highest sulfate reducing activity was observed in the center of the vent. Also Methanogenic archaea showed higher activities in the center of the vent compared to a transition zone site. Contrary to the results from Frerichs et al. (2013) in the Laacher See mofette, *Geobacteraceae* were in Latera mainly found at the CO_2 vent and only minor quantities were found at the reference site (Oppermann et al., 2010).

So far, only a few population datasets from dry mofettes are based on high throughput sequencing. The 454 pyrosequencing analyses of 16S rRNA genes from a natural mofette in centralsouthern Spain revealed that community richness, evenness, and diversity decreased with increasing CO_2 flux (Sáenz de Miera et al., 2014). An increase in abundance was thereby observed for OTUs related to the *Chloroflexi* phylum. Interestingly, Beulig et al. (2015) also showed that besides *Methanoregulaceae*, unclassified *Chloroflexi* might be involved in acetogenesis by DNA-SIP. The second 16S rRNA pyrosequencing dataset was established by Beulig et al. (2015) for a mofette located in the Plesná floodplain in the Cheb Basin. The community was dominated by methanogens (e.g., *Methanosarcinales* and *Methanomicrobiales*) and subdivision 1 *Acidobacteria*, which likely thrived under stable hypoxia and acidic pH. Recently, Krauze et al. (2017) investigated wet mofettes in the Cheb Basin by Illumina 16S rRNA amplicon sequencing and found a unique microbial community highly adapted to the anoxic conditions in the mineral and thermal waters and highlighted the connection between the groundwater or mineral waters and the deep biosphere. Deeper insights into the influence of CO_2 on the microbial community within the top 40 cm of a mofette in the Cheb Basin were gained by a metatranscriptomic and metagenomic approach (Beulig et al., 2016). One outcome of the study was that transcripts related to methanogenesis (*mcr*) and sulfate reduction (*dsr*, *cys*, *apr*) were remarkably increased in frequency.

However, until now, microbiological studies have focused only on near-surface soil layers (<70 cm) of dry mofettes, and deeper sediments have not yet been analyzed in

detail. The present study aims to characterize the influence of elevated CO_2 concentrations inside a CO_2 conduit on the geochemistry, microbial abundance, and community composition. Furthermore, this study intends to determine significant community-shaping environmental factors. To study the influence of mantle-derived CO_2, two 3-m drillings were performed, one of which was located in the center of the DDS and the other at the undisturbed border of the mofette field. To unravel the community structures a high-resolution sampling (every 5 to 10 cm) and Illumina 16S rRNA gene amplicon sequencing was conducted.

2.3 Material and methods

2.3.1 Site Selection, Description, and Sampling

The drilling campaign was conducted in September 2015 in the Hartoušov Mofette Field (HMF; 50°07′58″N, 12°27′46″E; **Figure 1B**). The study site is located in the Cheb Basin (NW Bohemia, Czechia), a shallow Neogene intracontinental basin filled with fluvial and lacustrine sediments (≤ 350 m thick; **Figure 1A**). The basin formed at the intersection of the Eger Rift (Kopecký, 1979) and the Regensburg–Leipzig–Rostock fault zone (Bankwitz et al., 2003b; Geissler et al., 2004) where four Quaternary volcanoes existed (Mrlina et al., 2009; Rohrmüller et al., 2018). The western Eger Rift has been well studied regarding structure of the lithosphere, seismic activity, sedimentology, and fault characteristics (Dobeš et al., 1986; Bucha et al., 1990; Špičáková et al., 2000; Bankwitz et al., 2003a; Kämpf et al., 2005; Kämpf et al., 2007; Flechsig et al., 2008; Kämpf et al., 2013; Fischer et al., 2014; Bussert et al., 2017). The seismic activity in this area occurs as “earthquake swarms”, which are typically numerous small earthquakes at upper crustal depths that cluster in time and space (Fischer et al., 2014). Earthquake swarms usually occur in volcanic areas, geothermal fields, and ocean ridges, whereas intraplate earthquake swarms that are not connected to active volcanism are present in continental rifts, such as the Rio Grande Rift, the Kenya Rift, and the western Eger Rift (Ibs-von Seht et al., 2008). Due to magmatic activity beneath the Cheb Basin, large-scale degassing of mantle-derived CO_2 (>99%)

occurs, and traces of gases such as He, N_2, Ar, and CH_4 are emitted (Weinlich et al., 1999; Kämpf et al., 2013; Hrubcová et al., 2017; Bräuer et al., 2018). The gas migrates through the upper lithospheric mantle and the crust to the surface and mixes with water of deep thermal and shallow groundwater aquifers (Bussert et al., 2017). Mofettes are local degassing phenomena that often occur as larger DDS on the scale of up to a few square kilometers. They are controlled by fluid migration in fault zones (Girault and Perrier, 2014; Nickschick et al., 2015) or in volcanohydrothermal areas (Chiodini et al., 2008; Girault et al., 2014; Inguaggiato et al., 2017). The investigated dry mofette is part of the Hartoušov mofette field (HMF or DDS Hartoušov) according to Kämpf et al. (2013), which covers an area of approximately 350,000 m^2 of grassland with two small ponds (2–6 m^2) close to the river Plesná. A total of 23–97 tons of CO_2 have been estimated to be released daily in the HMF (**Figure 1B**) (Nickschick et al., 2015).

The drilling sites were located along a NW-SE-oriented profile that is perpendicular to one of the main degassing areas of the HMF (**Figure 1B**). The CO_2 soil gas flux was repeatedly measured in June, August, September, and October 2012 along a 55-m profile that consisted of 11 stations (P1 to P11) with 5 m between each of them (Nickschick et al., 2015). The CO_2 soil gas flux measurements were performed by the accumulation chamber method, which uses a LiCOR 820 infrared gas analyzer for CO_2 discharge quantification and two accumulation chambers (West Systems, Italy). The profile encompasses low, medium, and high CO_2 soil degassing spots at the soil surface with strong degassing in the center of the profile (Nickschick et al., 2015). Places of high CO_2 soil gas flux form small hummocks (Flechsig et al., 2008).

Two 3-m cores were retrieved by hammered drilling using a motor-driven hammer (Wacker Neuson, Germany). The cores were taken from a dry mofette near station P6 and an undisturbed reference site in the direct vicinity of station P2 (Nickschick et al., 2015) (**Figures 1C,D**). The mean CO_2 soil gas flux of the mofette amounted to 27,961.6 g m^{-2} per day, while the CO_2 soil gas flux of the reference site amounted to 8.1 g m^{-2} per day (Nickschick et al., 2015). At the mofette site, which has a size of about 2 m^2, the growth of vegetation is hindered by continual CO_2 degassing (**Figure 1C**). A pond

about 4 m away from the sampled dry mofette is irregularly filled with groundwater or meteoric water.

Each core was subsampled in technical triplicates in the topmost 1 m in intervals of 5 cm and below in intervals of 10 cm. The inner part of the core material was subsampled using an ethanol flamed spatula. The core material for molecular biological analyses was immediately stored at -20°C after subsampling.

2.3.2 Geochemical Analysis

Pore water content in the sediment samples was too low to gain a sufficient amount of water for ion chromatographic analyses; therefore, a leaching procedure was applied in accordance with (Blume et al., 2011). Five grams of sediment were suspended in 25 mL of freshly autoclaved deionized water, shaken for 90 min in an anaerobic workstation (Don Whitley Scientific Limited, West Yorkshire, United Kingdom), and then centrifuged using airtight centrifuge tubes to remove solids. The water content of the fresh sediment was calculated from the difference in weight after being dried at 75 °C for 2 days. The pH and the conductivity of the pore water were analyzed with a Multi 3420 SET G digital measuring instrument (WTW, Weilheim, Germany).

Total organic carbon (TOC) and $\delta^{13}C_{org}$ values were measured using an elemental analyzer (NC 2500 Carlo Erba) coupled with a ConFlowIII interface on a DeltaPlusXL mass spectrometer (Thermo Fischer Scientific). Around 3 mg of sample material were weighed in unfolded Ag-capsules, added with 20% HCl, heated for 3 h at 75 °C, enfolded in the Ag-capsules, and measured. The calibration of $\delta^{13}C_{org}$ was performed by certified isotope standards (USGS24, CH-7) and proofed by an internal soil reference sample (Boden3). The isotopic composition is given in $\delta^{13}C_{org}$ notation relative to a standard: δ (‰) = $[(R_{sample} - R_{standard})/R_{standard}] \times 1000$. The ratio (R) and standard for carbon is $^{13}C/^{12}C$ and VPDB (Vienna PeeDee Belemnite).

The cation and anion concentrations in leached pore water were analyzed using ion

chromatography (IC) (Sykam Chromatography, Eresing, Germany) according to Vuillemin et al. (2016) protocol. For cations, the IC system consisted of a S5300 sample injector (Sykam), a 4.6 × 200 mm ReproSil CAT column (Dr. Maisch HPLC, Ammerbuch-Entringen, Germany), and a S3115 conductivity detector (Sykam). The eluent was 5 mM H_2SO_4, and the eluent flow rate was set at 1 mL min^{-1}. The column oven temperature was 45 °C. A Cation Multi-Element IC-standard (Carl Roth) was diluted ten times for calibration. Samples and standards were measured in technical triplicates. For anions, the suppressed IC system consisted of a SeQuant SAMS anion IC suppressor (EMD Millipore, Billerica, MA, United States), a S5200 sample injector, a 3.0 × 250 mm lithocholic acid (LCA) 14 column, and a S3115 conductivity detector (all Sykam). The eluent was 5 mM Na_2CO_3 with 20 mg L^{-1} 4-hydroxybenzonitrile and 0.2% methanol. The eluent flow rate was set at 1 mL min^{-1}, and the column oven temperature was set at 50 °C. A multi-element anion standard (Sykam) was diluted ten times for calibration. Samples and standards were measured in technical triplicates.

2.3.3 DNA Extraction and Purification

The total genomic DNA was isolated by the FastDNA™ SPIN Kit for soil and the FastPrep Instrument (MP Biomedicals, Santa Ana, CA, United States) with some protocol modifications. The FastPrep Instrument homogenizing time was set to 30 s, and the speed was set to 5.5 m s^{-1}. The mixing time of Binding Matrix and DNA crude extract solution was extended to 20 min. The Genomic DNA Clean & Concentrator™-10 (Zymo Research, Irvine, CA, United States) was utilized to remove humic acids and other substances that may have inhibited the PCR reaction. Three DNA isolations were extracted from each of the 44 sediment samples (22 samples from each core) as technical triplicates. In total, 132 samples were processed.

2.3.4 Quantitative PCR

The total bacterial abundance (16S rRNA gene) and the functional genes of sulfate-

reducing bacteria (SRB) (*dsrB* gene) and methanogenic archaea (*mcrA* gene) were determined by a quantitative polymerase chain reaction (qPCR). The qPCR Master Mix consisted of 12.5 ml iTaq^{TM} Universal SYBR Green Supermix (Thermo Fisher Scientific Inc., United States), 8.5 ml PCR water, 0.5 ml forward primer (20 mM), 0.5 ml reverse primer (20 mM), and 3 ml template. The quantification of the bacterial 16S rRNA gene was based on the primer pair of 331F (5'-TCCTACGGGAGGCAG-CAGT-3') and 797R (5'-GGACTACCAGGGTATCTAATCCTGTT-3') (Lane, 1991) and followed the protocol of 5 min at 98 °C, 40 cycles of 5 s at 98 °C, 20 s at 57 °C, and 60 s at 72 °C. The cloned 16S rRNA gene fragment from *E. coli* was used as standard. The qPCR efficiency for the 16S rRNA gene quantification was 90.2% and the R^2-value of the standard curve line was 0.996. The quantification of the dsrB gene was based on the primer pair of dsr2060F (5'-CAACATCGTYCAYACCCAGGG-3') and dsr4R (5'-GTGTAGCAGTTACCGCA-3') (Ben-Dov et al., 2007) and followed the protocol of 10 min at 95 °C, 40 cycles of 30 s at 95 °C, 60 s at 60 °C, 60 s at 72 °C. The cloned *dsrB* gene fragment of *Desulfovibrio vulgaris* was used as standard. The qPCR efficiency for the *dsrB* gene quantification was 93.4% and the R^2-value of the standard curve line was 0.999. The quantification of the *mcrA* gene was based on the primer pair of mlas-F (5'-GGTGGTGTMGGDTTCACMCARTA-3') and mcrA-R (5'-CGTTCATBGCGTAGTTVGGRTAGT-3') (Steinberg and Regan, 2009) and followed the protocol of 3 min at 95 °C, 40 cycles of 5 s at 95 °C, 20 s at 58.5 °C, 30 s at 72 °C, and 3 s at 80 °C. The cloned *mcrA* gene fragment of *Methanosarcina barkeri* was used as standard. The qPCR efficiency for the *mcrA* gene quantification was 97.7% and the R^2-value of the standard curve line was 0.997.

The qPCR was conducted on a CFX96 real-time thermal cycler (Bio-Rad Laboratories Inc., United States), and the analysis of the quantification data was performed with the CFX Manager^{TM} software (Bio-Rad Laboratories Inc., United States).

2.3.5 Illumina MiSeq Amplicon Sequencing

The 16S rRNA gene amplified from extracted total genomic DNA was used as a

template for the Illumina MiSeq highthroughput sequencing. The PCR reaction solution consisted of 12.5 ml MangoMix™ (Bioline, Taunton, United States), 9.2 ml PCR water, 0.3 ml bovine serum albumin, 0.25 ml forward primer (20 mM), 0.25 ml reverse primer (20 mM), and 2.5 ml template. Unique combinations of barcode-tagged 515F (5'-GTGCCAGCMGCCGCGGTAA-3') and 806R (5'-GGACTACHVGGGTWTCT AAT-3') (Caporaso et al., 2011) primers were assigned to each sample. The amplifications were performed on a T100 thermal cycler (Bio-Rad Laboratories Inc., United States) and followed the protocol of 3 min at 95 °C, 30 cycles of 30 s at 94 °C, 45 s at 56 °C, 60 s at 72 °C, and a final extension step of 10 min at 72 °C. The PCR products were cleaned up with AMPure XP magnetic beads (Beckman Coulter GmbH, Krefeld, Germany). After measuring the DNA concentration (CLARIO star plate reader, BMG LABTECH GmbH, Ortenberg, Germany), PCR products were pooled in equimolar amounts. The DNA pool was concentrated (Eppendorf Concentrator plus, Eppendorf AG, Hamburg, Germany) to meet the requirement of sequencing (DNA concentration ≥ 50 ng μl^{-1}). It should be noted that the used MangoMix™ (Bioline, Taunton, United States) does not supply a proof-reading polymerase, which may inflate species richness and interfere with recovery of certain genotypes (Brandariz-Fontes et al., 2015). However, (Pereira et al., 2018) showed that the choice of DNA polymerase did not significantly change the community profiling and composition.

2.3.6 Bioinformatics and Statistical Analysis

Sequencing was performed by Eurofins Scientific SE, Luxembourg, on an Illumina MiSeq (2 x 250 bp). Read pairs were merged using PEAR (Zhang et al., 2014). QIIME (Version 1.9.1) (Caporaso et al., 2010) was employed for microbiome analysis. More specifically, reads were demultiplexed, and USEARCH (Edgar, 2010) was used for the detection and removal of chimeric sequences. The SILVA database (Version 128) (DeSantis et al., 2006) was utilized for open-reference OTU clustering (97% sequence similarity) and taxonomic assignments. Rational taxonomic boundaries have been proposed for the high taxa (that is, genus and above) of the Bacteria and the Archaea on the basis of 16S rRNA gene sequence identities. These are: 94.5% for genus, 86.5%

for family, 82.0% for order, 78.5% for class, and 75.0% for phylum (Yarza et al., 2014). Within in this study the taxonomical data was discussed on genus-level and above. Singletons and OTUs assigned to chloroplasts were removed. The data received for the technical triplicates were merged for the downstream analyses. For alpha diversity analyses, the data were rarefied to 14,528 reads per sample. Alpha diversity and evenness were analyzed using the Shannon H index and the Shannon EH index. Beta diversity (PCoA) was determined by calculating the weighted UniFrac distance metric (QIIME), and samples from different depths were clustered and illustrated by 95% confidence ellipses. For multivariate statistics (including canonical correlation analysis, CCA), CANOCO 5 (Šmilauer and Lepš, 2014) and PAST3 (Hammer et al., 2001) were used. Sequencing data were submitted to the European Nucleotide Archive (http://www.ebi.ac.uk/ena) under accession numbers ERS 2039641 to ERS 2039772 (Bioproject PRJEB 22478).

2.4 Results

2.4.1 Stratigraphy and Geochemical Characterization

The reference core consisted primarily of fine- to medium- grained clayey sand that contained dispersed iron mottles (**Figure 2A**). A gravel-rich sand layer was reached at a depth of 80 to 100 cm, which roughly represented the groundwater level. The mofette core was dominated by humus or peaty sand and occasional by sandy peat. Clay or clayey sand occurred primarily in the topmost 20 cm. In the mofette field, the groundwater level was shallower (25–70 cm) than at the reference site. The very shallow groundwater level was also reflected in the high water content of the sediment (**Figure 2B**).

Ion concentrations, conductivity, and pH were obtained by sediment leaching (**Figures 2C, E, F**). The complete spectrum of measured anions, cations, and $\delta^{13}C_{org}$ values is provided in the **Supplementary Tables S1, S2**. The concentrations of sulfur, nitrate,

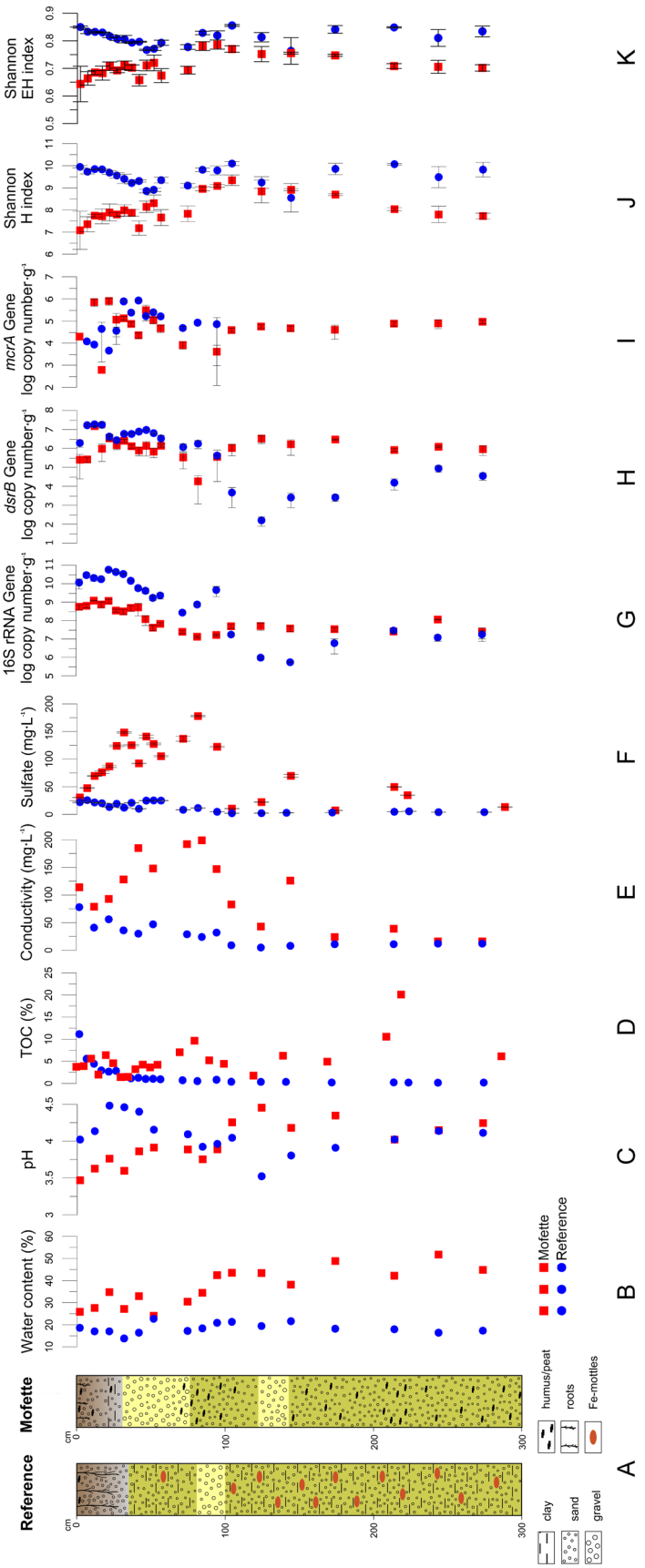

Figure 2 Lithological profile of the reference and mofette core (A). The water content (B), pH (C), TOC (D), conductivity (E), sulfate concentration (F), bacterial 16S rRNA gene copy number (G), *dsrB* gene copy number (H), *mcrA* gene copy number (I), Shannon H index (J) and Shannon EH index (K) of reference (blue dots) and mofette (red squares) core.

and nitrite were under detection limit. The pH values in the mofette core increased from around 3.5–4.3 down to a depth of 105 cm and varied from 4.0 to 4.6 between 105 and 275 cm in depth. In contrast, the pH values of the reference core ranged from 3.5 to 4.5 without displaying a clear trend. The conductivity of the mofette sediment was substantially higher compared with the reference core. Conductivity in the mofette site increased from 114 mg·L^{-1} at the surface to 199 mg L^{-1} at a depth of 85 cm and decreased downward to 16 mg L^{-1} at a depth of 275 cm. A conductivity peak of 126 mg L^{-1} was measured at a depth of 145 cm. In the reference core, the conductivity decreased from top to bottom from 78 mg L^{-1} to 12 mg L^{-1}.

The TOC content of the reference site decreased from 11.1% in the topsoil to 0.2% in the deepest sample at 275 cm in depth. The mofette site was characterized by a generally higher TOC content that varied significantly in the organic-rich peat layers (**Figure 2D**). The highest TOC contents were present at a depth of 224 cm (20.1%) and below the groundwater table at a depth of 82 cm (9.6%). $\delta^{13}C_{org}$ values were in the range of -25.3 to -28.5‰, and showed no significant differences between mofette and reference site.

In comparison with the reference core, sulfate concentrations were higher across the entire mofette core (**Figure 2F**). The sulfate most likely stems primarily from the oxidation of pyrite, which at Hartoušov (Flechsig et al., 2008) proved to be abundant in the mofette sites. The highest sulfate concentrations were measured in the top 65 cm of the reference (up to 25.74 mg L^{-1}) and in the top 100 cm of the mofette core (up to 177.92 mg L^{-1}). Sulfate concentrations were ten times higher than other measured anion and cation concentrations in the mofette and had a strong positive correlation with conductivity ($R = 0.8019$, $p < 10^{-5}$). Therefore, the high sulfate concentrations seem to be the main reason for the high conductivity.

2.4.2 Abundance of Microorganisms

The bacterial abundance (16S rRNA gene copy numbers) in the mofette core decreased within the upper 50 cm (**Figure 2G**). However, no decrease in abundance was observed

below 50 cm in sediment depth. From 0 to 100 cm in sediment depth, the gene copy numbers of the reference core were one order of magnitude higher than those of the mofette core. The highest bacterial abundance was analyzed at a depth of 12 cm in the mofette core (5.8 x 10^{10} gene copies g^{-1} sediment) and at 22 cm in the reference core (1.2 x 10^{9} gene copies g^{-1} sediment). From 100 to 280 cm in sediment depth, the gene copy numbers in the mofette core partially exceeded those of the reference site.

The abundance of SRB was estimated through the quantification of *dsrB* gene copies (**Figure 2H**). The *dsrB* gene copy numbers in the reference core followed a similar trend to that of the respective 16S rRNA gene copy numbers. The highest *dsrB* gene copy number (1.9 x 10^{7} gene copies g^{-1} sediment) was measured at a depth of 12 cm, and the lowest (1.6 x 10^{2} gene copies g^{-1} sediment) was measured at 125 cm. The *dsrB* gene copy numbers in the mofette core decreased with depth (1.5 x 10^{7} to 1.8 x 10^{4} gene copies g^{-1} sediment).

The abundance of methanogens was estimated via the quantification of *mcrA* gene copies (**Figure 2I**). Between a depth of 0 and 100 cm, the *mcrA* gene copy numbers of both the mofette site and the reference site varied in the range of 0 and 8.5 x 10^{5} gene copies g^{-1} of sediment. No *mcrA* genes were detected at depths greater than 100 cm at the reference site; however, *mcrA* gene copy numbers in the mofette site slightly increased with depth (3.9 x 10^{4} gene copies g^{-1} sediment at a depth of 105 cm to 9.3 x 10^{4} gene copies g^{-1} sediment at a depth of 275 cm).

2.4.3 Community Structure

In total 10,201,992 sequences were obtained in the 16S rRNA gene library after merging, demultiplexing, filtering, and excluding of chimeric sequences, chloroplast-like sequences, and singletons. The read numbers ranged from between 21,143 and 160,896, with a mean value of 77,287. Rarefaction analyses revealed that no sample exhibited a conspicuous increase in its Shannon H index when calculating more than 14,528 sequences per sample.

Except for the section of sediment between 85 and 145 cm in depth, the reference site showed a higher alpha diversity (**Figure 2J**). The alpha diversities of the mofette increased with depth from 0 to 85 cm, remained constant from 85 cm to 145 cm, and then decreased toward the end of the profile. The Shannon index of the mofette displayed a weak positive correlation with pH ($R = 0.582$, $p = 0.0045$) and water content ($R = 0.497$, $p = 0.0187$) (**Supplementary Tables S3, S4**). The Shannon EH equitability index was lower throughout the depth sequence at the mofette than at the reference site (**Figure 2K**), especially at the surface layers and the deepest part.

The relative abundance of each taxon is displayed by the percentage of total sequence reads. The dominant phyla at both the mofette site and the reference site were *Acidobacteria* (mofette: 20.4%; reference: 25.6%), *Actinobacteria* (mofette: 6.7%; reference: 10.9%), *Chloroflexi* (mofette: 9.4%; reference: 15.8%), *Firmicutes* (mofette: 14.9%; reference: 4.8%), and *Proteobacteria* (mofette: 24.9%; reference: 23.7%). The dominant archaeal phyla were *Bathyarchaeota* (mofette: 1.8%; reference: 1.7%), *Euryarchaeota* (mofette: <0.1%; reference: 0.4%), and *Thaumarchaeota* (mofette: 0.3%; reference: 1.0%). Moreover, a larger fraction of unassigned taxa were present in the mofette sediments (4.0%) compared with in the reference sediments (1.0%; **Figure 3**).

Beta diversities were obtained by calculating a weighted UniFrac distance metric (**Figure 4**). A distinct clustering of the microbial communities was observed for both sites. The microbial community structure of the upper sediment (0–95 cm) of the mofette was distinct from the deeper part of the core (100–275 cm), and we therefore defined two distinct clusters. Cluster A includes communities from 0 to 95 cm in depth, and Cluster B includes communities observed at depths between 100 and 275 cm.

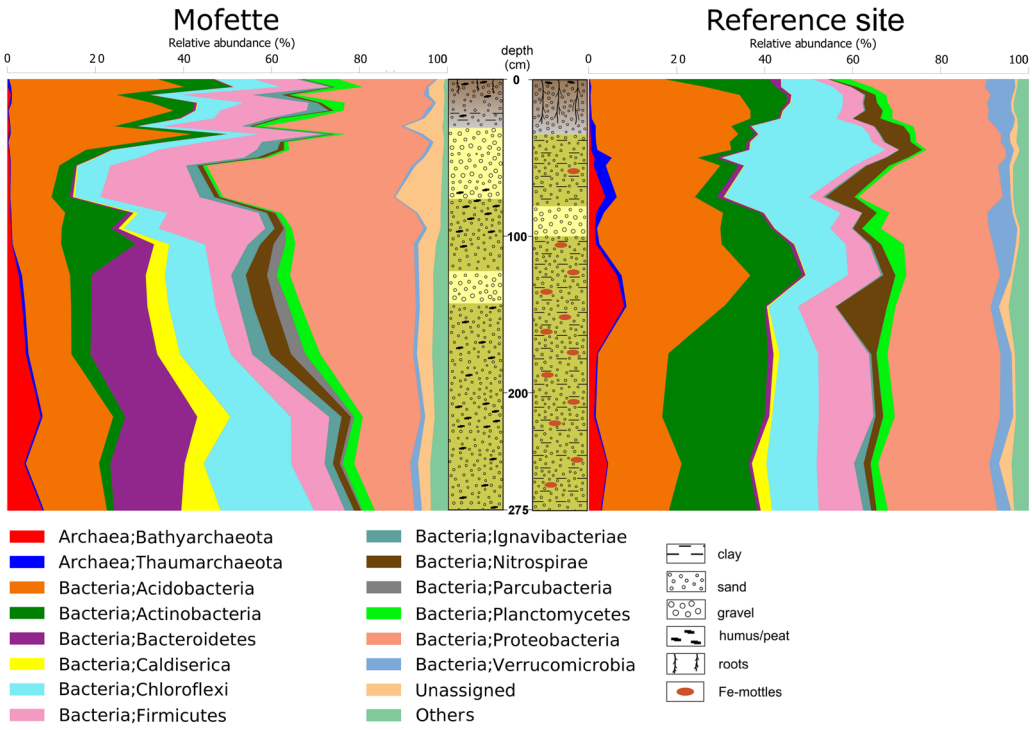

Figure 3 Community structures at phylum level (most abundant 14 phyla) and the lithological profiles of the cores.

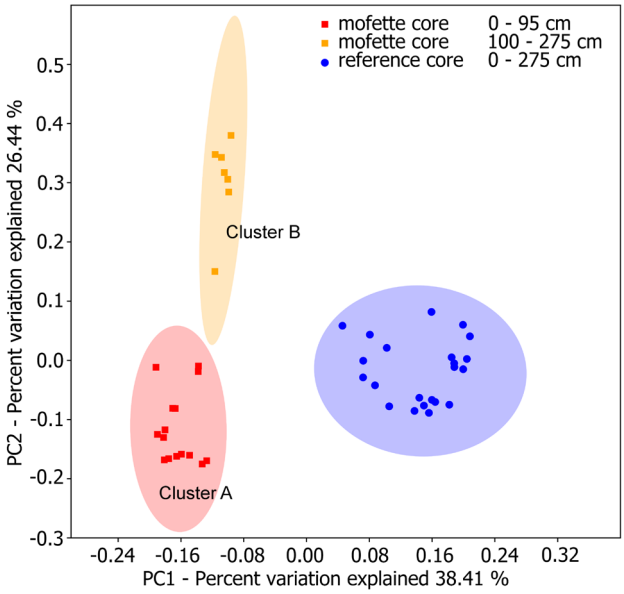

Figure 4 PCoA plot calculated by the weighted UniFrac distance of the microbial communities. Mofette samples are indicated by red and orange squares; reference site samples by blue dots. The 95% confidence ellipses indicate three different clusters.

At a depth of 0–100 cm (Cluster A), the dominant taxa were *Acidobacteriaceae* (Subgroup 1) (mofette: 12.4%; reference: 10.5%) – which contributed to 5.1% of the dissimilarity – followed by the genera *Acidithiobacillus* (mofette: 7.1%; reference: 0.5%) – which contributed to 4.6% of the dissimilarity (**Figure 5A**). At a depth of 100–275 cm (Cluster B), where the influence of the uprising CO_2 was stronger than in the atmospheric- and groundwater influenced upper part of the depth sequence, significant differences in the community structures were observed (**Figure 3**). *Acidothermus* (mofette: 0.5%; reference: 6.8%) and *Acidobacteriaceae* (Subgroup 1) (mofette: 2.0%; reference: 8.3%) were much more abundant in the reference site, and *Sulfurovum* (mofette: 4.2%; reference: 0.1%), *Anaerolineaceae* (mofette: 5.1%; reference: 2.0%), *Caldisericum* (mofette: 5.5%; reference: 1.2%), *Desulfobacca* (mofette: 5.7%; reference: 1.4%), *Thermoanaerobaculum* (mofette: 6.5%; reference: 0.3%), and *Bacteroidetes vadin HA17* (mofette: 4.1%; reference: 0.1%) were more abundant in the mofette (**Figure 5B**).

In the mofette site, microorganisms potentially involved in sulfur cycling were far more abundant (relative to the entire community) and comprised up to 14.4% of the sequence reads. In contrast, only 2.5% of the sequence reads were involved in sulfur cycling at the reference site. Observed taxa involved in sulfur cycling were sulfide/sulfur oxidizer *Acidithiobacillus* (mofette: 7.1%; reference: 0.5%) (Kelly and Wood, 2000), *Sulfuriferula* (mofette: 1.1%; reference: 0.1%) (Watanabe et al., 2015), *Sulfurovum* (mofette: 1.5%; reference: 0.1%) (Inagaki et al., 2004), SRB *Desulfobacca* (mofette: 3.1%; reference: 0.9%) (Oude Elferink et al., 1999), and *Desulfosporosinus* (mofette: 0.8%; reference: 0.2%) (Stackebrandt et al., 1997) (**Figure 6A**). Taxa involved in iron cycling were less abundant in the mofette (1.1%) than at the reference site (1.2%). The iron cycling-related taxa consisted of extremely acidophilic iron-oxidizer *Ferrithrix* (mofette: 0.18%; reference: 0.01%) (Johnson et al., 2009), acidophilic ironoxidizer *Ferrovum* (mofette: 0.72%; reference: 0.05%) (Johnson et al., 2014), *Gallionella* (mofette: <0.01%; reference: 0.04%) (Hallbeck and Pedersen, 1990), and the aerobic iron-oxidizer *Sideroxydans* (mofette: 0.20%; reference: 1.14%) (Emerson and Moyer, 1997) (**Figure 6B**). Methanogens were found in a relatively low proportion at both the

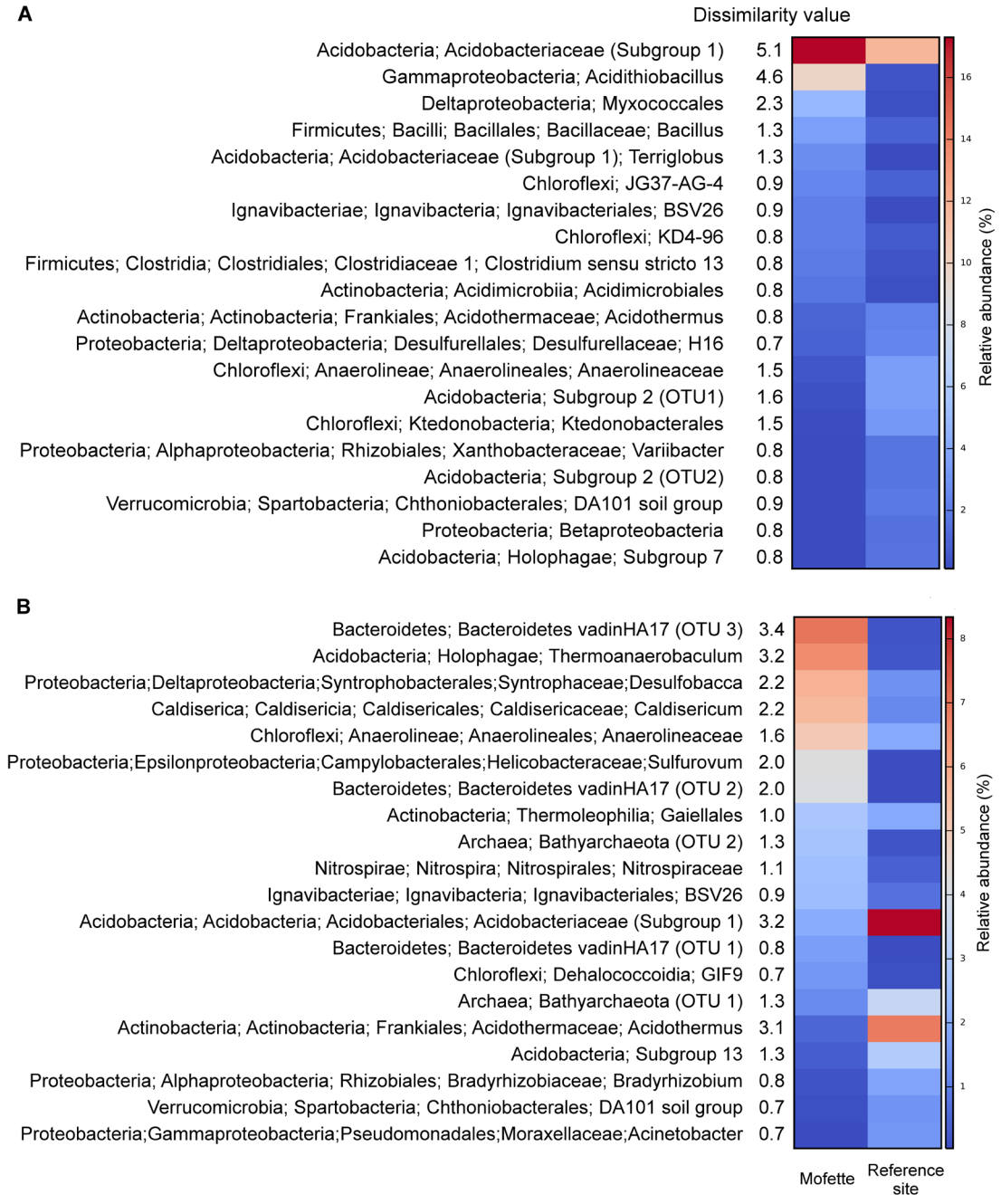

Figure 5 Heatmap of the top 20 taxa which explain most of the dissimilarity between the microbial communities of the mofette and the reference site based on the Bray–Curtis dissimilarity values. Cluster A (depths between 0 and 95 cm) (A) and Cluster B (depths between 100 and 275 cm) (B).

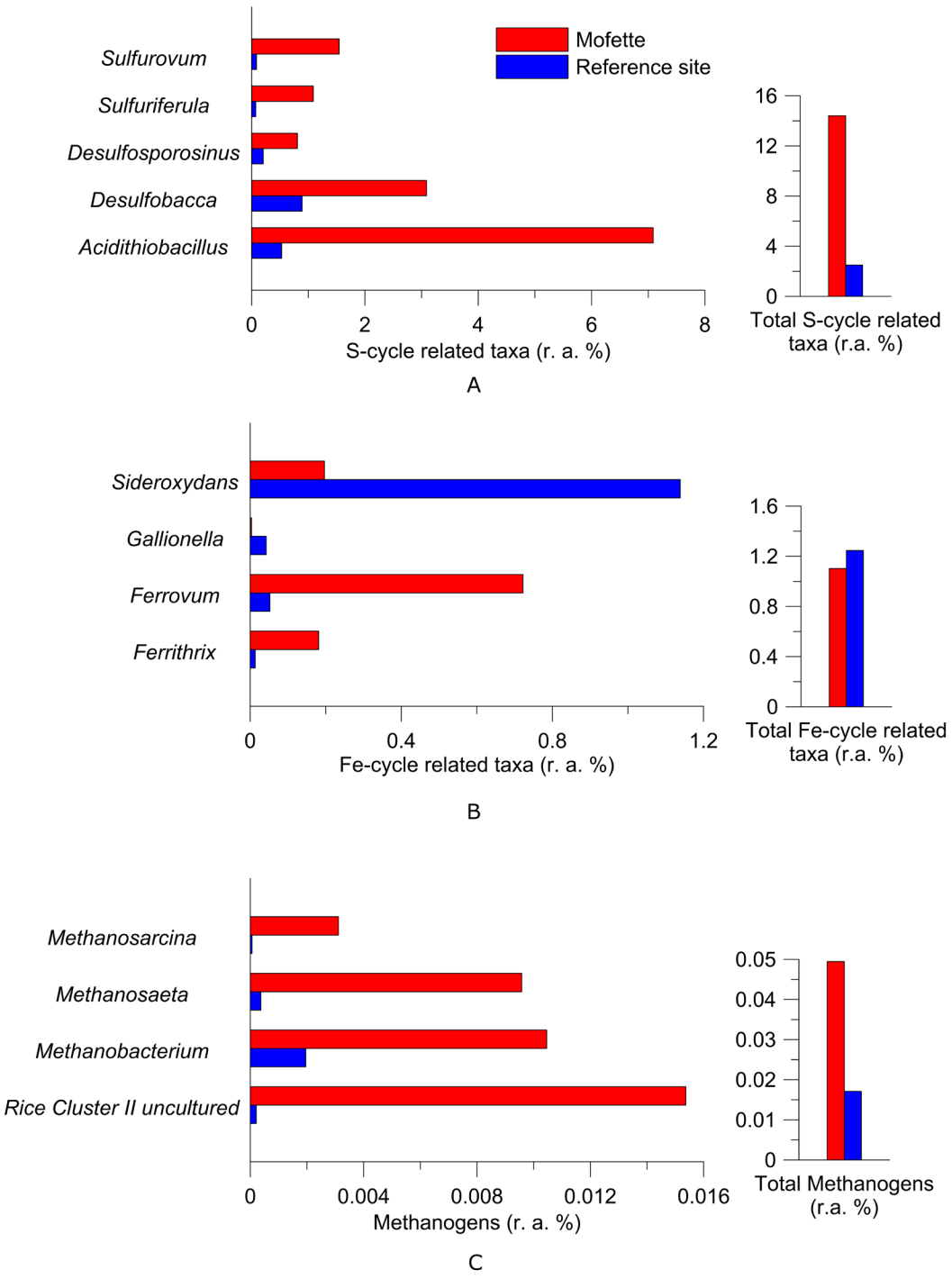

Figure 6 Relative abundance (r. a.) of the most abundant taxa and the total fraction involved in the sulfur-cycle (A), iron-cycle (B), and methanogenesis (C).

mofette site and the reference site (0.04 and 0.02%). Uncultured taxa from Rice Cluster II (Großkopf et al., 1998), *Methanobacterium* (Smith et al., 1997), *Methanosaeta* (Patel and Sprott, 1990), and *Methanosarcina* (Zinder et al., 1985) were the most abundant genera and were proportionally more common in the mofette microbial community (0.02, 0.01, 0.01, and <0.01%) in comparison with those of the reference site (<0.01%; **Figure 6C**).

The mofette and the reference site shared 1,626 taxa, and a small fraction of taxa only occurred in the mofette (138) or the reference site (128). At depths of between 100 and 275 cm, 1,336 taxa were shared, but 184 and 198 taxa were only observed in the mofette and at the reference site, respectively. A total of 1,045 taxa were detected in the deeper part (200–275 cm) of the mofette and the reference site, 124 taxa were detected only at the mofette, and 330 taxa were only detected at the reference site (**Supplementary Table S5**).

Interestingly, methanogenic archaea – such as *Methanosphaerula* – were only found in the mofette. *Methanoregula* was not observed at the reference site between depths of 100–275 cm. *Methanosaeta* and *Methanosarcina* were not observed in the deep layers (200–275 cm) of the reference site.

2.4.4 Multivariate Statistics

Canonical-correlation analysis was used to determine community-shaping environmental factors (**Figure 7**). Among all measured environmental parameters, only those with significant p_{adj}-values (*Bonferroni* corrected <0.05) were included in the analyses. pH, sulfate concentration, and TOC formed the optimal subset of parameters to explain the observed OTU distribution. The pH value explains 38.7% of the distribution pattern of taxa at the mofette site (**Figure 7A**) and 16.3% at the reference site (**Figure 7B**). Sulfate concentration explains 12.7% of the distribution pattern of microorganisms at the mofette (**Figure 7A**) and 8.4% at the reference site (**Figure 7B**). The TOC values explain 11.4% of the distribution pattern at the reference site (**Figure**

7B) and 4.5% at the mofette (**Figure 7A**). The differences in the community structure of the mofette and the reference site are mainly explained by pH (22.4%), sulfate concentration (10.6%), and TOC (9.9%) (**Figure 7C**). The 16S rRNA gene copy numbers at the reference site are positively correlated with pH ($R = 0.709$, $p = 0.0002$), whereas at the mofette site, a significant negative correlation with pH ($R = -0.655$, $p = 0.0009$) was observed (**Figure 2G**) (**Supplementary Tables S3, S4**). No significant correlation with any measured environmental parameter was found for the abundance of the *dsrB* or *mcrA* genes.

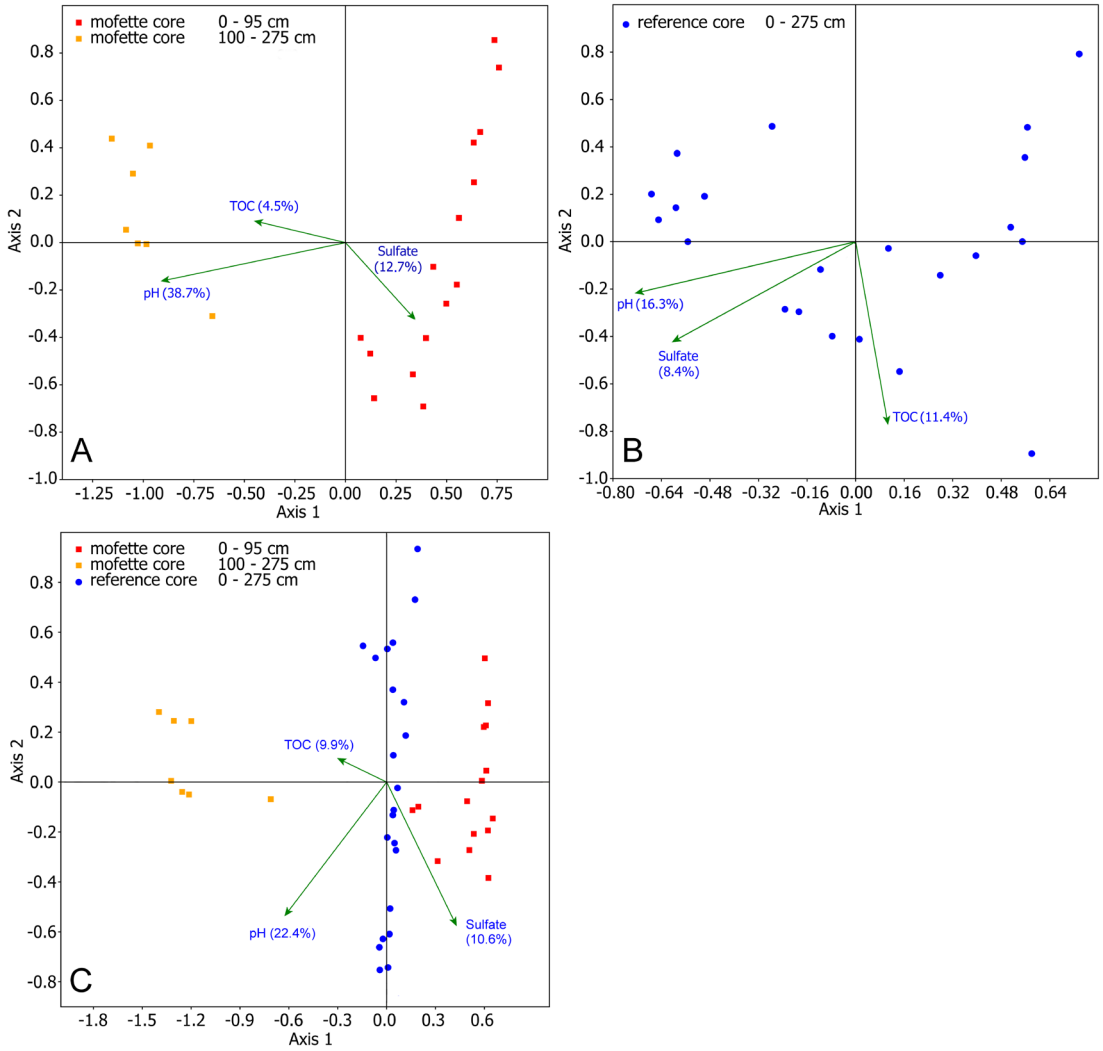

Figure 7 CCA analyses of the microbial communities of the mofette (A), reference site (B), and for both (C). The environmental parameters were selected based on the forward-selection method with significant padj-values (Bonferroni corrected <0.05).

2.5 Discussion

Dry mofettes – such as the HMF – allow for an investigation of geo–bio interactions that result from the permanent degassing of mantle-derived CO_2. In the uppermost soil layers – which have been the focus of other studies (Krüger et al., 2009; Blagodatskaya et al., 2010; Sáenz de Miera et al., 2014; Beulig et al., 2015) – the conditions are not necessarily permanent strictly anoxic, which also allows aerobic or microaerophilic heterotrophic microorganisms to grow. The input of oxygen can derive from meteoric water as well as horizontally via groundwater flow. The sampling depth and lithological profile are therefore of major importance in unraveling the influence of the CO_2 on the microbial communities. For the first time, the present study provides insights into the community structure in 3-m-deep sediments of a mofette and a nearby reference site. The combination of geochemical analyses and Illumina MiSeq highthroughput sequencing of 16S rRNA genes reveals the complexity of geo–bio interactions in the CO_2-influenced habitat.

We observed a strong influence of the emanating CO_2-rich fluid on crucial soil parameters, such as pH, water content, and ion composition (**Figure 2**). The relatively low pH may be an indication for the influence of CO_2 also at the reference site, and reflects the characteristics of the lithological profile. However, the CO_2 flux measurements at the surface of the reference site did not reveal any mofette activity; this is supported by the typical TOC profile and low sulfate concentration and conductivity. Both sampling sites were located in a wet land area (floodplain) with a high groundwater level. We assume that depending on the season (and flooding) an influence by CO_2-rich groundwater at both sites is possible. It is known that the groundwater level at the HMF may shift around 20 cm per day (Nickschick et al., 2017). Within the first 80 cm of the depth profile the pH of the reference site ($pH > 4$) was higher than at the mofette site ($pH < 4$). At the reference site the groundwater level is situated within a gravel-rich sand layer at a depth of 80 to 100 cm. The groundwater, which may migrate horizontally, presumably causes a decrease of the pH due to dissolved CO_2. Thereby, the fine- to medium-grained clayey sand in the reference site might function as a natural vertical barrier for the groundwater and CO_2 flow, especially

in depths deeper than the core sequence. In the mofette, the groundwater level was shallower (25–70 cm) than at the reference site. On the other hand the pH in the mofette was highest in the gravel-rich layer between depths of 130–140 cm. The high conductivity and sulfate concentration (**Figure 2**) may indicate that mineral water from greater depth is admixed with groundwater in the mofette. Mineral water found in the same mofette in a depth of ca. 82 m had a pH of 6.4 and a sulfate concentration 1470 mg L^{-1} (Bussert et al., 2017).

The different microbial community structures found in each depth and each core at the reference site and in the mofette cannot be explained by the variances in the lithology of the core material, however, the lithological setting is from a major importance for both habitats in greater depth (78 m) where a cap-rock like carbonate-rich layer largely seals the CO_2-rich aquifer and allows for a channelized CO_2 degassing (Bussert et al., 2017). Instead, the pH, TOC, and sulfate concentration formed the optimal subset of parameters to explain the abundance and distribution of the taxa at both sites. Multivariate statistical analyses and qPCR results revealed that at the reference site, the microbial abundance was positively correlated with pH (R = 0.709, p = 0.0002), while a significant negative correlation was observed at the mofette site (R = -0.655, p = 0.0009; **Figures 2C,G** and **Supplementary Tables S3, S4**). Therefore, several taxa of the microbial community at the mofette site seem to be adapted to the acidic conditions. However, the diversity and the evenness at the mofette site are positively correlated with the pH (R = 0.582, p = 0.0044, and R = 0.550, p = 0.008; **Supplementary Tables S3, S4**), indicating that it is mainly specialists that can withstand the extreme environmental conditions. It is remarkable that solely the pH value explains 38.7% of the distribution pattern of taxa at the mofette site (**Figure 7A**). Since the pH value at the reference site is hardly affected by the emanating CO_2, it only explains 16.3% of the OTU distribution (**Figure 7B**). However, since the pH is generally cocorrelated with CO_2 concentration, it is necessary to consider the fact that the abundance of autotrophic microorganisms in the mofette site is also positively correlated with the amount of CO_2-rich emanating fluids. The results of the geochemical analyses and the 16S sequencing lead to the assumption that in addition to pH, sulfate also plays an important role in

microbial matter cycling under anaerobic conditions in the mofette site. The sulfate concentration – which is five to fifteen times higher in the mofette site – explains 12.7% of the distribution pattern of microorganisms at the mofette (**Figure 7A**). In comparison with the mofette, the sulfate concentration at the reference site explains only 8.4% of the community structure (**Figure 7B**).

In comparison with the reference site, the TOC values were up to 100 times higher in the peat layers of the mofette (**Figures 2A, 2D**). While pH and ion concentrations are directly influenced by the emanating CO_2, the high TOC content at the mofette site can be explained by the consequences of acidification and anoxia on mesoscopic or macroscopic eukaryotes involved in the degradation of complex organic matter; additionally it was shown that acetogenesis is a prominent process in mofettes (Beaubien et al., 2008; Beulig et al., 2015; Beulig et al., 2016; Fernández-Montiel et al., 2016b). The TOC values explain 11.4% of the distribution pattern at the reference site (**Figure 7B**) and only 4.5% at the mofette (**Figure 7A**). Moreover, the top 10 abundant taxa at the reference site were heterotrophic microorganisms. In contrast, the high abundance of chemolithoautotrophic taxa in the mofette highlights the importance of an autotrophic- rather than a heterotrophic lifestyle in habitats with strongly elevated CO_2 concentrations (Oppermann et al., 2010). Autotrophic microorganisms can fix significant amounts of carbon from geogenic CO_2 (Nowak et al., 2015), whereas organic substrates remain undegraded and accumulate in the sediment. An interesting side effect can be seen in a long-term perspective because such an enormous accumulation of organic substances in sediments may be the precondition for the development of a paleo organic layer at a late stage.

The bacterial 16S rRNA gene copy numbers in the mofette varied from 10^5 to 10^9 copies g^{-1} of sediment. The highest gene copy numbers were found in the topsoil of the mofette (1.2×10^9 gene copies g^{-1} at a depth of 12 cm; **Figure 2G**). While the abundance of microorganisms at the reference site followed a classical trend and decreased with depth, the abundance of microorganisms in the mofette did not decrease with depth beyond 50 cm. The present study suggests for the first time that at a depth greater than 100 cm, the

microbial abundance in the mofette even partially exceeded that of the reference site. This trend was also observed for SRB and methanogenic archaea (**Figures 2H, 2I**). As discussed later, presumably the uprising CO_2-rich fluid feeds the ecosystem from underneath with substrates such as CO_2 and sulfate. However, compared with the reference site, the gene copy numbers at the mofette were about one order of magnitude lower for the uppermost 100 cm. Higher cell numbers in the surface soil of the reference site can be explained by the predominance of aerobic processes and a rather moderate pH. In general, the gene copy numbers per gram of subsurface sediment at the HMF were similar to soils with highly elevated CO_2 concentrations (10^9 to 10^{10} copies g^{-1} sediment) (Beaubien et al., 2008; Krüger et al., 2009; Oppermann et al., 2010; Frerichs et al., 2013; Beulig et al., 2015; Fernández-Montiel et al., 2016a; Fernández-Montiel et al., 2016b). The top 40 cm of the mofette site at the HMF was an exception, for here, the gene copies were one order of magnitude lower (10^8 to 10^9 copies g^{-1} sediment) compared with the Plesná floodplain site, which is located 1.8 km to the NW (Beulig et al., 2015). Reasons for the discrepancy could be the higher CO_2 flux at the HMF or different soil characteristics (Kämpf et al., 2013). Additionally, seasonal effects have to be considered. In April (Beulig et al., 2015), the surface water level is often higher, and substrates might be more easily accessible in comparison with September, when the HMF drilling took place.

Both diversity and evenness were lower at the mofette than at the reference site (**Figures 2J, 2K**). A lowered diversity was also observed at the La Sima mofette in Spain (Sáenz de Miera et al., 2014). The low evenness indicates a dominance of specialists, such as anaerobic acidophilic and acidotolerant taxa in the mofette community. In the mofette, the alpha diversity and the evenness were higher at depths between 85 and 125 cm. This shift can be explained by the surface water table and the admixture of surrounding aerobic communities.

The results of the Beta diversity of the community highlight the assumption that only the deeper sediments are almost unaffected by oxygen. The PCoA plot of the weighted UniFrac distance metric revealed that the mofette harbors two distinct communities

(**Figure 4**). One cluster includes communities from shallow depths between 0 and 95 cm (Cluster A), and the other cluster includes communities in the deep anoxic sediments from 100 to 275 cm (Cluster B). The microbial communities from the reference site cluster apart from all mofette samples, which highlights the fact that the mofette community is strongly influenced by the degassing phenomenon.

Site-specific effects – such as a low pH and changes in ion composition – do not sufficiently explain the differences between Cluster A and Cluster B, but the oxygen availability could be identified as the major stress factor. In the mofette, the oxygen-dependent depth gradient was clearly reflected in the antagonistic shift of the relative abundance of aerobic and anaerobic taxa in Cluster A and Cluster B. The relative abundance of obligate and facultative anaerobic microorganisms affiliated with *Bacteroidetes*, *Bathyarchaeota*, *Caldiserica*, and *Parcubacteria* gradually increased with depth. At the same time, the relative abundance of versatile *Proteobacteria* strongly decreased with increasing depth (**Figure 3**). Strictly anaerobic and facultative aerobic microorganisms affiliated with *Acidithiobacillus*, *Clostridiaceae 1*, *Bacillus*, and *Ignavibacteriales* that were observed in Cluster A were much more abundant at the mofette than at the reference site. In Cluster B, strictly anaerobic microorganisms within the taxa *Thermoanaerobaculum*, *Bacteroidetes vadin HA17*, *Desulfobacca*, *Caldisericum*, *Anaerolineaceae*, and *Sulfurovum* shaped the community and explained most of the differences (14.5% dissimilarity) between the communities of the deep sediments of the mofette and reference site (**Figures 5A, 5B**). Neither in Cluster A nor Cluster B were any of the strictly aerobic taxa more abundant in the mofette than at the reference site, except for *Acidobacteriaceae* (Subg. 1). Additionally, the family *Acidobacteriaceae* (Subg. 1) was the most abundant taxa in both study sites (mofette: 12.4%; reference site: 10.5%). Members of this group are heterotrophic, aerobic, or microaerophilic, and some species are facultative anaerobes (Pankratov et al., 2012). Therefore, the occurrence at both sites under both aerobic and anaerobic conditions is plausible. The HMF multivariate statistics indicate a strong negative correlation of the taxon with pH, and the same correlation has been observed by (Mannista et al., 2007) in tundra soils. Moreover, the proportion of unassigned taxa (4.0%) was much higher

in the mofette compared with the reference site, indicating that mofettes are unique environments that harbor a large fraction of novel, as-of-yet undescribed organisms.

The sulfate-rich mofette with a pH < 4.0 offers ideal growth conditions for obligate acidophilic bacteria such as *Acidithiobacillus* (Kelly and Wood, 2000). Accordingly, these bacteria's abundance is positively correlated with the sulfate concentration (R = 0.699, p = 0.0003; **Supplementary Tables S3, S4**). In both clusters, taxa potentially involved in sulfur cycling had a more substantial proportion (14.4%) and a higher diversity (e.g., of *Desulfobacca*, *Desulfosporosinus*, *Sulfurovum*, and *Sulfuriferula*) in the mofette in comparison with the reference site (3.0%; **Figure 6A**). *Desulfobacca* was also recently found in a Plesná floodplain site (Beulig et al., 2016). A higher abundance of SRB was also observed in CO_2 vents (Beaubien et al., 2008) and CO_2-affected soils (Frerichs et al., 2013). Striking differences between the mofette and reference site were also observed for taxa potentially involved in iron-cycling. The results lead to the assumption that in addition to sulfate reduction, iron-cycling is also an important feature under aerobic conditions at the reference site and under anaerobic conditions in the mofette. The aerobic or microaerophilic taxa – such as *Gallionella* and *Sideroxydans* (Hallbeck and Pedersen, 1990; Emerson and Moyer, 1997) – were more abundant at the reference site, whereby acidophilic obligate and facultative anaerobic genera – such as *Ferrithrix* and *Ferrovum* (Johnson et al., 2009; Johnson et al., 2014) – dominated in the mofette (**Figure 7B**).

The extreme environmental conditions in the mofette also favor the growth of methanogenic archaea. *Methanosphaerula* (Cadillo-Quiroz et al., 2009) occurred solely in the mofette, whereby other genera – such as *Methanoregula* (S. L. Bräuer et al., 2011), *Methanosaeta* (Patel and Sprott, 1990), and *Methanosarcina* (Zinder et al., 1985) – were abundant at all depths in the mofette core but occurred only in low abundances close to the surface in the reference site, presumably because oxygen is spatially depleted by aerobic processes. Other archaea potentially involved in acetogenesis and methane cycling – such as *Bathyarchaeota* and ammonia-oxidizing *Thaumarchaeota* affiliated with South African Gold Mine Gp 1 (SAGMCG- 1) (Takai et al., 2001a) –

were found at the mofette and the reference site in almost the same relative abundances (1.7 and 0.2%). These organisms have been found in marine sediments, deep aquifer waters, a CO_2 vent, as well as in water from wet mofettes and in thermal water in the Eger region (Kubo et al., 2012; Frerichs et al., 2013; Evans et al., 2015; Krauze et al., 2017). Additionally, several other microorganisms found in the deep mofette sediments (e.g., *Thermoanaerobaculum*, *Caldisericum*, *Sulfurovum*, and *Mobilitalea*) have been isolated from hot springs, hydrothermal sediments, or thermal water from a 2.8-km-deep well (Oude Elferink et al., 1999; Inagaki et al., 2004; Losey et al., 2013; Podosokorskaya et al., 2014). These microorganisms most likely derive from the deep biosphere, indicating that the mofette is connected to the deep subsurface via ascending fluids. The environmental conditions in the mofette at 1–3 m in depth are similar to deep sediments or deeply originating thermal waters with respect to the availability of oxygen and ion composition and may therefore also provide adequate growth conditions for such taxa.

The microbial communities from both Cluster A and Cluster B at the HMF share many abundant taxa with the communities described by Sáenz de Miera et al. (2014) in the shallow sediments at the La Sima CO_2 gas vent (top 10–20 cm; **Supplementary Table S6**) and a CO_2-influenced floodplain site at Plesná (Beulig et al., 2015). Although the relative abundances of these common taxa display clear differences, they represent an outline of the characteristic core community of CO_2-influenced surface habitats. The occurrence of unshared sitespecific taxa can be explained by the differing environmental conditions. For example, higher oxygen concentrations (<7%) (Peinado et al., 2009) and historical thermal anomalies might specifically trigger the growth of aerobic or facultative anaerobic thermophiles – such as members of *Ktedonobacteria* (e.g., *Thermogemmatispora*) – at the La Sima mofette. The high resemblance of the Cluster A communities to the microbial communities at the CO_2-influenced Plesná floodplain site (Beulig et al., 2015) lead to the assumption that the environmental conditions at both mofettes located in the Cheb Basin are rather similar compared with those the La Sima site. The low pH at the HMF and the floodplain particularly favors the growth of acidophilic taxa (e.g., *Acidobacteria*, Subg. 1), which have a rather low

abundance at the La Sima site.

The high relative abundance of sulfate reducers, methanogens as well as further autotrophs indicate that the community is supported by hydrothermal originating substrates, delivered by the mantle-derived CO_2. The geochemical data demonstrate that electron acceptors such as sulfate and CO_2 are sufficient available. This is in good accordance with the findings from Beulig et al. (2016) who showed that in the mofette transcripts related to methanogenesis (*mcr*) and sulfate reduction (*dsr*, *cys*, *apr*) were remarkably increased in the frequency. In the Eger Rift, hydrogen, which is a key electron donor in the deep biosphere (Stevens and McKinley, 1995; Chapelle et al., 2002; Nealson, 2005; Spear et al., 2005; Hinrichs et al., 2006), becomes available during radiolytic decay in the underlying fissured granite or stress-released during earthquake swarms (Bräuer et al., 2005; Bräuer et al., 2007).

2.6 Conclusion

Our study of a dry CO_2 degassing mofette in Hartoušov, NW Bohemia, as central part of a CO_2 conduit deepens the knowledge of geo–bio interactions in extreme environments with elevated CO_2 concentrations. The mofette ecosystem is characterized by anoxic conditions, a low pH, high TOC content and due to the admixing of mineral waters a relatively high sulfate concentration and conductivity. Our study shows that the exceptional environmental conditions provoke a decrease in diversity and favor the occurrence of anaerobic, acidophilic taxa, whereby sulfate reduction and methanogenesis become distinct processes. However, the deeper mofette sediments alone provide strictly anaerobic conditions, and accordingly, two distinct community clusters were found at different depth intervals. Electron acceptors such as CO_2 and sulfate are provided by the permanently ascending fluid which is admixed with deep thermal waters, thereby forming a kind of anoxic deep biosphere habitat close to the surface level. Hydrogen, originating from deep fissured granites may thereby function as an electron donor. This study is limited to taxonomical assignments, further studies focusing on deep mofette sediments should implement metagenomic or

transcriptomic approaches to unravel the functional repertoire of the communities.

2.7 Acknowledgment

QL gratefully acknowledges financial support from the China Scholarship Council. The authors would like to thank André Friese and Axel Kitte (GFZ German Research Centre for Geosciences) for their guidance and assistance with anion/cation measurements. Special thanks to Oliver Burckhardt and Axel Kitte (GFZ German Research Centre for Geosciences) for their valuable help during the sampling campaigns and support in the lab.

3 Microbial signatures from a deep saline CO_2-saturated aquifer of the Hartoušov mofette system (Eger Rift, NW Czech Republic)

3.1 Abstract

The Hartoušov mofette system is a natural CO_2 degassing site located in the central Cheb Basin (Eger Rift, Central Europe). In early 2016 a 108 m deep borehole was drilled into this system to investigate the impact of ascending geogenic CO_2 on the indigenous deep microbial communities and their surrounding life habitat. During drilling a CO_2 blow out occurred at a depth of 78.5 meters below surface (mbs) suggesting a CO_2 reservoir related to a deep low-permeable CO_2-saturated saline aquifer at the transition from Early Miocene terrestrial to lacustrine sediments. Past microbial communities were investigated by hopanoids and glycerol dialkyl glycerol tetraethers (GDGTs) reflecting rather the environmental conditions during the time of deposition than showing a signal of the current deep biosphere. The composition and distribution of the deep microbial community potentially influenced by the upward migration of CO_2 starting during Late Pleistocene time were investigated by intact polar lipid (IPL), quantitative polymerase chain reaction (PCR) and deoxyribonucleic acid (DNA) analysis. The deep biosphere is characterized by a similar abundance and diversity independent from the lithology over the entire investigated depth profile suggesting an overall impact of the ascending CO_2-saturated groundwater on the microbial community structure. The results revealed that a high relative abundance of *Acidovorax* and *Aquabacterium* as well as specialized members of unknown and uncultured genera within the family *Comamonadaceae* are indicative for CO_2-dominated environments. A set of new IPLs are suggested to be indicative for microorganisms associated with CO_2 accumulation in the mofette system.

3.2 Introduction

The Hartoušov mofette system is located in the center of the Cheb Basin (Eger Rift) at the central part of the Počatky-Plesná Fault Zone (PPZ) (Bankwitz et al., 2003a; Bankwitz et al., 2003b; Flechsig et al., 2008)(**Figure 1A**). The region is known for periodically occurring earthquake swarms and widely distributed natural cold gas exhalation systems in form of mofette sites and mineral water springs releasing CO_2-rich gas into the atmosphere (Fischer et al., 2014). The CO_2 originates from active magma chambers at the crust-mantle boundary and at lithospheric mantle depths of about 65km depth. The CO_2 preferentially migrates as a component of supercritical fluids in the lower crust or either dissolved in water or as a free gas phase along deep-seated faults in the upper crust to the surface (Weinlich et al., 1999; Weise et al., 2001; K. Bräuer et al., 2011; Kämpf et al., 2019). Both, the PPZ and the Hartoušov mofette system started to develop in the Late Pleistocene (Bankwitz et al., 2003a; Bankwitz et al., 2003b).

Previous investigations from sediments of the upper 9 m at the Hartoušov mofette system revealed that ascending CO_2-containing fluids cause sediment fluidization, hydrofracturing and geochemical alterations e.g. sediment bleaching, mobilization of metals and the preservation of organic matter (Flechsig et al., 2008; Rennert et al., 2011; Mehlhorn et al., 2016; Rennert and Pfanz, 2016; Bussert et al., 2017; Liu et al., 2018; Mehlhorn et al., 2018). At the surface, CO_2 exhalation occurs in form of diffuse degassing structures (DDS, namely dry mofettes) and localized water-filled, pool-like structures (wet mofettes) (Flechsig et al., 2008; Kämpf et al., 2013; Nickschick et al., 2015; Nickschick et al., 2017; Kämpf et al., 2019).

Dry mofette areas display high CO_2 soil gas concentrations, low soil pH, accelerated silicate weathering, leaching of base cations, anomalous vegetation patterns, low taxonomic and functional biodiversity of soil biota and limited microbial degradation of soil organic matter (SOM) (Rennert et al., 2011; Hohberg et al., 2015; Rennert and Pfanz, 2016; Kämpf et al., 2019). In comparison to reference sites, the microbial community obviously differs in composition and is dominated by anaerobic

chemolithoautotrophic microorganisms, e.g. acidophilic, methanogenic and sulfur-cycling organisms (Beulig et al., 2015; Beulig et al., 2016; Liu et al., 2018). Additionally, a higher microbial abundance was observed even in deeper parts of the sedimentological profile (Liu et al., 2018) and estimates for microbial fixation of ascending geogenic CO_2 reach up to 27 % of the total SOM (Nowak et al., 2015). Similar characteristics were also found at other mofette sites, e.g. the Laacher See in Germany (Krüger et al., 2009; Frerichs et al., 2013), the Latera caldera in Italy (Oppermann et al., 2010) and the Stavešinci mofette in Slovenia (Šibanc et al., 2014). Hydrogeochemical investigations of waters from wet mofettes and mineral springs in the Cheb Basin by Krauze et al. (2017) and in the adjacencies (Wagner et al., 2007; Schuessler et al., 2016) unraveled different water sources with surface water being co-sourced by a deep saline aquifer at some locations. The microbial communities in all of these CO_2-influenced waters were generally dominated by chemolithoautotrophic microorganisms (iron- and sulfur-cycling organisms) and methanogenic archaea. Similar to dry mofettes, the microbial degradation of complex dissolved organic carbon (DOC) is also restricted in these anaerobic environments (Krauze et al., 2017) suggesting that upstreaming CO_2 is one of the main carbon sources for microorganisms as well. The connection to a deep saline aquifer at some mofettes (e.g., Bublak, approximately 1.5 km NNE of the Hartoušov mofette) was indicated by the occurrence of specialists from the deep subsurface biosphere and marine paleoenvironments pointing to a broadly distributed deep saline aquifer as a general deep microbial habitat in this region (Krauze et al., 2017).

Subsequently, further deep biosphere habitats may exist related to CO_2 reservoirs in geological trapping structures indicated by an increase in gas flow rates after swarm earthquakes pointing to a gas release after seismically induced fracking of sealing layers (Sandig et al., 2014; Sauer et al., 2014; Schuessler et al., 2016; Fischer et al., 2017). Moreover, Bräuer et al. (2005) described dm- to m-sized cavities in sediments of the nearby open-cast mine Nová Ves II at 50 mbs (meter below surface) which developed along fluid migration pathways. This suggests the presence of restricted gas-filled cavities potentially acting as distinct habitats for the deep biosphere. An important hint

for a CO_2-related deep biosphere was recognized by Bräuer et al. (2005) after the swarm earthquake activity in 2000. They detected an increase in methane concentrations at the Wettinquelle (Bad Brambach, Germany) about 20 km north of the Hartoušov mofette system with a significant decrease of $\delta^{13}C_{methane}$ attributed to microbial methane production from magmatic CO_2 and pre- or co-seismically released hydrogen from the granitic basement. Similarly, higher methane concentrations were detected at the Bublak mofette after the swarm event in 2011 (Bräuer et al., 2018).

These previous investigations show that ascending geogenic CO_2-containing fluids locally alter the sedimentary overburden and thus change the environmental conditions for microbial life. Additionally, there are indications for subsurface structures that may harbor CO_2-influenced deep microbial habitats which could act as deep microbial hotspots. However, studies investigating the potential for CO_2-related deep microbial life in the Cheb Basin and the Eger Rift are still missing. Thus, in early 2016 a 108.5 m deep borehole was drilled by the German Research Centre for Geosciences (GFZ) as a test case for the International Continental Scientific Drilling Program (ICDP) project "*Drilling the Eger Rift"* (Dahm et al., 2013). The borehole was positioned in the Hartoušov mofette system (HJB-1) (50°07′58″N, 12°27′46″E) and described in detail by Bussert et al. (2017). During drilling, CO_2-rich sediments were recovered between 71 and 81 mbs. At a depth of 78.5 mbs, a CO_2 blow out occurred suggesting the penetration of a subsurface CO_2 accumulation. This CO_2 reservoir is related to a basal low-permeable CO_2-saturated and saline aquifer (1892 mg L^{-1} of free dissolved CO_2) that occurs between 79 and 85 mbs at the transition from Early Miocene terrestrial to overlying lacustrine sediments. Hydrogeochemically, the aquifer is characterized by Na-Ca-HCO_3-SO_4-type water with a high Fe content of up to 13.7 mg L^{-1} and a pH of 6.4 (Bussert et al., 2017). Due to the potential of the CO_2–saturated aquifer to harbor a very specialized microbial community we focussed on the core interval between 65 and 95 mbs. Thereby, we aimed to identify the impact of geogenic CO_2 on deep microbial communities and to figure out whether the low-permeable CO_2-saturated and saline aquifer might act as a hotspot for active and abundant deep microbial life. The methodological approach to characterize the microbial community included lipid

biomarker analysis of past and living microbial biomass (hopanoids, GDGTs and intact polar lipids) as well as DNA analysis such as quantitative Polymerase Chain Reaction (qPCR) and Illumina 16S rRNA gene amplicon sequencing. Furthermore, the microbial signals were compared to lithological background information and sedimentological bulk parameters.

3.3 Methods

3.3.1 Drilling, coring and pump test

A detailed description of the fieldwork including drilling, coring and a pump test was published by Bussert et al. (2017). The drilling was performed with a Drillmec G-25 device installed on a Tatra 815 drilling lorry and discovered core material in PVC liners with a length of 3 m and a diameter of 0.1 m. The drilling mud consisted of homogeneously blended pure bentonite. Fluorescein was added as a tracer to monitor potential drill mud contamination of the retrieved core material according to Pellizzari et al. (2013). Subsamples for further analysis were taken about every 0.5 m and stored in gasbags flushed with nitrogen at -80 °C directly after core recovery in the field. After the drilling campaign, a 24-hour pump test within the deep low-permeable CO_2-saturated saline aquifer was performed. The groundwater was filtered, the obtained water samples geochemically analyzed and the obtained filters were stored at -20 °C, respectively.

The initial lithological description of the sample material and the drill mud contamination control were performed in the lab. The frozen core segments were stored overnight at 5 °C to initiate the thawing of the external sample layer and to avoid fluid migration from the rim to the center of the samples. The thawed rim (approx. 1 cm) was removed (inner coring), the still frozen inner core described (e.g. in **Supplementary Figure S1**), material from the removed rim (outer rim) tested in triplicates for fluorescein (Pellizzari et al., 2013) and the samples again stored at –80 °C. To ensure that the samples are not contaminated by external DNA the inner coring technique was

repeated in a clean bench (Thermo Scientific, Waltham, USA). The removed material and the outside of the inner core were again tested in triplicates for fluorescein (inner rim). Inner core samples (sample) exceeding the background fluorescence were excluded from further analysis (**Supplementary Figure S1**). The fluorescein concentration was measured with a CLARIO star® plate reader (BMG LABTECH GmbH, Ortenberg, Germany). The background fluorescence signal was obtained from samples of a shallow drilling campaign (3 m) drilled in 2015 adjacent to our study side without the application of drill mud and fluorescein (Liu et al., 2018).

3.3.2 Bulk carbon and nitrogen analyses

Total carbon (TC), total organic carbon (TOC), total nitrogen (TN) and the bulk $\delta^{13}C_{org}$ were all analyzed with the same equipment consisting of a NC2500 Carlo Erba elemental analyzer coupled with a ConFlo_III interface on a DELTAplusXL isotope ratio mass spectrometer (IRMS) (Thermo Fischer Scientific). Prior to analysis, the sample material was freeze-dried, powdered and homogenized. In order to determine the TC and TN approximately 25 mg of sample material was loaded into tin capsules and the content was calibrated against acetanilide. For the investigation of TOC and bulk $\delta^{13}C_{org}$ the carbonate content was removed using in situ decalcification. Therefore, around 3 mg sample material was loaded into Ag-capsules and decalcified by drops of 3 % HCl followed by 20 % HCl and heated for 3 h at 75 °C. The calibration was performed using elemental urea and certified isotope standards (USGS24, IAEA-CH-7) and proofed with an internal soil reference sample (Boden3, HEKATECH). All isotope compositions are given relative to the VPDB (Vienna Pee Dee Belemnite) standard in the conventional delta notation. The total inorganic carbon (TIC) was calculated by subtraction of TOC from TC.

3.3.3 Lipid biomarker extraction and chromatographic column separation

The freeze-dried, powdered and homogenized sediment samples (about 80 g) were extracted with a modified extraction method after Bligh and Dyer (1959) using methanol:dichloromethane (DCM):ammonium acetate buffer (pH 7.5) (2:1:0.8) as extraction solvent mixture. The sample material was centrifuged for 10 min with 2500 rpm. The supernatant was transferred to a separation funnel and the solvent ratio changed to 1:1:0.9 (methanol:DCM:ammonium acetate buffer) to achieve phase separation. Afterward, the organic phase containing the lipid extract was collected in a turbovap glas and the solvent was removed (TurboVap 500). Each fifth sample was a blank. After extraction 5α-Androstane and deuterium-labeled phosphatidylcholine (PC_{d54} = 1,2-dimyristoyl-d54-sn-glycerol-3-phosphocholine) were added as standards for compound quantification in the aliphatic and intact polar lipid fractions, respectively. The obtained total extracts were chromatographically separated into a low polar lipid (20 ml chloroform), free fatty acid (50 ml methyl formiate with 0.025 % glacial acetic acid), glycolipid (20 ml acetone) and intact polar lipid (IPLs, 25 ml methanol) fraction using two glass syringe columns filled with dried pure silica (1 g silica gel 63–200 µm, dried at 110 °C for 2 h) and Florisil (1 g magnesium silica gel 150–250 µm) with the silica column on top of the Florisil column. The IPL fraction was only eluted from the silica column (Zink and Mangelsdorf, 2004). To improve IPL recovery the silica column was eluted with 25 ml methanol:water (60:40) for a second time. Phase separation was conducted as described above. Finally, the IPL fractions were combined and the solvent was removed. Afterward, the IPL fraction was split into two halves: one for the direct detection of IPLs and one for the detection of polar lipid fatty acids (PLFAs) after saponification (Müller et al., 1993).

After removal of asphaltenes, the low polar lipid fraction was further subdivided by Medium Pressure Liquid Chromatography (MPLC) into an aliphatic, aromatic and NSO fraction (Radke et al., 1980). The aliphatic fraction was analyzed for hopanoids and the

NSO fraction for glycerol dialkyl glycerol tetraethers (GDGTs). GDGTs have been quantified as an external archaeol standard.

3.3.4 Determination of the lipid biomarkers

Analysis of IPLs was performed on a Thermo Scientific Ultimate 3000 RS Ultra high performance liquid chromatography (UHPLC) coupled to a Q Exactive Plus Orbitrap mass spectrometer (MS) with a heated electrospray (H-ESI II) probe. Samples were separated with a LiChrospher 100 diol column (2x125 mm, 5 µm; CS-Chromatographie Service) equipped with a pre-column filter. The eluents used for compound separation were (A) *n*-hexane:isopropanol:formic acid:ammonia (25 % in water) 79:20:1.2:0.04 v/v and (B) isopropanol:water:formic acid:ammonia (25 % in water) 88:10:1.2:0.04 v/v (solvent gradients: 1 min 100 % A, linear increase of B to 65 % within 20 min and 40 min for reconditioning). The flow rate was set to 0.35 ml/min (modified after Rütters et al., 2001). ESI source conditions were as follows: spray voltage -2.2 kV; capillary temperature 300 °C; nitrogen sheath gas at 49 and auxiliary gas at 12 arbitrary units at a temperature of 419 °C, S-Lens 65 V. The obtained data were acquired in negative and positive ion mode with dependent MS/MS acquisition at ranges of m/z 400 to 2000. The full scan and fragment spectra were collected at a resolution of 280 000 and 70 000 (at m/z 200), respectively.

The aliphatic fraction and PLFAs were determined on a Thermo Trace GC Ultra equipped with a Thermo PTV injection system and an SGE BPX5 fused silica capillary column (50 m length, 0.22 mm ID, 0.25 µm film thickness) coupled to a Thermo Trace DSQ Quadrupole MS. Helium was used as carrier gas. The temperature of the GC oven was programmed from 50 °C (hold 1 min) to 310 °C at a rate of 3 °C min^{-1}, followed by an isothermal phase of 30 min. The injector temperature was programmed from 50 to 300 °C at a rate of 10 °C s^{-1}. The MS was operated in electron impact ionization mode (EI) at 70 eV. Full scan mass spectra for compound identification were recorded from m/z 50 to 600 at a scan rate of 1.5 scans s^{-1}.

GDGT analysis was conducted on a Shimadzu LC10AD HPLC instrument coupled to a Finnigan Triple Stage Quadrupol (TSQ) 7000 MS with an atmospheric pressure chemical ionization (APCI) interface. Samples were separated at 30 °C with a Prevail Cyano column (2.1x150 mm, 3 µm; Alltech) equipped with a pre-column filter. The mobile phase consisted of (A) *n*-hexane and (B) isopropanol and compound separation was achieved using the following solvent gradients: 5 min 99 % A and 1 % B, linear gradient to 1.8 % B within 40 min, increase to 10 % B within 1 min and holding time for 5 min to clean the column, back to initial solvent conditions within 1 min and 16 min for column equilibration (Schouten et al., 2007). The flow rate was set to 200 µl min^{-1}. The APCI adjustments were: corona current 5 µA giving a voltage of around 5 kV, vaporizer temperature 350 °C, capillary temperature 200 °C and nitrogen sheath gas at 60 psi (no auxiliary gas). Mass spectra were generated by selected ion monitoring in the positive ion mode for the masses 1295.0, 1302.1, 1049.5, 1035.5, 1021.5 and 654.2 each with a width of 7 amu (to also obtain neighboring masses) at a scan rate of 0.33 s.

Compound specific $\delta^{13}C$ values of the aliphatic fraction (hopanoids) were determined with a GC-isotope ratio monitoring (IR)-MS system consisting of an Agilent 7890 GC (USA) connected with an open split GC-C/TCIII-Interface for compound-specific carbon and hydrogen isotope analysis to a Delta V Plus IRMS (Thermo Fischer Scientific, Germany). The GC-separated organic substances were oxidized to CO_2 in a combustion furnace at a temperature of 940 °C on a CuO/Ni/Pt catalyst. CO_2 was transferred to the mass spectrometer to determine carbon isotope ratios. 3 µL of the aliphatic fraction was injected with a split ratio of 1:2 and an initial temperature of 230 °C to a programmable temperature vaporization inlet (PTV, Agilent Technology, USA). The injector was heated to 300 °C with a heating rate of 12 °C s^{-1}. The separation of the aliphatic fractions was attained by a fused silica capillary column (HP Ultra 1, 50 m x 0.2 mm ID, 0.33 µm FT, Agilent Technology, Germany) with a temperature program starting from 40 °C to 300 °C, with a heating rate of 4 °C min^{-1} and the maximum temperature held for 45 min. The carrier gas was Helium with a flow rate of 1.0 ml min^{-1}. All samples were measured in triplicates with a usual standard deviation of ≤0.5 ‰. The quality of the results was checked by measuring *n*-alkane standards (*n*-

C_{15}, *n*-C_{20}, *n*-C_{25}) with the known isotopic composition (Campro Scientific, Germany). Isotopic compositions are given in the delta notation relative to the Vienna Pee Dee Belemnite (VPDB) standard.

3.3.5 DNA extraction and purification

Due to the extremely low amount of biomass in the core samples, 10 g of powdered sample material was used to extract the total genomic DNA with the DNeasy® PowerMax® Soil Kit (QIAGEN, Venlo, Netherlands). Afterward, the obtained DNA was dissolved in 5 ml of DNA-free water (Carl Roth, Karlsruhe, Germany). For each sampling depth, three independent samples were taken from different positions of the core horizon as technical triplicate. The 5 ml DNA solution was concentrated to 100 µL by an Eppendorf Concentrator Plus (Eppendorf AG, Hamburg, Germany). The Genomic DNA Clean & Concentrator™-10 (Zymo Research, Irvine, CA) was utilized to remove humic acids and other substances that may inhibit the polymerase chain reaction (PCR). Three DNA extractions were done from separated sample triplicates. DNA from 1 mL DNA-free water (Carl Roth, Karlsruhe, Germany) was extracted as a negative control.

In addition to the core material, approximately 1 L of the fluid samples from the pump test were filtered (0.2 µm) to collect insoluble particles. The total genomic DNA trapped on the filters was extracted by the FastDNA™ SPIN Kit for Soil and the FastPrep® Instrument (MP Biomedicals, Santa Ana, CA) with standard protocols. The FastPrep® Instrument homogenizing time and the homogenizing speed were modified to 30 s and 5.5 m s^{-1} according to Liu et al. (2018).

3.3.6 Quantitative PCR

The bacterial 16S rRNA gene copies were determined by a quantitative polymerase chain reaction (qPCR) to reveal the total bacterial abundance. The qPCR Master Mix

consisted of 10 µl SYBR® FAST qPCR Master Mix (2X) Universal (KAPA Biosystems, Wilmington, Massachusetts, USA), 5.92 µl PCR water, 0.04 µl forward primer (100 µM), 0.04 µl reverse primer (100 µM), and 4 µl template. The quantification of the bacterial 16S rRNA gene was based on the primer pair 341F (5'- CCTACGGGAGGCAGCAG -3') and 534R (5'- ATTACCGCGGCTGCTGG -3') (Degelmann et al., 2010). The qPCR was programmed as 3 min at 95 °C, 40 cycles of 3 s at 95 °C, 20 s at 60 °C, 30 s at 72 °C, and 3 s at 80 °C for the plate read. A cloned 16S rRNA gene fragment from *Escherichia coli* was used as standard. The qPCR was conducted on a CFX96 real-time thermal cycler (Bio-Rad Laboratories Inc., USA) and the analysis of the quantification data was performed with the CFX Manager™ software (Bio-Rad Laboratories Inc., USA). The concentration range of the standard was optimized and set from 10^3 to 10^7 16S rRNA gene copies. The R^2-value of the standard curve line was 0.994 to 0.997.

3.3.7 Illumina MiSeq amplicon sequencing

The 16S rRNA gene was amplified with OptiTaq™ polymerase (Roboklon, Berlin, Germany) which has a proofreading capability due to the extremely low concentration of extracted total genomic DNA. The PCR reaction solution consisted of 2.5 µl10x Buffer Pol C, 0.125 µl OptiTaq™ polymerase, 1 µl dNTP Mix (5 mM each), 1 µl $MgCl_2$ (25 mM), 17.075 µl PCR water, 0.3 µl bovine serum albumin, 0.25 µl forward primer (20 µM), 0.25 µl reverse primer (20 µM) and 2.5 µl template. Unique combinations of barcode-tagged 515F (5'- GTGCCAGCMGCCGCGGTAA -3') and 806R (5'- GGACTACHVGGGTWTCTAAT -3') (Caporaso et al., 2011) primers were assigned to each sample. The amplifications were performed on a T100™ thermal cycler (Bio-Rad Laboratories Inc., USA). The PCR program was 5 min at 95 °C, 35 cycles of 30 s at 95 °C, 45 s at 56 °C, 60 s at 72 °C and a final extension step of 7 min at 72 °C. A cloned 16S rRNA gene fragment from *E. coli* was used as the positive control. The PCR products were cleaned up with AMPure XP magnetic beads (Beckman Coulter GmbH, Krefeld, Germany). After measuring the DNA concentration with a CLARIO star® plate reader (BMG LABTECH GmbH, Ortenberg, Germany)

PCR products were pooled in equimolar amounts. The pooled DNA solution was concentrated with Eppendorf Concentrator plus (Eppendorf AG, Hamburg, Germany) to meet the requirement of the Illumina MiSeq high-throughput sequencing. The final pooled DNA concentration was 77.05 ng μl^{-1}.

3.3.8 Bioinformatics and statistical analysis

Sequencing was performed by Eurofins Scientific SE (Luxembourg) on an Illumina MiSeq (2 x 250 bp). Dual-indexed reads were demultiplexed using CutAdapt (Martin, 2011) allowing for 10 % errors in the primer and no errors in the barcodes. Read pairs were merged using PEAR (Zhang et al., 2014) and trimmed using Trimmomatic (Bolger et al., 2014). The orientation of the target sequences was standardized using the information obtained from demultiplexing. The QIIME-pipeline (Version 1.9.1) (Caporaso et al., 2010) was employed for OTU clustering and taxonomic assignment. More specifically, USEARCH (Edgar, 2010) was used for the removal of chimeric sequences and open-reference OTU clustering (97 %). The SILVA database (Version 128) (DeSantis et al., 2006) was the reference database for chimera removal, OTU clustering and taxonomic assignment. Singletons and OTUs assigned to chloroplasts and mitochondria were removed from the obtained OTU table. After the filtering processes, 11,063,679 sequences were obtained in the 16S rRNA gene library in total. The read numbers ranged between 11,446 and 296,694 with a mean value of 112,895. Due to its presence in the negative control, *Undibacterium* was treated as contamination and removed from the library before further analyses. The alpha diversity was estimated by using the Shannon H and Shannon EH indices. Beta diversity was determined by the non-metric multidimensional scaling (NMDS) with PAST3 (Hammer et al., 2001). Sequencing data were submitted to the European Nucleotide Archive (http://www.ebi.ac.uk/ena) under accession numbers PRJEB22478 (ERS4382097 to ERS4382146 and ERS4382395 to ERS4382400).

3.4 Results

3.4.1 Stratigraphy and sample material

The core section between 65 and 95 mbs depth was lithologically composed of three different units which were from bottom to the top: i) a weathered Paleozoic mica schist (95 – 91.5 mbs, Paleozoic basement), ii) sandy to peaty Early Miocene mudstones of the Main Seam Formation (Fm.) with lignite fragments and root structures suggesting paleo-soil horizons in the lower and upper sections (91.5 – 78.5 mbs) and iii) laminated, calcareous, sandy or peaty Early Miocene mudstones interbedded with bioclastic carbonates, dolomite beds and gypsum layers of lacustrine origin (78.5 – 65 mbs) belonging to the Cypris Fm. (**Figure 8a**) (Bussert et al., 2017). Identified macrofossils in the Cypris Fm. were bark fragments, seeds, plant debris and ostracod shells (**Figure 8a** and **Supplementary Figure S1**). Both sediments, Main Seam and Cypris Fm. revealed vein-like structures indicating CO_2 ascending pathways with potentially mineral alteration and precipitation. These features were siderite-rich veins and bubble structures in the Main Seam Fm. and small fractures, dykes and sills with sediment color changes in the Cypris Fm. The CO_2 blow out during the drilling campaign occurred at the transition from the Cypris Fm. to the underlying Main Seam Fm. This indicates that a carbonate layer (about 30 cm thick) found at this transition or the lacustrine sediments itself act as a sealing layer for the low-permeable CO_2-saturated saline aquifer in the upper Main Seam Fm. resulting in a zone characterized by a high CO_2 pore pressure (**Figure 8a**).

3.4.2 Bulk carbon and nitrogen

Carbonates were detected in all three lithological units expressed as total inorganic carbon (TIC) (**Figure 8b**). In the Paleozoic basement and the Main Seam Fm. the carbonates were dominated by zoned siderite spheres and veins that could have been precipitated from the low-permeable CO_2-saturated saline aquifer. At the transition from the Main Seam Fm. to the Cypris Fm. carbonates were essentially absent except

for the thick (30 cm) carbonate layer at 78.5 mbs. In the Cypris Fm. calcite predominated pointing to an origin from the lacustrine environment which was supported by the finding of ostracod shells.

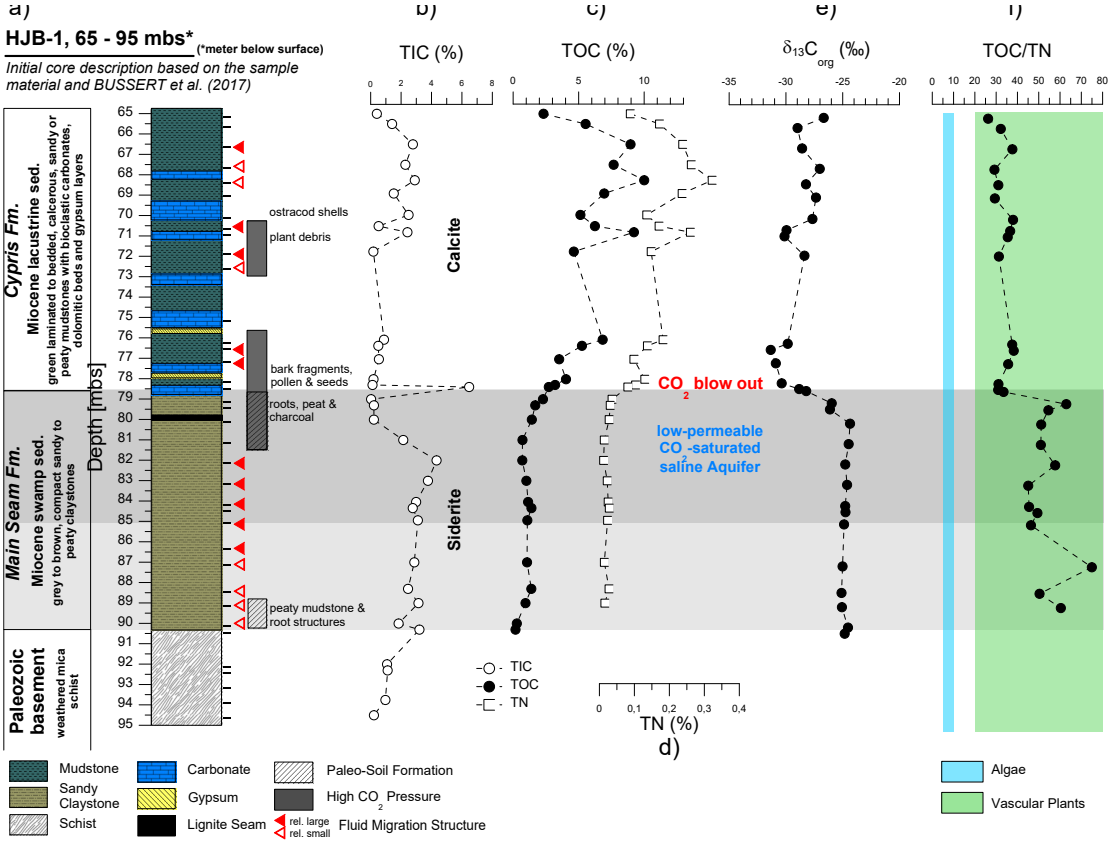

Figure 8 a) Stratigraphical and lithological description of the Hartoušov mofette core HJB-1 (2016) between 65 and 95 mbs based on visual inspection of the sample material and data from Bussert et al. (2017). Depth profiles of bulk sedimentological parameters showing b) total inorganic carbon (TIC), c) total organic carbon (TOC), d) total nitrogen (TN), e) bulk $\delta^{13}C_{org}$ and f) the TOC/TN ratio.

Organic matter was not detected in the Paleozoic basement. TOC contents of the Main Seam Fm. ranged between 0.2 % and 2.3 %. After a small increase, the TOC contents remained relatively constant at ca. 1 % before increasing to 2.3 % at the top of the Main Seam Fm. (**Figure 8c**). In the overlying lacustrine Cypris Fm. the TOC contents were significantly higher and show strong fluctuations between 2.3 % and 10 %. Bulk $\delta^{13}C_{org}$ data also changed with the lithological transition from the Main Seam to the Cypris Fm.

showing relative constant values around -24 ‰ in most parts of the Main Seam Fm. and a strong decrease down to -30 ‰ at the top (**Figure 8e**). In the Cypris Fm. the organic carbon isotope signals fluctuate between -31 ‰ and -27 ‰.

The total nitrogen content (TN, **Figure 8d**) was mainly positively correlated with the TOC content (R^2 = 0.98). Values were low in the Main Seam Fm. ranging between 0.01 % and 0.04 % and increase at the top. In the Cypris Fm. TN values were significantly higher ranging between 0.08 % and 0.32 %. The TOC/TN ratio ranged in the Main Seam Fm. between 45 and 75 and in the Cypris Fm. between 26 and 41 (**Figure 8f**).

3.4.3 Microbial biomarker signals

Hopanoids, representing membrane regidifiers and ordering components in bacterial cell membranes (Sáenz et al., 2015), could be detected as unsaturated hopenes (22,23,30-trisnor-17(21)-ene, 30-norhop-17(21)-ene, hop-17(21)-ene, neohop-13(18)-ene) and saturated hopanes with the steric 17β(H), 21β(H)-, 17β(H), 21α(H)- and 17α(H)β(H)-configuration (ββ–C_{27}, ββ–C_{29}, βα–C_{29}, ββ–C_{30}, αβ–C_{30}, ββ–C_{31}, βα–C_{31}, αβ–C_{31}R, αβ–C_{31}S) (**Figure 9b**). In the Paleozoic basement, hopanoids were essentially absent. In the Main Seam Fm. the hopanoid signal was usually low and dominated by the αβ-C_{31}R-hopane. However, at the top to the Main Seam Fm. the hopanoid concentrations especially the αβ-C_{31}R signal distinctly increased to the highest values in the entire investigated core interval (**Figure 9b**). In the Cypris Fm., hopanoids were generally more abundant than in the Main Seam Fm. (with exception of the top part) and hop-17(21)-ene supplemented by ββ-hopanes were the predominating hopanoid compounds (**Figure 9b**). The $\delta^{13}C_{hopanoid}$ values in the Main Seam Fm. plotted in a range between -22 ‰ and -37 ‰ and shifted to significantly lower values between -42 ‰ and -60 ‰ in the Cypris Fm. (**Figure 9c**).

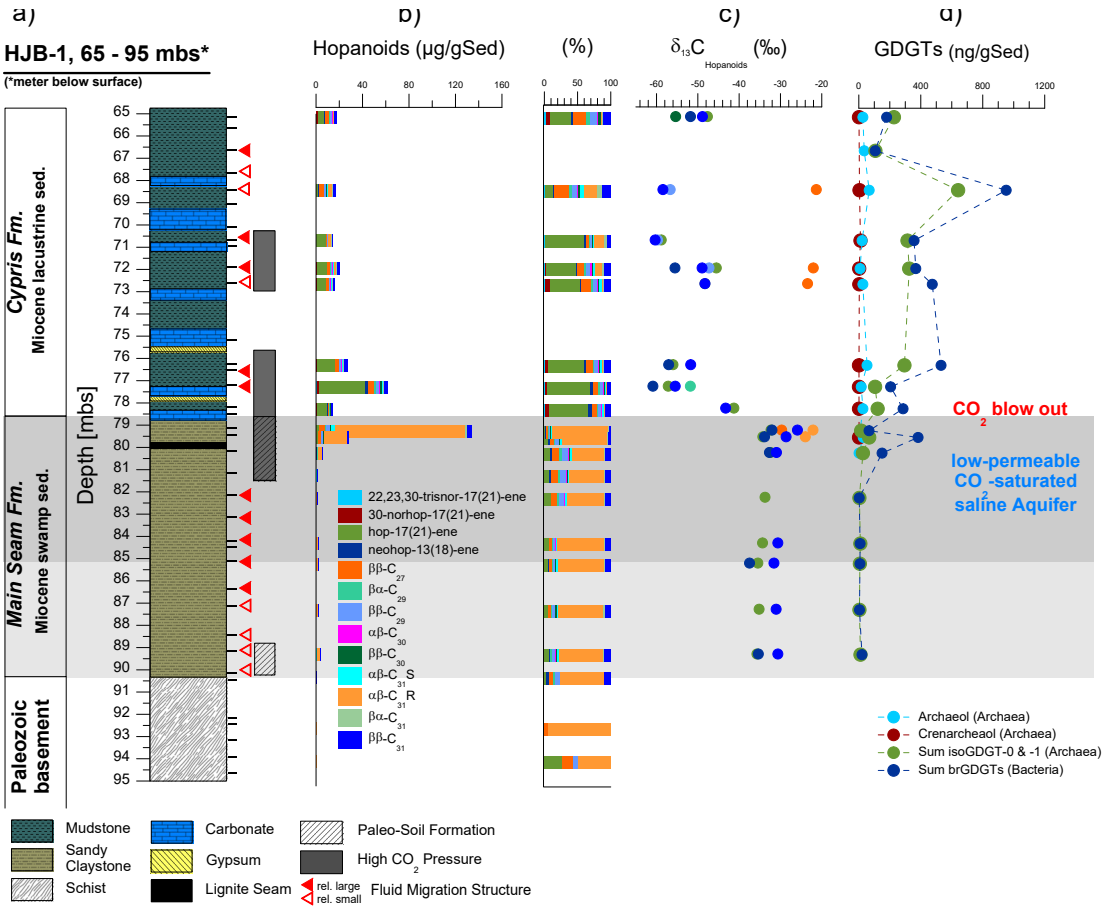

Figure 9 a) Stratigraphical and lithological description of the Hartoušov mofette core HJB-1 (2016) and depth profiles of b) the hopanoid distribution and its relative abundance (%), c) $^{13}C_{hopanoids}$ of different hopanoids and d) archaeol, crenarchaeol, the sum of isoGDGTs-0 and isoGDGTs-1 and the sum of all branched GDGTs.

GDGTs are known to derive from membrane lipids of soil bacteria (branched (br)GDGTs) and aquatic archaea (isoprenoid (iso)GDGTs) (Schouten et al., 2013). Both GDGT types were absent in the basement and occurred at low concentrations with similar proportions (1 to 20 ng $gSed^{-1}$) in most parts of the Main Seam Fm. (**Figure 9d**). At the top of the Main Seam Fm. branched GDGTs significantly increased to 382 ng $gSed^{-1}$. Subsequently, the highest relative concentrations of branched GDGTs and isoprenoid GDGT-0 and -1 occurred in the Cypris Fm. ranging between 100 and 950 ng $gSed^{-1}$. Archaeol and Crenarchaeol showed low concentrations (0.5 to 11 ng $gSed^{-1}$ and 1.5 to 67 ng $gSed^{-1}$) and only appeared at the top of the Main Seam Fm. and in the Cypris Fm. (**Figure 9d**).

In contrast to the hopanoids and GDGTs both representing past microbial biomass, intact polar lipids (IPLs) provide information on present microorganisms, since these biomarkers are only stable in living microbes over longer periods (White et al., 1979; Zink et al., 2003). The chromatogram of IPLs revealed no common phospholipids, but a double peak which represented to the best of our knowledge two yet unknown lipid compound groups. These groups were tentatively referred to as compound group A and B (**Figure 10a**). The mass spectra of these two compound groups showed a cluster of six individual mass peaks with a maximum at m/z 631 or 617, respectively (**Figure 10b and 10c**). The masses differed by 14 mass units indicating an increase of the lipid side chain length by a CH_2-group. The individual masses of the two compound groups were essentially the same indicating the same elemental composition. This and the close vicinity of the chromatographic signals suggested that these compounds bear the same head group but show different configurations in their side chains (e.g. OH-group vs. ether-group), causing slightly different elution behaviors. Microbial membrane lipids usually consist of a polar head group and two long-chain ether or ester side chains linked to a glycerol backbone (Mangelsdorf et al., 2019). To elucidate whether ester bond fatty acids formed the lipid side chains, MS-MS and saponification experiments (polar lipid fatty acid (PLFA) analysis) were conducted indicating that the side chains are not ester bound fatty acids and that alkyl and ether bound side chains are more likely. The Orbitrap MS allowed high-resolution analysis of the unknown compounds resulting in a proposed elemental formula. This together with the isotope patterns of the individual molecular masses indicated the presence of sulfur (^{34}S-isotope) presumably a sulfonic acid (R-SO_2-OH) as the head group part. An example for the suggested lipid structure for the mass peak at 617 m/z within compound group A is shown in **Figure 10d** and further experiments have to be conducted to determine the full structure of compound groups A and B.

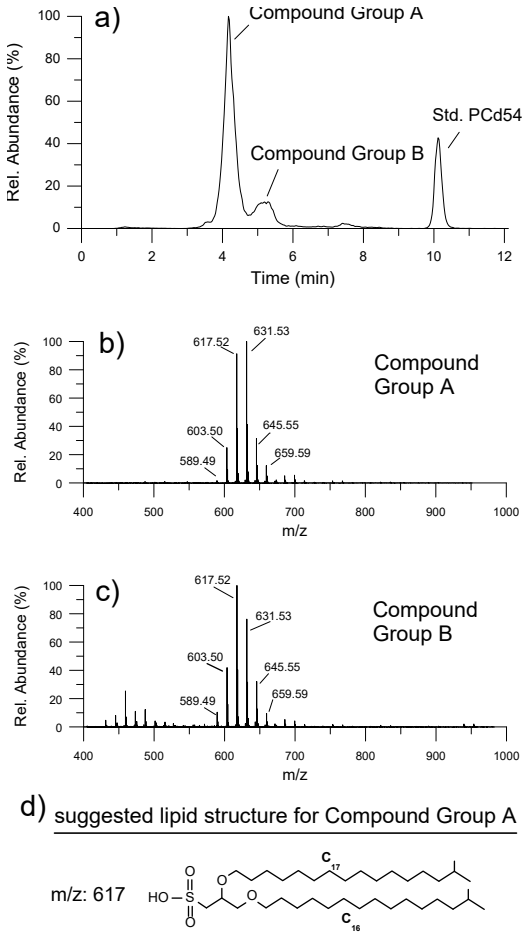

Figure 10 a) HPLC chromatogram of two yet unknown groups of intact polar lipids (IPLs) referred to as compound group A and B. The associated mass spectra b) and c) show both a cluster of six individual mass peaks differing by 14 mass units with a maximum at m/z 631 or 617, respectively. d) Suggested lipid structure for the mass peak at m/z 617 of compound A.

Both lipid groups were almost absent in the basement and Main Seam Fm. (0 – 7.6 µg/gSed; **Figure 11g**). However, they showed their highest abundance (475.2 µg/gSed) at the top of the Main Seam Fm. with its high CO_2 pressure. In the Cypris Fm. the signal decreased significantly again but was still a bit higher in CO_2 influenced core intervals (up to 116 µg/gSed; **Figure 11g**).

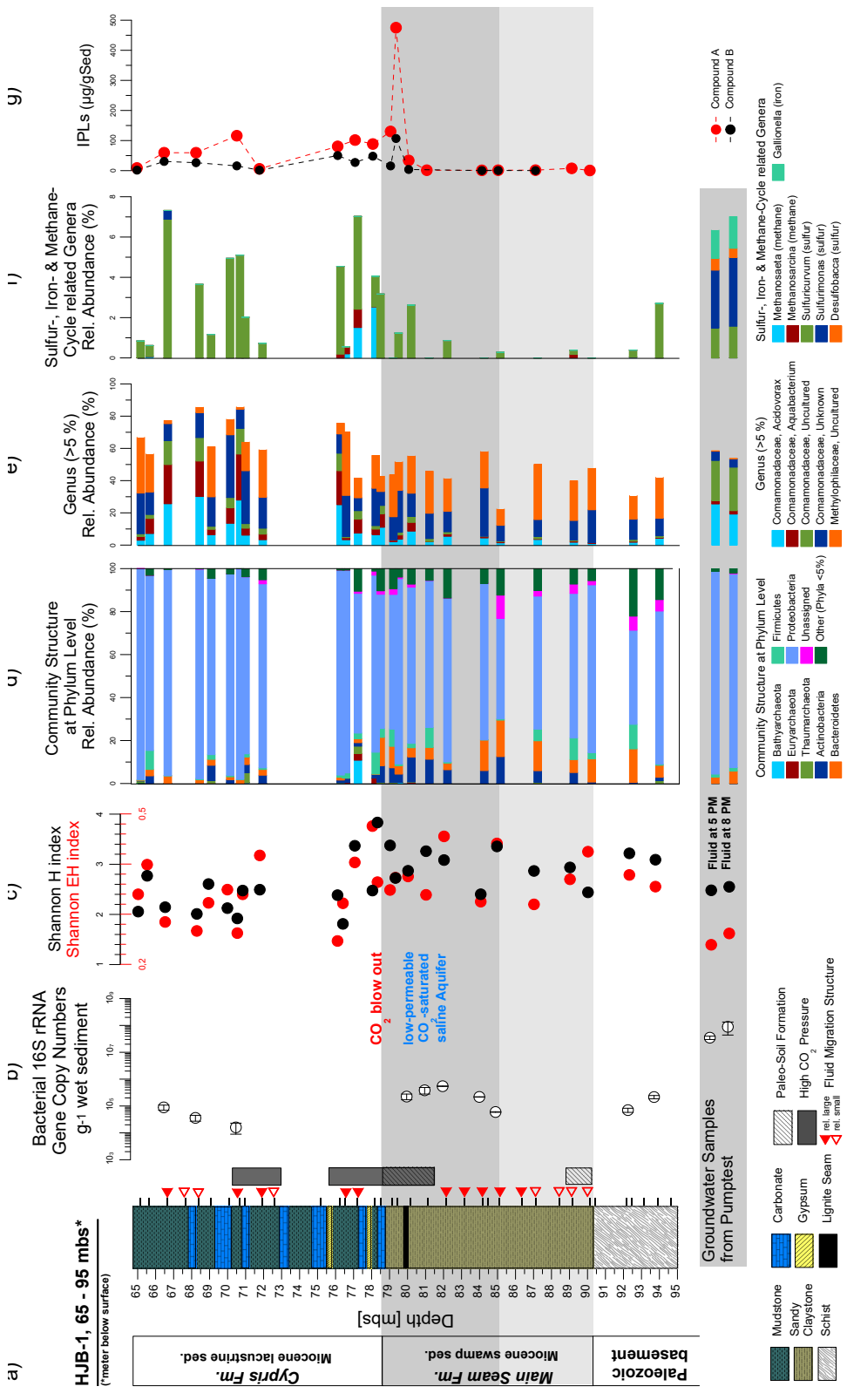

Figure 11. a) Stratigraphical and lithological description of the Hartoušov mofette core HJB-1 (2016) and depth profiles of b) bacterial 16S rRNA gene copy numbers, c) the Shannon H and Shannon EH indices, d) the community structure on phylum and e) genus (>5 %) levels, f) specific genera with respect to their metabolism and g) intact polar lipids (IPLs).

3.4.4 Abundance of microorganisms

The bacterial 16S rRNA gene copy numbers could not be quantified for all investigated samples, but revealed results between 10^4 and 10^6 16S rRNA gene copies g^{-1} wet sediment for a substantial portion of the samples in the Paleozoic basement, the low-permeable CO_2-saturated saline aquifer in the upper Main Seam Fm. and in the upper part of the investigated Cypris Fm. showing fluid migration structures (**Figure 11b**). The fluid filter samples from the pump test contained gene copy numbers ranging between 10^7 and 10^8 16S rRNA gene copies L^{-1} (**Figure 11b**).

3.4.5 Microbial community composition

The alpha diversity of the microbial community for the whole lithological profile was expressed by the Shannon H index (diversity) ranging between 1.9 and 3.3 and the Shannon EH index (evenness) ranging between 0.2 and 0.5 (**Figure 11c**). Relatively higher Shannon H and Shannon EH indices were detected in the Paleozoic basement, the Main Seam Fm. and at the bottom of the Cypris Fm. In the upper investigated Cypris Fm. the Shannon H and EH indices were lower, but similar to the fluid filter samples.

The relative abundance of each phylum in the community structure was demonstrated by the percentage of total sequence reads (**Figure 11c**). The composition of the bacterial community in the lithological units was strongly dominated by *Proteobacteria* (78.2 %) and in addition contained *Bacteroidetes* (5.8 %), *Actinobacteria* (3.8 %) and *Firmicutes* (3.0 %) in the Paleozoic basement and Main Seam Fm. Archaea were represented by the phyla *Bathyarchaeota* (0.6 %), *Euryarchaeota* (0.3 %) and *Thaumarchaeota* (0.3 %) mainly in minor amounts at the transition from the Main Seam Fm. to the Cypris Fm. characterized by a higher CO_2 influence (**Figure 11d**).

The community of the groundwater filter samples from the pump test was also dominated by *Proteobacteria* (92.2 %) accompanied by low amounts of *Bacteroidetes*

(4.3 %) and showed similarities to the community structure of the upper lacustrine sediments (**Figure 11d**).

The genera with a relative abundance of more than 5 % within the mofette system revealed a predominance of the families *Comamonadaceae* and *Methylophilaceae*, which both belong to the phylum *Proteobacteria* (**Figure 11e**). The identified genera of *Comamonadaceae* were *Acidovorax* (8.1 %), *Aquabacterium* (6.1 %) and uncultured (4.7 %) and unknown *Comamonadaceae* (16.0 %) and occurred in the sediment and groundwater filter samples. All investigated *Methylophilaceae* were uncultured genera (18.8 %) and only appeared in the sediment samples (**Figure 11e**).

In general, nearly the whole lithological profile was dominated by unknown *Comamonadaceae* and uncultured *Methylophilaceae* genera. In addition, minor amounts of *Acidovorax*, *Aquabacterium* and uncultured *Comamonadaceae* genera were detected in the upper Main Seam Fm. with the low-permeable CO_2-saturated saline aquifer. Subsequently, the above described general community structure was in the Cypris Fm. intercalated with sections characterized by a predominance of *Acidovorax*, *Aquabacterium*, uncultured and unknown *Comamonadaceae* genera as well and only minor amounts of uncultured *Methylophilaceae* genera. The community structure of these intercalations was comparable to the community of the groundwater filter samples which certainly contained only low amounts of *Aquabacterium* and no uncultured *Methylophilaceae* genera (**Figure 11e**).

Regarding the findings of the deep environmental setup of the investigated lithological profile (Bussert et al., 2017) and results from previous microbiological surface investigations from the Hartoušov and Bublák mofette systems (Beulig et al., 2015; Krauze et al., 2017; Liu et al., 2018) microorganisms involved in the sulfur-, iron- and methane-cycle could be expected (**Figure 11f**). Generally, the Illumina 16S rRNA gene analysis revealed low abundances of these genera. Sulfur-cycle related genera were represented by the abundance of sulfur-oxidizing *Sulfuricurvum* and *Sulfurimonas* showing a predominance of *Sulfuricurvum* in the sediments and a predominance of

Sulfurimonas in the groundwater filter samples (**Figure 11f**). Sulfate reducing bacteria were rare and the only detected genus was *Desulfobacca* restricted to the groundwater. A mentionable iron-cycling related genus was the iron oxidizer *Gallionella* also restricted to the groundwater filter samples. Methanogens were represented by *Methanosarcina* and *Methanosaeta* and had been found at the base of the Cypris Fm. (**Figure 11f**).

The analysis of the Beta diversity compares the microorganism distribution within the lithological profile and was obtained by non-metric multidimensional scaling (NMDS) with calculating the Bray-Curtis dissimilarity (**Figure 12**). The microbial communities of the different lithological units formed two clusters. The first cluster was characterized by major core segments with predominating unknown *Comamonadaceae* genera and uncultured *Methylophilaceae* genera within nearly the whole lithological profile. The second cluster comprised the intercalated core sections within the Cypris Fm. and the groundwater filter samples with a predominance of *Acidovorax*, *Aquabacterium* and uncultured *Comamonadaceae* genera. Additionally, from each lithological unit one sample was not included in these clusters (samples at 77.2 mbs, 84.2 mbs and 92.5 mbs). These samples had a high Shannon H index in common.

3.5 Discussion

3.5.1 Depositional environment and past microbial signatures

Based on the lithological description by Bussert et al. (2017) the Early Miocene Main Seam Fm. is characterized by terrestrial sediments deposited in a swamp environment. This is confirmed by the low TN values, the high TOC/TN ratio and the bulk $\delta^{13}C_{org}$ values at -26 ‰ indicating that vascular C3 plants are the major source of organic matter (OM) (Meyers, 1997, 2003) (**Figure 8**). Two intervals of paleo-soil and peat formation at the bottom and the top of the Main Seam Fm. are suggested from the abundance of roots, peat and charcoal in the sample material (**Figure 8a**) as well as increases in the TOC contents (**Figure 8c**).

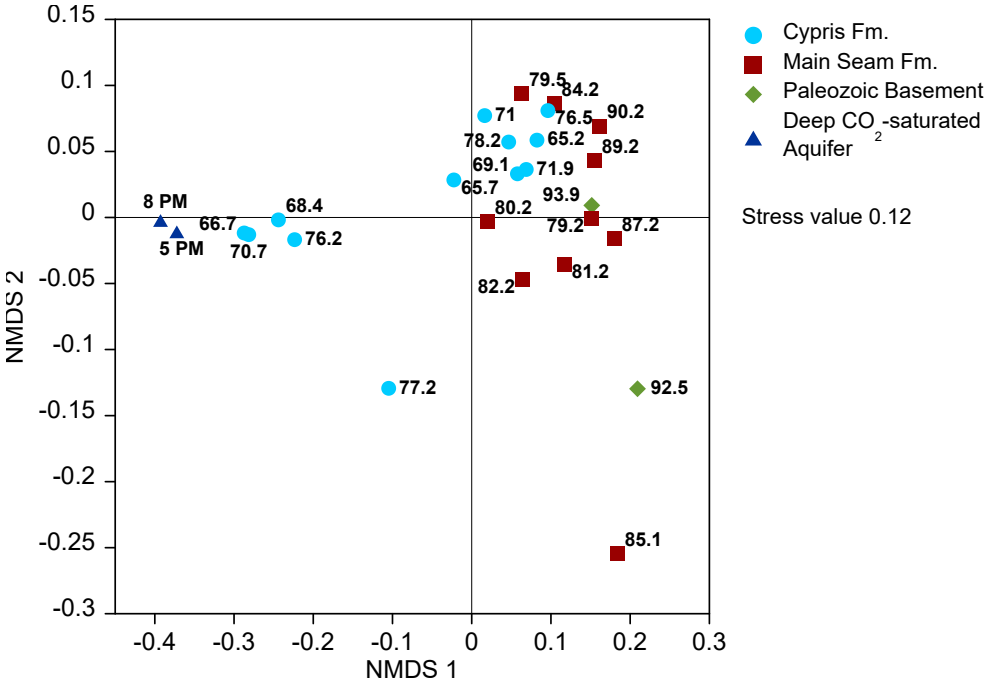

Figure 12 Beta diversity obtained by non-metric multidimensional scaling (NMDS) based on the Bray-Curtis dissimilarity to compare the relative abundance of microorganisms within the samples concerning their distribution within the lithological profile, i.e. Paleozoic basement, Main Seam Fm. and lacustrine Cypris Fm. as well as the groundwater of the deep CO_2-saturated aquifer.

The Early Miocene Cypris Fm. is described as a lacustrine deposit which is lithologically more heterogeneous and revealed phases during which carbonate precipitation interrupted the prevailing siliciclastic sedimentation (Bussert et al., 2017). The high and fluctuating TOC contents point to changes in OM production related to changing environmental conditions (**Figure 8c**). Fossil ostracod shells and higher TN values indicate planktonic biomass (**Figure 8a** and **8d**) (Meyers, 1997, 2003). Compared to the Main Seam Fm. the TOC/TN ratio is significantly lower, but with values between 25 and 40 still in the range of land plant material (**Figure 8f**). This indicates that the lacustrine OM is a mixture of autochthonous aquatic and allochthonous terrestrial biomass.

The hopanoids, representing dead microbial biomass, show indeed increased abundances during the intervals influenced by higher CO_2 concentrations making on a first view the impression that the hopanoid distribution is linked to the CO_2 occurrence.

However, the compositional change of the hopanoid types from the Main Seam Fm. ($\alpha\beta$–C_{31}R-hopane dominated) to the Cypris Fm. (Hop-17(21)-ene dominated) suggests that the hopanoid distribution is rather the result of hopanoid preservation during the time of deposition. This is confirmed by the shift in the $\delta^{13}C_{hopanoid}$ values (**Figure 9c**) showing a clear decrease related to the transition from the Main Seam to the Cypris Fm. and not to the occurrence of increased CO_2 concentrations. Compared to the bulk $\delta^{13}C_{org,}$ the relatively similar $\delta^{13}C_{hopanoid}$ signal in the Mean Seam Fm. points to a heterotrophic degradation of terrestrial OM and the dominance of $\alpha\beta$-C_{31}R-hopane is associated with bacteria known from terrestrial and more specific peat environments (Quirk et al., 1984; Huang et al., 2015; Inglis et al., 2018). In contrast, the decrease of the $\delta^{13}C_{hopanoid}$ signal in the Cypris Fm. indicates that aerobic methanotrophs might have formed a significant part of the source bacteria for the deposited hopanoids dwelling on microbially derived methane at the water-sediment interface (Nealson, 1997; Whiticar, 1999; Hoefs, 2018).

A similar picture, resulting from the depositional environment can be seen from the depth distribution of the GDGTs. The upper Main Seam Fm. is dominated by branched GDGTs (brGDGTs) characteristic for soil and swamp environments (**Figure 9d**) (Weijers et al., 2007; Weijers et al., 2010; Schouten et al., 2013). The lacustrine Cypris deposits show high but fluctuating amounts of isoprenoid GDGTs (isoGDGTs) and brGDGTs representing a mixture of aquatic microbial biomass produced in the lake and terrestrial biomass from the catchment area (Weijers et al., 2007; Weijers et al., 2010; Schouten et al., 2013), respectively. The relatively high brGDGT content might reflect good preservation conditions within the lake. Abundant isoGDGTs point to the presence of aquatic methanogenic and methanotrophic archaea (Schouten et al., 2013; Naeher et al., 2014; Bale et al., 2019). Both, the results from the GDGT and hopanoid analysis indicate that methane cycling processes particularly of methanogenic and methanotrophic archaea and methane oxidizing bacteria (hopanoid signal) play a significant role within the lake (**Figure 9c**).

Overall, this shows that the biomarkers representing dead microbial biomass rather represent ancient microbial communities during the time of deposition and that they cannot be used to elucidate the signal of the present deep biosphere. This might already indicate that the currently living microbial community is rather small leaving only small traces in the sediments.

3.5.2 Deep biosphere structure and lipid markers in the CO_2-saturated mofette system

The investigation of the microbial DNA in the deep subsurface of the Hartoušov mofette system (65 to 95 mbs) revealed a limited abundance but unique distribution of the microbial community. In comparison with findings from shallow mofette sediments of the same location (Liu et al., 2018), relatively low bacterial 16S rRNA gene copy numbers are determined for the deep biosphere communities (deep subsurface: 10^4 to 10^6 copies g^{-1} wet sediment; surface: 10^7 to 10^9 copies g^{-1} wet sediment; **Figure 11b**). Regarding the relatively equal distributed microbial abundance in both profiles, the lower microbial abundance in the subsurface can mainly be attributed to a low pore space of the lithology, the saline CO_2-saturated groundwater and a missing influence of meteoric waters (Bussert et al., 2017). Compared to the surface (Liu et al., 2018), the lower microbial diversity expressed by a low Shannon H index and its correlating Shannon EH index (evenness) (**Figure 10c**) points to a smaller but well adapted community in the deeper part of the mofette system. The dominance of *Proteobacteria* (**Figure 10d**) and therein high amounts of uncultured or even unknown genera of the families *Comamonadaceae* and *Methylophilacea* hint to a very specialized community that occurs independently from the background lithology over the whole depth profile (**Figure 10e**). This similarity might indicate, that the ascending CO_2–saturated and saline groundwater acts both as transport mechanisms and main ecosystem shaping factor for the deep biosphere. However, the relatively high abundance of uncultured *Methylophilaceae* genera is restricted to most of the lithological samples (**Figure 10e**) pointing to a more lithoautotrophic lifestyle of these genera and since the groundwater

is CO_2 saturated (Bussert et al., 2017) these uncultured *Methylophilaceae* genera may have a sedentary lifestyle.

Within this major deep ecosystem, we find two additional distinct minor niches. The first one is a transition zone at the bottom of the Cypris Fm. characterized by a strong rising TOC content and a high CO_2 concentration related to CO_2 accumulation and migration from the below located CO_2-saturated aquifer (**Figure 8a** and **8c**). Therein both potentially produced acetate from organic matter degradation and the ascending CO_2 might act as substrates for abundant methanogenic archaea, namely *Methanosaeta* and *Methanosarcina* (Zinder et al., 1985; Patel and Sprott, 1990) (**Figure 11f**). At this interval part of the isoGDGT past microbial signal representing methanogenic archaeal biomass (Schouten et al., 2013; Naeher et al., 2014) might also derive from the current deep biosphere (**Figure 9d**).

The second type of identified distinct minor microbial ecosystem is a couple of small habitats in the form of intercalations within the Cypris Fm. (e.g. 66.7 mbs, 68.4 mbs, 70.6 mbs and 77.1 mbs) being characterized by a higher relative abundance of the genera *Acidovorax* and *Aquabacterium* which correlate with fluid migration structures mentioned in the lithological description from the subsampling (**Figure 11a** and **11e**, **Supplementary Figure S1c**). The microbial community of these intercalations is relatively similar to that of the groundwater filter samples (**Figure 11e**) and both sample types correspond to the same cluster obtained from the beta diversity analysis (**Figure 12**). This leads to the interpretation that these zones represent a higher influence of fluid migration which might be caused by a locally increased pore space of the commonly argillaceous sediments.

Mu et al. (2014) reported a general shift from *Firmicutes* to *Proteobacteria* and therein a mainly high increase of members in the family *Comamonadaceae* after pumping a mixture of supercritical CO_2 and groundwater into the Paaratte sandstone aquifer (Southern Australia). Furthermore, Ham et al. (2017) also reported a predomination of *Comamonadaceae* in a CO_2-dominated aquifer from South Korea and Krauze et al.

(2017) detected members of *Comamonadaceae* in wet mofettes of the Cheb Basin close to the Hartoušov site as well. Thus, the dominance of members from the family *Comamonadaceae* in the deep successions of the Hartoušov mofette seems to reflect a typical microbial community for CO_2 influenced sediments and good adaptation potential of the identified community to the prevailing conditions. Hence, our study assumes that some members of *Comamonadaceae*, especially the determined sequences of uncultured and unknown genera as well as *Acidovorax* and *Aquabacterium* are very adoptive to CO_2-dominated ecosystems and can be suggested as an indicator for such environments.

From a chemolithoautotrophic perspective, a highly adopted community is indicated by the abundant occurrence of the genus *Sulfuricurvum* which was detected in higher amounts by Gulliver et al. (2018) after a CO_2 injection into a freshwater aquifer at Plant Daniel in Escatawpa (Massachusetts, USA). Moreover, the genus *Sulfurimonas* was also found in surficial pools of several mofette systems within the Cheb Basin (Krauze et al., 2017) and a CO_2-driven geyser on the Colorado Plateau (Utah, USA) (Probst et al., 2018). Thus, *Sulfuricurvum* and *Sulfurimonas* occurring together with high SO_4^{2-} contents in groundwater might represent indicator organisms for CO_2 influenced ecosystems.

Common intact phospholipids (PLs) and their corresponding fatty acids (PLFAs) have not been detected in significant amounts in the investigated sediments, which is in contrast to the finding of bacteria using the DNA approach. The reason for the lack of these major bacterial membrane lipids might be the generally low abundance ($< 10^6$ gene copy numbers per g^{-1} wet sediment) of the microbial community in the investigated interval (**Figure 11b**).

However, two uncommon and previously unknown intact polar lipid groups (A and B) are detected (**Figure 10a** and **11g**) in the sediments of the Main Seam and Cypris Fm. The first structural assessment suggests that they bear a sulfur-containing head group (presumably a sulfonic acid group) and ether- or alkyl-linked long hydrophobic side

chains. This would also explain why they were not detected during the PLFA analysis targeting ester-linked side chains. The fact that two clusters of up to six compounds representing individual lipids with the same head group but different side chain lengths (-CH_2- differences) were detected, which point to the origin of these lipids from bacteria or a single bacterium. Archaea also contain ether-linked side chains, but they do not show this side chain length variability (Mangelsdorf et al., 2019). Due to the ether-linked side chains with its higher stability against initial degradation, it might be argued that the potential of these IPLs to act as a life marker is restricted (Logemann et al., 2011). However, these IPLs show their highest concentration in the sediments with increased CO_2 abundance especially below the interface between the Main Seam and the Cypris Fm. This suggests that the source bacteria are related to the high CO_2 concentrations in the deep subsurface of the Hartoušov mofette and that the new IPLs act here as a life marker for some specifically adapted bacteria. A direct link to the DNA results could not be drawn based on the lipid and microorganism profiles (**Figure 11**) and further analysis has to be conducted to elucidate the exact structure and origin of these uncommon membrane lipids.

3.6 Conclusion

The lithological setup of the deep Hartoušov mofette system (65 – 95 mbs) represents a paleoenvironmental change from a terrestrial swamp-like to a lacustrine ecosystem. This system became overprinted by migration and accumulation of geogenic CO_2 which forms a potential habitat stimulating deep microbial life.

Past microbial lipid biomarkers essentially reflect the environmental conditions during the time of deposition and they cannot be used to trace the deep biosphere at the Hartoušov Site. This already indicates that the current biosphere signal in the deep mofette system is rather small compared to the paleo microbial biomass.

The overall low abundance of microbial signatures from the deep biosphere in the Hartoušov mofette system suggests that mainly related to the low pore space of the

lithology, the low-permeable CO_2-saturated aquifer interval does not reflect a hotspot for deep microbial life as might be expected from a substrate point of view. However, the data indicates that related to the ascending CO_2 a specialized microbial community developed with a depth distribution independent from the lithology over the whole explored core interval. In addition, our results imply that the high relative abundance of *Acidovorax* and *Aquabacterium*, members of uncultured and unknown genera of the family *Comamonadaceae* as well as the occurrence of *Sulfuricurvum* and *Sulfurimonas* together with high sulfate contents in the CO_2-saturated groundwater can be indicative for CO_2-dominated deep subsurface ecosystems. A cluster of yet unknown intact polar membrane lipids indicates the presence of microbial life associated with higher accumulations of CO_2 in the deep subsurface of the Hartoušov mofette. These lipids show the potential to act as biomarkers for such environmental settings.

3.7 Acknowledgements

QL gratefully acknowledges financial support from the China Scholarship Council. The authors would like to thank the Deutsche Forschungsgemeinschaft (DFG) and all involved scientists, technicians and student research assistants of the GFZ - German Research Centre for Geosciences for support and guidance through the sample preparation, analysis and interpretation. These important people, who kept the system running are in alphabetical order; Oliver Burckhardt, Anke Kaminsky, Cornelia Karger, Axel Kitte, Sebastian Kreutz, Hartmut Liep, Joana MacLean, Doreen Noak, Sylvia Pinkerneil, Anke Saborowski and Andrea Vieth-Hillebrand.

4 Direct link between earthquake and subsurface microbial methane production

4.1 Abstract

The Hartoušov mofette field is situated in a seismically active area in the Cheb Basin/Czech Republic, which is located in the western part of the Eger Rift, central Europe. During seismic events, released H_2 may serve as the electron donor for microbial hydrogenotrophic processes, such as methanogenesis. In the present study, we aimed to strengthen the hypothesis that seismic events can trigger methanogenesis by conducting laboratory simulation experiments with sediments down to 94.7 m at the Hartoušov mofette field. The laboratory simulation experiments show that after the addition of hydrogen, substantial amounts of methane were produced in incubations with mofette sediment. The methanogenic hydrogenotrophic genera *Methanobacterium* was highly enriched during the incubation. The modeling of the in-situ observation of the earthquake swarm period in 2000 at the Novy Kostel focal area/Czech Republic and our laboratory simulation experiments reveals a close relation between seismic activities and biological methane production via earthquake-induced H_2 release. We thus conclude that H_2 – which is released during seismic activity – can potentially trigger methanogenic activity and thus microbial life in the deep subsurface. Based on the conclusion, we further hypothesize that the hydrogenotrophic early life originated in hydrothermal vents was boosted by the Late Heavy Bombardment induced seismic activity in approximately 4.2 to 3.8 Ga.

4.2 Introduction

In general, microbial growth in the deep terrestrial biosphere is restricted by anaerobic conditions, the lower availability of water, and the exchange and support of substrates, such as organic carbon (Kallmeyer and Wagner, 2014). The deep subsurface biosphere

is considered supported by geological energy sources that migrate upward from the Earth's mantle (Gold, 1992). The availability of the electron donors and acceptors necessary for microbial processes usually decreases with sediment depth (Froelich et al., 1979; Middelburg, 1989). At greater depth, electron acceptors such as O_2, NO_3^-, Mn^{4+}, Fe^{3+}, and SO_4^{2-} become depleted, and H_2 becomes the major controlling and limiting factor for microbial activity in the terrestrial deep biosphere (Stevens and McKinley, 1995; Nealson, 2005; Spear et al., 2005). Molecular H_2 can be produced not only during fermentative processes and the radiolysis of water (Vovk, 1987; Savary and Pagel, 1997; Lin et al., 2005) but also by water-rock interactions and tectonic activity (Stevens and McKinley, 1995; Chapelle et al., 2002). Furthermore, molecular H_2 has been observed to be released in connection with tectonic stress (Sugisaki and Sugiura, 1985) and may, therefore, act as an indicator of fault activity (Wakita et al., 1980; Sato et al., 1986). During earthquakes, H_2 has been experimentally demonstrated to be capable of being generated by a mechano-chemical reaction between groundwater and fresh surfaces of crushed rock material (Kita et al., 1982). Following the idea that seismicity influences the availability of H_2 in the subsurface, Bräuer et al. (2005) hypothesized that seismic events may mobilize H_2 and trigger methanogenesis. The hypothesis was based on the observation that the H_2 concentration – and subsequently the concentration of biogenically produced methane – had increased in the emanating gas at a wellhead at Wettinquelle, Bad Brambach/Germany after the 2000 earthquake swarm period (**Figure 1A**). The shift of the $\delta^{13}CH_4$ values indicated a microbiological origin of the emanating methane, which had presumably been produced by hydrogenotrophic methanogens, in the deep fissured granite where the Wettinquelle was captured using stress-released H_2 as an energy source (Bräuer et al., 2005). Previous studies revealed hydrogenotrophic methanogens were detected in shallow sediments in the Cheb Basin (Beulig et al., 2016; Liu et al., 2018), but it remained unclear whether they were related to hydrogen released by seismic activity.

In this study, we now provide evidence that methanogenic archaea in the diffuse degassing structure (DDS) of Hartoušov mofette field (HMF) responds to a temporally increased availability of hydrogen, as expected after an earthquake activity. The

methanogenic activity was estimated in experiments with sediments retrieved from coring that reached a depth of up to 108.5 m below surface level (**Figure 1B**) where the sediments were anaerobically incubated under varying gas compositions (mixtures of CO_2, N_2, and H_2) in the headspace to simulate the influence of seismicity on the microbial methane production activity. Based on these experimental results, we show that the observed methane increase after the 2000 swarm activity can be very well fitted through a simple quantitative model.

4.3 Geological, geophysical, and geomicrobiological settings

The Cheb Basin (Czech Republic) is a shallow Neogene intracontinental basin filled with fluvial and lacustrine sediments ($\leqslant$ 350 m thick; **Figure 1A**), which is well-known for the recurrence of intense seismic swarms related to fluid pressure buildup (Hainzl and Ogata, 2005; Fischer et al., 2014). Those highly active seismic episodes lasting for weeks with thousands of recorded small earthquakes lastly occurred in 1985/86, 2000, 2008, 2011, 2014 and 2018, all activated a distinct part of the Novy Kostel fault zone. Particularly, the year 2000 swarm, with its more than 7000 events in the magnitude range between 0 and 3.3 (Fischer, 2003) is of interest, because of the close-by, continuous fluid monitoring (free gas + water) at the same time (Bräuer et al., 2005; Bräuer et al., 2007).

The Cheb Basin is known for its large-scale degassing of mantle-derived CO_2 (> 99%) — which is combined with traces of gases (e.g., He, N_2, Ar, and CH_4) — due to magmatic activity beneath the crust (Kämpf et al., 2013; Hrubcová et al., 2017). 56,6 tons of CO_2 is estimated to be released every day at the diffuse degassing Hartoušov mofette field over an area of 0.78 km^2 (Nickschick et al., 2015). The emanating mantle-derived gas has created specific diffuse degassing structures on the surface soil, which are called “wet” mofettes if gas is bubbling through the water at the surface and “dry” mofettes if gas escape at the soil of grassland or forest areas (Kämpf et al., 2013). DDS is controlled by fluid migration in fault zones (Nickschick et al., 2015) and can be analogs to the deep subsurface in terms of restricted availability of oxygen and

hydrogen (Liu et al., 2018). Moreover, the upstreaming fluids have been suggested to provide substrates for microbial life not only in the near-surface mofette soil but also in the CO_2 conduits of deep subsurface sediments (Krauze et al., 2017). Therefore, the microbial communities of both shallow and deep DDS sediments may depend on substrates originating from the deep subsurface.

4.4 Cultivation based earthquake simulation experiment

To prove whether methanogenic archaea can use both the CO_2 supplied by the upstreaming mantle-derived fluids and the H_2 provided during seismic events as a source of carbon and energy respectively, we performed cultivation-based simulation experiments under controlled environmental conditions with shallow and deep originating DDS sediment (**Figure 13**). No methanogenic activity was observed in simulation experiments without hydrogen as an additional substrate. Combined with the long-term observations of the gas composition by (Bräuer et al., 2005), during times with no measurable seismic activity, the *in-situ* methane production can be deemed negligible due to the lack of hydrogen as a substrate. After the addition of hydrogen to the incubations (which simulates the side-effects of seismic activity), methane production in the shallow sediments (< 2.95 m) began after a lag phase of 28–42 days. The lag phase observed during the incubations of the mofette soils is shorter than the observation in the field (Bräuer et al., 2005), because this lag phase only represents the time that the methanogenic population needs to grow and adapt to the changing conditions and the production of key enzymes but does not include the time for H_2 and in-*situ* methane transport. The 16S rRNA Illumina sequencing revealed that the microbial community structures were significantly influenced by the addition of hydrogen to the headspace (**Figure 14**). After the addition of hydrogen, *Euryarchaeota* showed a strong increase in relative abundance and became the dominant Archaeal phylum in all three active samples and sequences affiliated with the hydrogenotrophic genera *Methanobacterium* (Smith et al., 1997) was the most abundant genera within the *Euryarchaeota*.

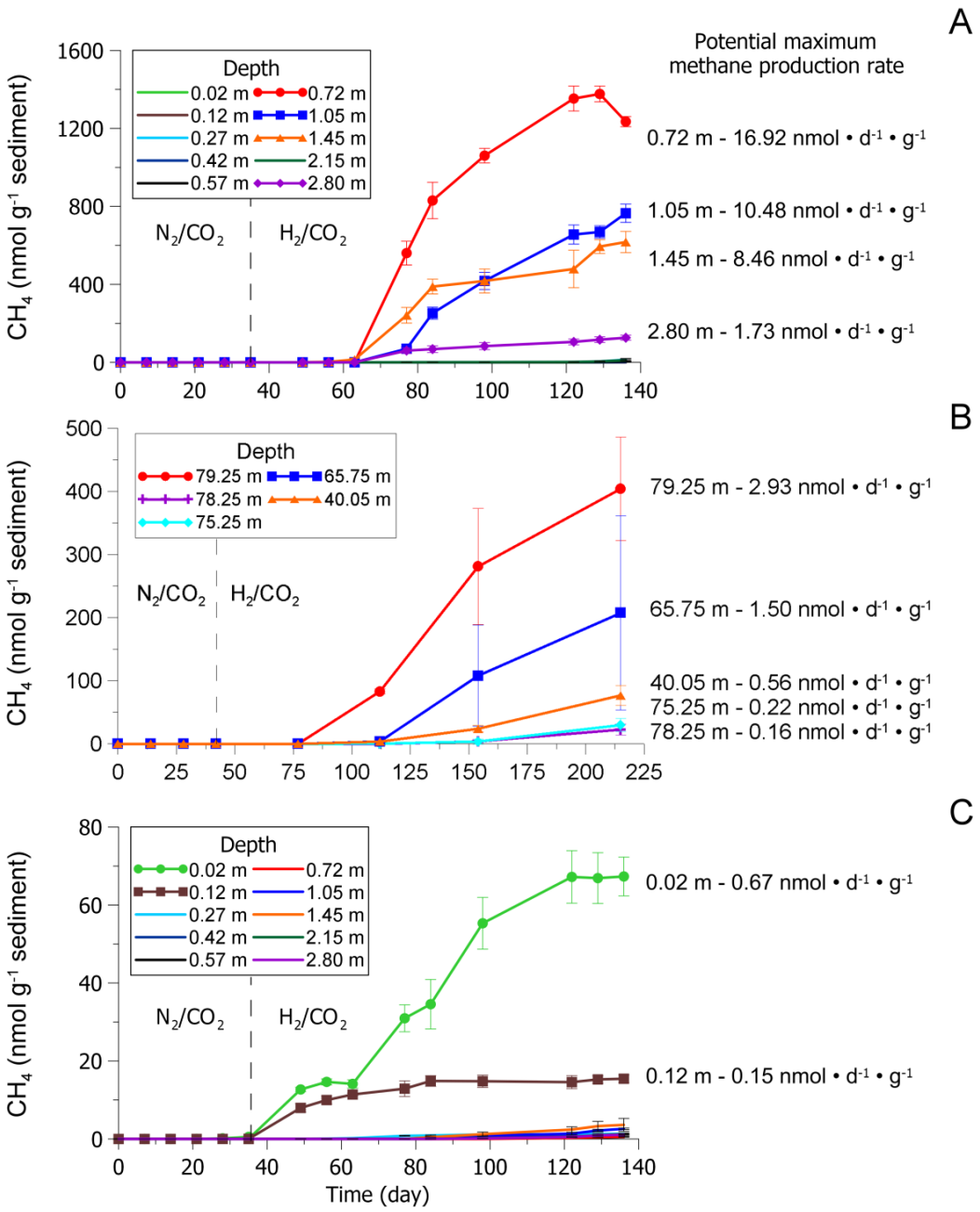

Figure 13 During the simulation experiments of earthquake swarms, methane was not produced in the "pre-earthquake" phase before hydrogen was supplied. Vast methane production (maximum 16.92 nmol·d^{-1}·g^{-1} wet soil) in the incubations from the shallow mofette sediments occurred between 28 and 35 days after changing the headspace gas phase from N_2/CO_2 to H_2/CO_2 (A). The incubations from deep subsurface material indicate only five samples have observable methane production, therefore the rest twenty-nine samples were not illustrated. The active methane production layers have a much longer lag phase (around 70 days), a much lower methane production rates (2.93 nmol·d^{-1} g^{-1} wet sediment) and a much larger standard deviation compare with that of the shallow

mofette sediments due to the extremely low number of microorganisms in the deep biosphere of the HMF (B). The highest measured methane production rates at the reference site (0.67 nmol·d^{-1}·g^{-1} wet soil) were around 20 times lower than those of the mofette and the in vitro methane production at the reference site was restricted to the uppermost soil layer (< 27 cm) (C). The control groups of both mofette and reference samples with N_2/CO_2 gas in the headspace showed no increase or only a negligible increase of methane (results are not shown).

The methanogenic activity was also observed in incubations provided with hydrogen gas for deep subsurface sediments (from 15 to 94.5 mbs). Only five sampling depth show detectable methane production compare with 34 total sampling depth and the period of the lag phase between changing the headspace gas composition and the starting point of methane production in the incubation experiment with the deep mofette sediment was up to 42 days longer (lag phases between 35 and 70 days) in comparison with that of the shallow HMF mofette soil (**Figure 13B**). Additionally, the highest methane concentration and the highest measured potential methane production rate of the deep sediments (0.2–2.9 nmol d^{-1} g^{-1} sediment) were significantly lower compared with that of the shallow mofette samples (1.7–16.9 nmol d^{-1} g^{-1} soil). This phenomenon can be explained by the initially extremely low abundance of methanogens at greater depths as well as by a reduced transport of all substances due to low water- and gas permeability and entrapment in the heavily compressed, claylike deep sediment (Wang et al., 1993), which cause a very limited geological H_2 availability to the methanogens via subsurface DDS. However, a direct comparison of the lag phases observed in the simulation experiments under laboratory conditions and the complex *in-situ* conditions during earthquakes remains difficult. Although the potential methane production rate is relatively low, the large extension of the degassing area in the Eger Rift fault system has to be considered for its large surface area and depth, which extends down to several kilometers. According to the positive response of the methanogens to the elevated H_2 concentration, we conclude that seismic activity can potentially trigger methanogenic activity by releasing H_2 and thereby change the gas composition of emanating fluids in the western Eger Rift region.

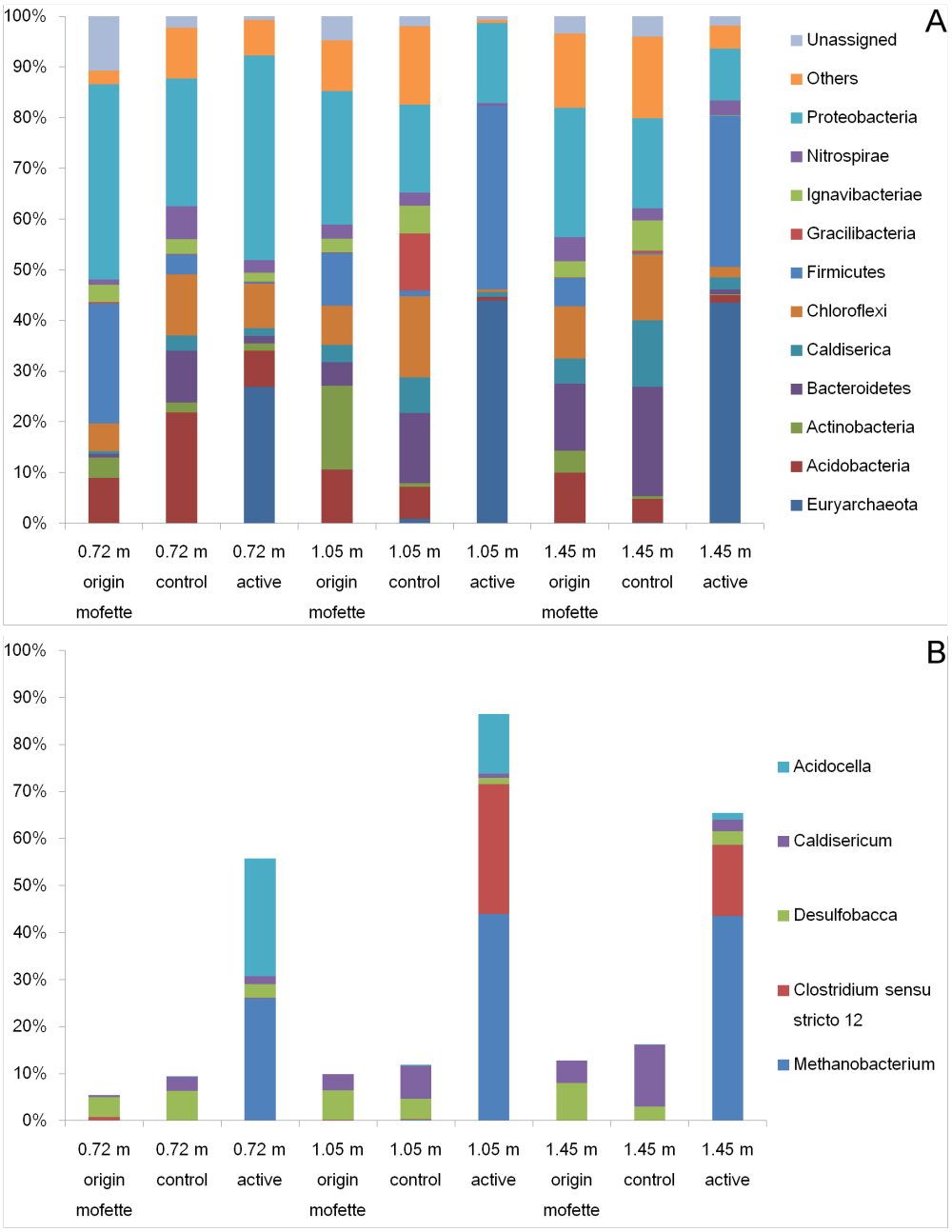

Figure 14 Relative abundances (A: phyla with a relative abundance of at least 5% and B: the most abundant 5 genera) of the mofette samples with active methanogenesis (0.72 m, 1.05 m and 1.45 m), their relevant control groups after incubations and the original samples without incubations. Triplicates are merged. Incubations with hydrogen significantly influence the microbial communities. The common difference caused by sufficient hydrogen supply is the increase of *Methanobacterium*, which belongs to the Archaea phylum Euryarchaeota. The relative abundance of *Methanobacterium* increases from almost 0 to 26.0 ~ 44.0%.

4.5 Linking of earthquake activity and microbial response

In accordance with the finding of Hainzl & Ogata (2005), we assume that the earthquake activity was triggered by earthquake-fluid interactions, where earthquake ruptures facilitate fluid flow and vice versa. Furthermore, we assume that the earthquake-related pressure changes at depth are proportional to the energy released by the earthquakes and that those pressure changes migrate upwards by pore-pressure diffusion. Direct evidence of such a fluid pressure pulse was found for the 2014 activity at the same place, where a postseismic pressure change has been observed at the Hartoušov mofette which fits the fluid-driven seismicity migration patterns (Hainzl et al., 2016). Fischer et al. (2017) showed that the surface observation can be very well fitted assuming fluid diffusion within a connecting fault zone with high hydraulic diffusivity of 12 m^2/s. Here we use the same values (8 km distance and D = 12 m^2/s) to model the pressure changes at a depth of 50 meters, as a representative value for the depth of the microbes. The pressure pulse is expected to open existing fractures and mobilize H_2 of the surrounding rock. Thus $H_2(t)$ is simply assumed to be proportional to the pressure pulse induced by the observed seismicity (**Figure 15C**). The additional $H_2(t)$ leads to a blooming of the microbe population and CH_4 production, according to our simple microbial growth model described in the methods part. The transport of the CH_4 to the surface is again assumed to follow a diffusion process with the same hydraulic diffusivity. **Figure 15E** shows the fit of the full model based on seismic activity. Here we use T = 20 and T_{lag} = 35 days according to the calibration test for the depth range between 40 to 80 m, thus the factor X is the only free parameter which affects the shape of the expected CH_4-response function. The good fit of our simplified model to the field observations is a strong indication that the seismic activity caused H_2 releases which finally triggered the growth of hydrogenotrophic methanogens.

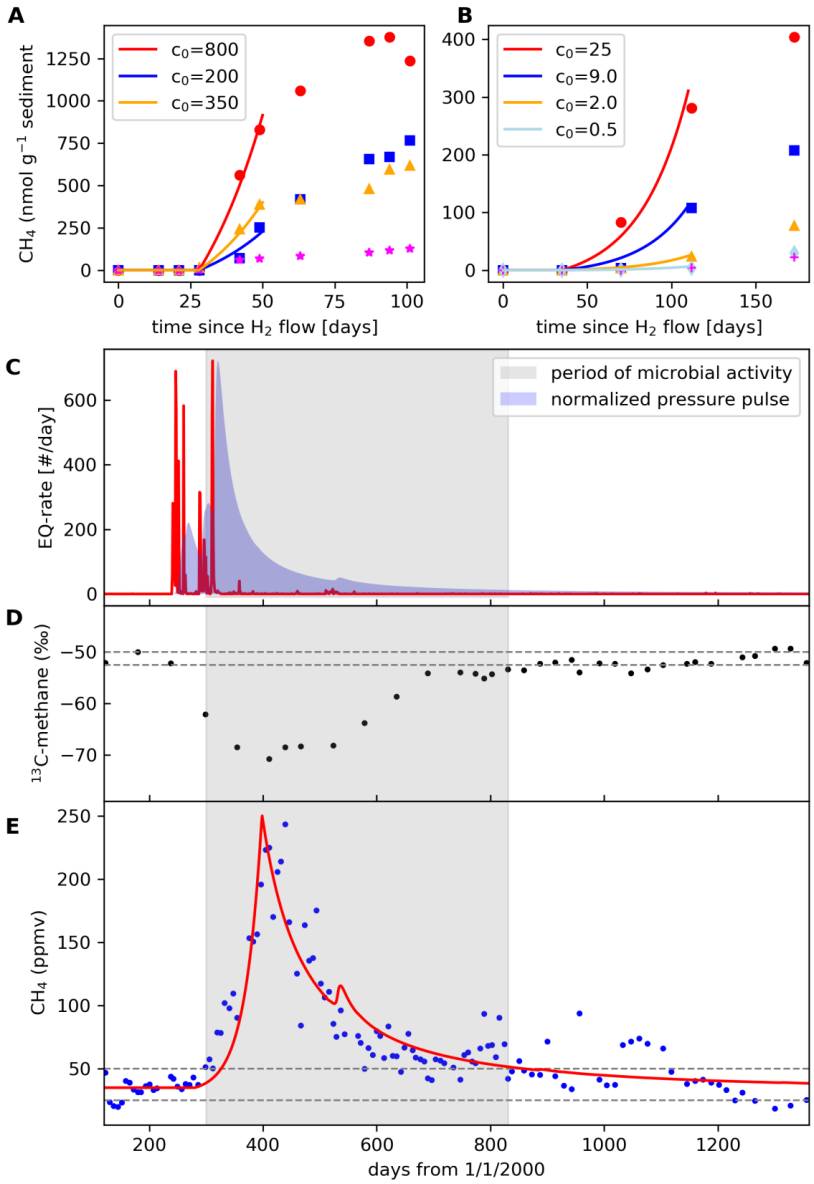

Figure 15 Model application to experimental (A, B) and observed data (C - E according to Bräuer et al., 2005, 2007). The calibration to the experimental values (**Figure 13**) is performed for the depth range 0-3 m (A) and 40-80 m (B). In all cases, the model fits are done with T=20 days, while the lag-times are 28 and 35 days in (A) and (B), respectively. (C) Observed daily earthquake numbers (m>0) versus time, where additionally the calculated normalized pore pressure response at the assumed depth level of the microbes (50m) is shown in blue; (D-E) observed values at the surface.

In (E), the red line refers to the normalized response which adds to the background CH_4-level according to our simplified model.

4.6 The impact of early life

It is believed that life arose on Earth before 3.5 Ga (Schopf, 1993; Schopf, 2006) after the formation of the oceans; approximately in the same period when a critical event - the Late Heavy Bombardment (LHB) - is suspected to have happened between 4.1 and 3.8 Ga (Tera et al., 1974). During this interval, a disproportionately large number of asteroids have collided the earth (Claeys and Morbidelli, 2011). Despite the debate of the existence, the LHB was considered catastrophic to the environment (Maher and Stevenson, 1988; Oberbeck and Fogleman, 1989; Sleep et al., 1989; Chyba, 1993). However, recent studies estimated that the energy input from impact asteroids is not enough to evaporate the ocean and sterilize the planet (Valley et al., 2002), indicating that the existence of life is possible in non-surficial environments during the LHB. Many studies speculate that life originated in submarine hydrothermal vents (Martin and Russell, 2007; Martin et al., 2008; Dodd et al., 2017). Interestingly, the functions and properties of the last universal common ancestor (LUCA) are characterized as anaerobic, CO_2- and N_2-fixing, thermophilic, and H_2-dependent with a Wood-Ljungdahl pathway (Weiss et al. 2016). This means that geological H_2 (fermentational H_2 production in H_2-dependent microorganisms with a Wood-Ljungdahl pathway is impossible) may play an important role at the early stage of life. As an example of the energy input from asteroids impacts, the study of Chicxulub meteorite crater - which was produced about 65 million years ago by an asteroid impact and has an approximate 180 km outer diameter of the crater depression - estimated the impact energy varied from 2.2×10^{22} to 7.4×10^{22} J (Ivanov, 2005). The seismic energy released by this impact is roughly comparable to a magnitude 10-11 earthquake, which means, the impact radiated approximately 100 times the energy of the largest ever recorded earthquake (Ivanov, 2005). The total estimated energy of asteroid impacts on both earth and moon during the LHB are estimated in the range between 10^{24} and 10^{26} J (Sleep and Zoback, 2007). The static and dynamic stress changes related to these impacts

likely induced extensive co- and postseismic fracturing in the early crust; in particular, the impact and its subsequently induced seismic activities created new cracks, cavities, or through-going new faults (Sleep and Zoback, 2007; Lowe, 2013). As indicated by our present-day example, this fracturing of the crust probably released a large amount of H_2 via degassing vent systems which - as an extra substrate - would subsequently stimulate the growth and replication of the existing hydrogenotrophic early life. The fracturing indicated by energy input from impact asteroids might have created magma chambers and numerous new hydrothermal vents with geological H_2 and other mantle gas releases, leading to an expansion of possible habitats for the H_2-dependent early life. Therefore, the spreading of H_2-dependent and newly evolved early life may be promoted. In conclusion, our study of a present-day terrestrial hydrothermal-vent-like degassing site supports the hypothesis that the LHB may influence and boosted the development and thrive of H_2-dependent early life in hydrothermal vents.

4.7 Methods

4.7.1 Study site and sampling

The drilling sites were located perpendicular to one of the main CO_2 degassing areas of the Hartouš ov mofette field (50° 07′ 58″ N, 12° 27′ 46″ E) and the Wettinquelle mineral spring, Bad Brambach/Germany (50° 22′ 07″ N, 12° 30′ 38″ E) in the Eger Rift. A map and detailed description of the drilling and sampling procedure had been provided previously (Liu et al., 2018). The drilling campaign of two 3-m-shallow cores was conducted at the HMF in September 2015. The cores were retrieved by hammered drilling using a motor-driven hammer (Wacker Neuson, Germany). One shallow mofette core was taken from a dry mofette, and one reference core was taken from an undisturbed reference site in the direct vicinity (Liu et al., 2018). The mean CO_2 soil gas flux at the mofette amounted to about 28 kg m^{-2} d^{-2}, while the CO_2 soil gas flux at the reference site amounted only to about 8 g m^{-2} d^{-2} (Liu et al., 2018). As part of the characterization of the ecosystems, the cores were sedimentologically and geochemically characterized and Illumina MiSeq sequencing of 16S rRNA amplicons

highlighted the differences between the microbial community structure in the shallow mofette core and a reference core within the same study (Liu et al., 2018). Additionally, sediments from a 108.5-m-deep drilling into the major degassing system of the Hartoušov mofette field were analyzed and the deep drilling, coring and the contamination control were described by Bussert et al. (2017).

The samples were taken along the depth profile. Core material from both drilling campaigns that had been intended for use in the activity tests was immediately removed suspicious contaminated out-layer. Then the sample material was flushed and stored with sterile CO_2 (via a 0.02µm filter) in gas-tight bags at 4°C. In total, 20 samples from the two 3-m cores (10 samples for each core) and 34 samples from the 108.5-m-deep drilling core were analyzed. A triplicate was subsampled and analyzed for each sample depth.

4.7.2 Cultivation-based activity test

To simulate the elevation of the H_2 concentration during and after seismic activity in the Cheb basin. the potential of methane production from both 3-m-shallow cores and the 108.5-m-deep drilling samples was tested through anaerobic cultivations and measurements of the headspace methane concentrations. The experimental methods were modified from the study by Barbier et al. (2012). The sample materials of the earthquake simulation experiments were prepared in an anaerobic workstation (Don Whitley Scientific Limited, West Yorkshire, England). 0.5 g of homogenized sediment was placed in 20-ml serum bottles with 0.5 ml of filter-sterilized (0.02 µm) tap water. Each sample was prepared and separated into the test group and the control group with triplicates in each group. The serum bottles with samples were flushed and filled with N_2/CO_2 (v/v 80:20) and cultivated at 18 °C to simulate “pre-earthquake” *in-situ* conditions. After 35 days (for the 3-m-shallow cores) and 42 days (for the 108.5-m-deep drilling samples), the headspace in the serum bottles of the test group was flushed and changed to H_2/CO_2 (v/v 80:20) to simulate “post-earthquake” conditions. The experiment lasted for 136 days (for the 3-m-shallow cores) and 215 days (for the 108.5-

m-deep drilling samples). The methane concentration in each serum bottle was measured every seven days by gas chromatography (Agilent 7890A, Agilent Technologies, Santa Clara, CA).

4.7.3 DNA extraction and sequencing the activity test samples

The total genomic DNA from the activity test group and the corresponding control group after the cultivation processes were isolated by the FastDNA™ SPIN Kit for soil and the FastPrep® Instrument (MP Biomedicals, Santa Ana, CA) with small modifications. The homogenizing time of the FastPrep® Instrument was changed to 30 seconds, and the speed was set to 5.5 m s^{-1}.

The microbial diversity within the incubations that showed the highest methane production was revealed by Illumina MiSeq 16S rRNA gene sequencing. The PCR reaction solution consisted of 12.5 µL of MangoMix™ (Bioline, Taunton, USA), 9.2 µL of PCR water, 0.3 µL of bovine serum albumin, 0.25 µL of forward primer (20 µM), 0.25 µL of reverse primer (20 µM), and 2.5 µL of the template. Unique combinations of barcode-tagged 515F (5'-GTGCCAGCMGCCGCGGTAA-3') and 806R (5'-GGACTACHVGGGTWTCTAAT-3') primers were assigned to each sample (Caporaso et al., 2011). The amplifications were performed on a T100™ thermal cycler (Bio-Rad Laboratories Inc., USA). The following protocol was used for the amplification: 3 minutes at 95 °C, 30 cycles of 30 seconds at 94 °C, 45 seconds at 56 °C, 60 seconds at 72 °C, and a final extension step of 10 minutes at 72 °C.

The PCR products were cleaned with AMPure XP magnetic beads (Beckman Coulter GmbH, Krefeld, Germany). After measuring the DNA concentration (CLARIO star® plate reader, BMG LABTECH GmbH, Ortenberg, Germany), PCR products were pooled in equimolar amounts. The DNA pool was concentrated (Eppendorf Concentrator plus, Eppendorf AG, Hamburg, Germany) to meet the requirement of the Illumina MiSeq high-throughput sequencing (DNA concentration ≥ 50 ng μL^{-1}).

Sequencing was performed by Eurofins Scientific SE, Luxembourg, on an Illumina MiSeq (2 x 250 bp). Detailed data processes followed the same procedure described previously[1]. After sorting, merging, trimming, and chimera removal, 5,849,228 sequences were obtained in total. Sequences range from 56,803 to 561,567 for each sample. Sequencing data were submitted to the European Nucleotide Archive (http://www.ebi.ac.uk/ena) under access number ERS2911355 to ERS2911364 (Bioproject PRJEB22478).

4.7.4 Model of microbial methane production

In order to quantify the link between the observed seismicity and methane concentration in the year 2000, we consider a simplified model of CH_4 production by microbes. In particular, we assume an existing population of N_0 microbes which starts to bloom after a lag-phase (T_{lag}) when an excess of H_2 is available. As long as enough H_2 is available, the population doubles after time T, which leads to an exponential increase according to $N(t) = N_0 * 2^{t/T}$. Considering that the CH_4 production is just proportional to the number of microbes, $CH_4(t) = c * N(t)$, the CH_4 production also increases exponentially, $CH_4(t) = c_0 * 2^{t/T}$ with $c_0 = c * N_0$. Calibration of this model to the experimental data is presented in **Figure 15A** and **15B**, showing that the onset of the laboratory data can be fitted of T = 20 days and T_{lag} = 28 days of the first 3 m, respectively T = 20 days and T_{lag} = 35 days of the depth range between 40 to 80 m.

However, the growth is limited by the finite availability of H_2. Assuming that each microbe consumes a certain amount Y of H_2 per time unit, the maximum number of active microbes is limited by the value of H_2-influx rate at time t, namely $N_{max}(t) = H_2(t) / Y$, which is equivalent to a maximum CH_4 production of $CH_{4max}(t) = c * N_{max}(t)$.
For the application to the observed seismicity data, the H_2-influx rate is assumed to be proportional to the earthquake-induced pressure, $H_2(t) = \kappa * p(t)$. Here we assume that the lag-phase starts at time t_0 when the H_2-influx rate exceeds 1% of its maximum value, and the exponential growth then starts at $t0+T_{lag}$ until N(t) reaches $N_{max}(t) = p(t)/X$ with $X=Y/\kappa$.

4.8 Acknowledgements

QL gratefully acknowledges financial support from the China Scholarship Council (CSC). Special thanks are also due to Oliver Burckhardt, Axel Kitte, Susanne Boteck, Maria Börger, and Kai Mangelsdorf (GFZ German Research Centre for Geosciences) for their valuable help during the 108.5-m-deep drilling and various sampling campaigns as well as for their support in the lab.

5 Synthesis and Outlook

5.1 Introduction

The microbial processes closely relate to the surrounding environments. The environmental factors – e.g. oxygen availability, water contents, pH and ion concentrations – shape the microbial communities. Therefore, the variation of these environmental factors usually leads to the shift of microbial composition, distribution, and activity. The geological processes in active fault systems – such as seismic activity, volcanic activity, gas emission, and fluid flow – can substantially change the environmental factors (Wakita et al., 1980; Sato et al., 1986; Rennert and Pfanz, 2016) and therefore shift the microbial communities. However, the microbial responses to the geological processes – namely the geo-bio interactions – are not well understood.

The Eger Rift region – which is characterized by active seismicity in form of so-called "earthquake swarms" and massive mantle-derived CO_2-rich gas flux (Bräuer et al., 2005; Dahm et al., 2013) – provides an ideal natural lab to study the interaction between microbial processes and geological processes. The primary goal of this thesis is to reveal the bio-geo interactions between microbial communities and the CO_2 ascending/seismic active environment in the Cheb Basin, western Eger Rift region by investigating geological properties and microbial communities in a mofette as well as deep subsurface sediments. Furthermore, this thesis provides a simple model to clarify whether microbial methane production can be triggered by seismic activity. Based on the modeling, the Late Heavy Bombardment favored the early life on Earth is hypothesized.

5.2 Microbial communities in ascending CO_2 affected surface and subsurface environments in the Hartoušov mofette field

In the Cheb Basin, the mantle-derived CO_2 migrates preferentially dissolved in water

or as a free gas phase along deep-seated faults to the surface (Weise et al., 2001; Bräuer et al., 2008). The migration and accumulation of geogenic CO_2 forms potential habitats for specialized microbial communities in both surface and subsurface sediments. The elevated CO_2 concentration (>99%) on the surface causes soil hypoxia and acidification (Rennert and Pfanz, 2016). The hypoxic to anaerobic and acidic environment substantially alters and differentiates the mofette communities compared with the undisturbed reference site. Additionally, the ascending high saline mineral water from the deep saline aquifer is also an essential influencing parameter due to the dissolved substrates (such as CO_2 and sulfate) feed the ecosystem in mofettes and subsurface fluid migration structures. The microbial community in the Hartoušov mofette system is characterized by their unusual abundance and distribution which is independent of the lithology setup under the significant influence of ascending CO_2.

An interesting characteristic of microbial life in the Hartoušov mofette system is the abundance of microorganisms is not decreasing with depth (**Figure 2** and **11b**). This can be explained by the acid adaptive, acid-tolerant or acidophilic bacteria, and anaerobic chemolithoautotrophs in the mofette (Liu et al., 2018). Within the deep subsurface sediments, the samples with high 16S rRNA gene copies are considered as CO_2-saturated fluid migration structures with a relatively higher pore space and more access to the CO_2-saturated groundwater compared with the other lithology setup.

The hypoxic to anaerobic and acidic conditions in the mofette significantly influences the distribution of microorganisms. The beta diversity shows that the mofette and the reference communities formed distinct clusters (**Figure 4**). Interestingly, there is also a gap that distinguishes the upper mofette (<95 cm) to the deeper mofette (>105 cm) (**Figure 4**). The variation of pH – as a result of the elevated CO_2 concentration as well as the buffing of meteoric water and groundwater – explains the distribution of the microbial communities (**Figure 7**). The 16S rRNA sequencing results pointed out the acidophilic, aerobic or facultative anaerobic genus *Acidithiobacillus* (Kelly and Wood, 2000) and the family *Acidobacteriaceae* (Subgroup 1) (Pankratov et al., 2012) dominated the upper mofette but strictly anaerobic and less acid-tolerant genus

Thermoanaerobaculum, *Bacteroidetes Vadin HA17*, *Desulfobacca*, *Caldisericum*, and *Sulfurovum* thrived in the deeper mofette. However, the acidification is no longer the influencing factor of the microbial distribution in the deep subsurface sediment. In a terrestrial deep biosphere, with the development of the sedimentary processes, the availability of nutrients necessary for microbial processes usually decrease with increasing depth (Froelich et al., 1979; Middelburg, 1989) and nutrient flux is usually extremely low due to the limitations of sediment chemistry and hydrology (Stevens and McKinley, 1995). However, mantle-derived CO_2 is ascending to surface at large scale through cracks and conduits within the Eger Rift mofette system (Kämpf et al., 2013; Nickschick et al., 2015; Nickschick et al., 2017). The ascending CO_2 carries high saline groundwater and provides substrates to the surface (Krauze et al., 2017; Liu et al., 2018). The saline and CO_2-saturated groundwater could only migrate through small cracks which were considered as fluid migration structures and therefore significantly influence the microbial communities. The 16S rRNA sequencing data indicated a higher relative abundance of the genera *Acidovorax* and *Aquabacterium* which correlate with fluid migration structures (e.g. 66.7 mbs, 68.4 mbs, 70.6 mbs, and 77.1 mbs) (**Figure 11E**). The microbial community of these intercalations is relatively similar to that of the groundwater (**Figure 11E**) and correspond to the same cluster obtained from the beta diversity analysis (**Figure 12**). The similarity leads to the interpretation that these intercalations represent a higher influence of fluid migration which “bleached out” the pristine sediment microorganisms.

Although both mofette and subsurface sediments are influenced by ascending CO_2, the deep subsurface community is dominated by the family *Comamonadaceae*, which is distinct from the mofette community. The family *Comamonadaceae* was described as having a remarkable phenotypic diversity including aerobic and anaerobic, autotrophic and heterotrophic species isolated from both water and soil habitats (Willems, 2014). The *Comamonadaceae* was reported widely spreads in the subsurface related hydrological systems such as wells, springs, and wet mofettes in Cheb Basin (Krauze et al., 2017). Sequences close to *Comamonadaceae* were abundant in springs and wells with elevated CO_2 concentration in South Korea (Ham et al., 2017). Interestingly, after

150 tons of supercritical CO_2 and groundwater were pumped into the sandstone Paaratte aquifer, the relative abundance of *Comamonadaceae* increased and caused a general shift from *Firmicutes* to *Proteobacteria* (Mu et al., 2014). Hence, it is assumed that within the family *Comamonadaceae*, not only known genera *Acidovorax* and *Aquabacterium*, but also a large relative abundance of uncultured and unknown genera are highly adaptive to CO_2-dominated habitat and can be suggested as indicators for CO_2-rich environments (**Figure 11**).

This thesis also highlights the importance of an autotrophic- rather than a heterotrophic lifestyle in mofette and deep subsurface environments with elevated CO_2 concentration. The high sulfate concentration in the ascending fluid (Bussert et al., 2017) results in a substantial proportion of sulfur-cycle related microorganisms. *Desulfobacca*, *Desulfosporosinus*, and *Acidithiobacillus* were found in high relative abundance in the mofette (**Figure 6**) while *Desulfobacca, Desulfomonile, Sulfuricurvum*, and *Sulfurimonas* were found in the subsurface fluid (**Figure 11**). The abundance of SRBs was much higher in the mofette compared with that in the deep subsurface sediments. The inhibited degradation of organic compounds in CO_2 affected mineral water (Krauze et al., 2017) and limited access of low molecular carbon organic compounds due to the impermeable strata – which resulting in immobilization of organic matter – might be the reason of the exclusion of SRBs in the subsurface sediments. On the other hand, the sulfate-rich mofette leads to a high abundance of SRBs and the reduced sulfur compounds feed the sulfur oxidizers. In a highly acidic environment (pH<4.0), the sulfur compounds offer ideal growth conditions for obligate acidophilic *Acidithiobacillus* (Kelly and Wood, 2000), which accounted for 7.1% of the mofette communities. However, in the deep subsurface environment, *Acidithiobacillus* was replaced by *Sulfuricurvum* and *Sulfurimonas*. Both genera were reported in subsurface related hydrological systems in Cheb Basin (Krauze et al., 2017) and other CO_2 influenced aquifers (Gulliver et al., 2018; Probst et al., 2018).

5.3 Methanogenic response to the seismic activity

Bräuer et al. (2005) observed an increasing concentration of biogenic produced methane, which indicated by low $\delta^{13}CH_4$ values in the emanating gas at the Wettinquelle mineral spring after the swarm earthquake 2000. This finding hints that the hydrogenotrophic methanogenesis in the deep subsurface environment might be triggered by H_2 released in seismic activity. To determine the methanogenic response to the seismic activity, laboratory incubation experiments were conducted to prove whether methanogenic archaea in the retrieved sediments can use both the degassing CO_2 and the H_2 provided during seismic events as the source of carbon and energy (**Figure 13**). No methanogenic activity was detected before the addition of hydrogen indicates the *in-situ* methane production can be deemed negligible not only because of the lack of hydrogen as a substrate for the hydrogenotrophic methanogens before the seismic event, but also the lacking of acetate due to the inhibited organic matter degradation (Beulig et al., 2016) for the heterotrophic and facultative methanogens (e.g. *Methanosarcina* and *Methanosaeta* in the mofette). Besides, the competition with SRBs for acetate and hydrogen (Kristjansson et al., 1982; Schönheit et al., 1982) should be taken into consideration because of the high abundance of SRBs, which indicated by a large amount of *dsrB* gene copies and the high relative abundance of *Desulfobacca* and *Desulfosporosinus* in the mofette (Liu et al., 2018). Substantial amounts of methane were produced after the addition of hydrogen with a lag phase of 28–42 days in the shallow mofette samples (**Figure 13A**). This finding indicates the availability of hydrogen is crucial for the hydrogen-depending methanogenic community in the mofette. The dominant hydrogenotrophic methanogenic genus in the mofette was *Methanobacterium* (Zeikus and Wolfe, 1972; Smith et al., 1997) and consequently became the dominant taxon in the samples showing the highest potential methanogenic activities (**Figure 14**).

The methanogenic activity was also observed in incubations with deep subsurface sediments (samples from the depth of 40.05 mbs, 65.75 mbs, 75.25 mbs, 78.25 mbs, and 79.25 mbs). However, the period of the lag phase was up to 42 days longer (lag phases between 35 and 70 days) compared with that of the shallow mofette samples in

the cultivation-based simulation experiments (**Figure 13**). Additionally, the highest methane concentration and the highest measured potential methane production rate of the deep sediments (0.2–2.9 nmol d^{-1} g^{-1} sediment) was also much lower compared with that of the shallow mofette samples (1.7–16.9 nmol d^{-1} g^{-1} soil), which can be explained by the initial extremely low abundance of methanogens at greater depth as well as the *in-situ* limited geological H_2 availability.

A simple model was introduced to reveal the potential link between the laboratory simulation experiments and the field observation made by Bräuer et al. (2005) in the emanating gas at a wellhead at Wettinquelle in the Eger Rift region after an earthquake swarm at 2000. The energy input from earthquake-induced pressure (Hainzl and Ogata, 2005) was introduced to model the curve of H_2 releases and further model the microbial methane production with the length of lag-phase and the doubling time of methanogens from the laboratory simulation experiments of the deep drilling samples. The good fit of our simplified model to the field observations (**Figure 15**) is a strong indication that the seismic activity caused H_2 releases which subsequently triggered the growth of hydrogenotrophic methanogens. Following this result, the large-scale seismic activities in the Archaean Eon caused by the Late Heavy Bombardment is hypothesized had favored the hydrogenotrophic early life on Earth. The energy of the asteroid collisions was estimated between 10^{24} and 10^{26} J (Sleep and Zoback, 2007) and such an energy input would induce extensive co- and postseismic fracturing in the early crust; in particular, the impact and its subsequently induced seismic activities created new cracks, cavities, or through-going new faults (Sleep and Zoback, 2007; Lowe, 2013) which would benefit the growth and replication of the hydrogenotrophic early life by creating habitats with largely H_2 releases.

5.4 Conclusion

This thesis provides insights into the microbial community in a CO_2 degassing mofette and in its correlated deep subsurface sediment from the Hartoušov mofette field of the western Eger Rift region. This thesis additionally expands our knowledge on geo–bio

interactions in extreme environments with elevated CO_2 concentrations and seismic activity.

The investigation of the microbial communities in the mofette and the deep subsurface CO_2-saturated degassing environment indicates that the microbial community varies independently from the lithology setup over the entire explored core interval. The hypoxic to anaerobic conditions, low pH, high TOC content, and relatively high sulfate concentration in the mofette favor the occurrence of anaerobic, acidophilic taxa as well as SRBs and methanogens. The lithological setup of the deep subsurface sediment represents a paleo-environmental change from a terrestrial, swamp-like ecosystem to a lacustrine ecosystem. This subsurface system became overprinted by migration and the accumulation of geogenic CO_2, which forms a potential habitat for a specialized microbial community but lack evidence to support the "hotspot" hypothesis. In addition, our results imply that the high relative abundance of *Acidovorax* and *Aquabacterium*, as well as of members of uncultured and unknown genera of the family *Comamonadaceae* can be indicative of CO_2-dominated deep subsurface ecosystems and novel high CO_2-adapted species remain to be discovered. In summary, The degassing of mantle-derived CO_2 and mobilized high-saline mineral water strongly influence the microbial communities in both surface and subsurface environments (**Figure 16**).

This thesis further investigated the potential of methane production in the mofette and deep subsurface sediments. The simulation of a seismic event and the link between the simulation results and the field observation – which was revealed via a subsequent modeling procedure – led to the conclusion that seismic activity can potentially trigger methanogenic activity due to the release of geogenic H_2 (**Figure 16**). The biological methane production is hypothesized to have benefited from the seismic activity, which leads to the release of H_2 during the Late Heavy Bombardment in the Archaean Eon and could support early life on Earth.

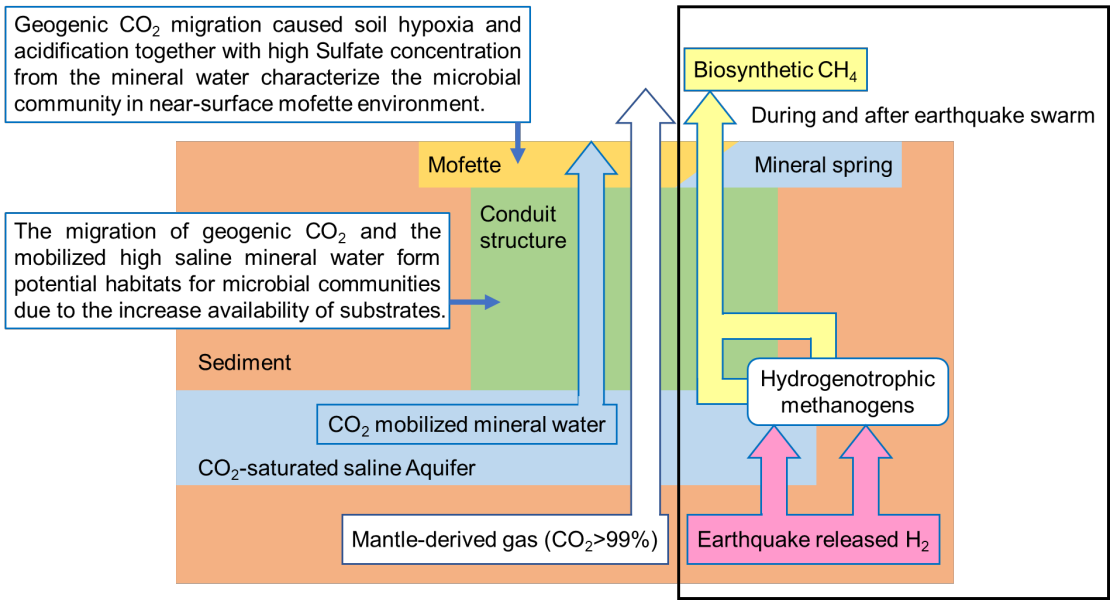

Figure 16 Graphic summary of the thesis, indicating the influence of geogenic CO_2 and earthquake swarm on the microbial communities in both surface and subsurface environments.

5.5 Outlook

This thesis provides insights into the geo–bio interactions between the microbial communities and the geological activities with geochemical, molecular ecological, and cultivation-based activity test methods. This thesis points out a highly CO_2-adapted microbial community in a sulfate-rich saline aquifer. However, a large fraction of yet undescribed microorganisms were revealed via 16S rRNA sequencing and lipid biomarker analyses. The metabolic capacities of these undescribed microorganisms are unclear. Furthermore, the accurate description of the metabolic capacity based on individual microbial taxa is vague due to the demonstrated mixotrophic growth of autotrophs (Wu et al., 2016; Probst et al., 2017). In order to investigate the metabolic potential of the entire community, metagenome-based analyses should be carried out in the future. Probst et al. (2017) analyzed the carbon cycle in a subsurface high-CO_2 aquifer in Crystal Geyser (Utah, USA) and indicated H_2 as an important inter-species energy currency even under gaseous CO_2-saturation. As a study prospect, the

metagenomic analysis can provide deep insights into the geo-bio interaction by unraveling the functional repertoire of the communities.

Moreover, this thesis also reveals a close relationship between seismic activity and biological methane production via earthquake-induced H_2 release. Based on the lab simulation and modeling, the hypothesis that early life on Earth might be benefited from the earthquake released H_2 could hint the early life study. The life may originate not only from hydrothermal vents but also from environments with the temporary support of earthquake released H_2, such as deep-reaching tectonic faults (Schreiber et al., 2012). The wider range of potential habitats of early life can also be of interest to astrobiological studies that search for life on other planets. A long-term *in situ* monitoring of seismicity, groundwater flow, CO_2 ascending, and microbial variation should be set in the Eger Rift region. The data collected in subsequent seismic activities would develop the understanding of the earthquake favored biological methane production and may further support the above-mentioned hypothesis.

6 References

Alawi, M., Lerm, S., Vetter, A., Wolfgramm, M., Seibt, A., and Würdemann, H. (2011). Diversity of sulfate-reducing bacteria in a plant using deep geothermal energy. *Grundwasser* 16, 105.

Alt, J. C., and Shanks, W. C. (2011). Microbial sulfate reduction and the sulfur budget for a complete section of altered oceanic basalts, IODP Hole 1256D (eastern Pacific). *Earth and Planetary Science Letters* 310, 73–83.

Anantharaman, K., Brown, C. T., Hug, L. A., Sharon, I., Castelle, C. J., Probst, A. J., et al. (2016). Thousands of microbial genomes shed light on interconnected biogeochemical processes in an aquifer system. *Nature communications* 7, 13219.

Ariztegui, D., Thomas, C., and Vuillemin, A. (2015). Present and future of subsurface biosphere studies in lacustrine sediments through scientific drilling. *International Journal of Earth Sciences* 104, 1655–1665.

Bale, N. J., Sorokin, D. Y., Hopmans, E. C., Koenen, M., Rijpstra, W. I. C., Villanueva, L., et al. (2019). New Insights Into the Polar Lipid Composition of Extremely Halo(alkali)philic Euryarchaea From Hypersaline Lakes. *Front. Microbiol.* 10, 377.

Bankwitz, P., Bankwitz, E., Brauer, K., Kampf, H., and Storr, M. (2003a). Deformation structures in Plio-and Pleistocene sediments (NW Bohemia, central Europe). *Special Publication-Geological Society of London* 216, 73–94.

Bankwitz, P., Schneider, G., Kämpf, H., and Bankwitz, E. (2003b). Structural characteristics of epicentral areas in Central Europe: study case Cheb Basin (Czech Republic). *J. Geodyn.* 35, 5–32.

Barbier, B. A., Dziduch, I., Liebner, S., Ganzert, L., Lantuit, H., Pollard, W., et al. (2012). Methane-cycling communities in a permafrost-affected soil on Herschel Island, Western Canadian Arctic: active layer profiling of mcrA and pmoA genes. *FEMS Microbiol Ecol* 82, 287–302.

Beaubien, S. E., Ciotoli, G., COOMBS, P., DICTOR, M., Krüger, M., LOMBARDI, S., et al. (2008). The impact of a naturally occurring CO2 gas vent on the shallow

ecosystem and soil chemistry of a Mediterranean pasture (Latera, Italy). *Int. J. Greenhouse Gas Control* 2, 373–387.

Ben-Dov, E., Brenner, A., and Kushmaro, A. (2007). Quantification of Sulfate-reducing Bacteria in Industrial Wastewater, by Real-time Polymerase Chain Reaction (PCR) Using dsrA and apsA Genes. *Microb. Ecol.* 54, 439–451.

Beulig, F., Heuer, V. B., Akob, D. M., Viehweger, B., Elvert, M., Herrmann, M., et al. (2015). Carbon flow from volcanic CO2 into soil microbial communities of a wetland mofette. *The ISME journal* 9, 746–759.

Beulig, F., Urich, T., Nowak, M., Trumbore, S. E., Gleixner, G., Gilfillan, G. D., et al. (2016). Altered carbon turnover processes and microbiomes in soils under long-term extremely high CO2 exposure. *Nature microbiology* 1, 15025.

Biddle, J. F., White, J. R., Teske, A. P., and House, C. H. (2011). Metagenomics of the subsurface Brazos-Trinity Basin (IODP site 1320): comparison with other sediment and pyrosequenced metagenomes. *The ISME journal* 5, 1038–1047.

Blagodatskaya, E., Blagodatsky, S., Dorodnikov, M., and Kuzyakov, Y. (2010). Elevated atmospheric CO 2 increases microbial growth rates in soil: results of three CO 2 enrichment experiments. *Global Change Biol.* 16, 836–848.

Blazejak, A., and Schippers, A. (2011). Real-Time PCR Quantification and Diversity Analysis of the Functional Genes aprA and dsrA of Sulfate-Reducing Prokaryotes in Marine Sediments of the Peru Continental Margin and the Black Sea. *Frontiers in microbiology* 2, 253.

Bligh, E. G., and Dyer, W. J. (1959). A Rapid Method of Total Lipid Extraction and Purification. *Can. J. Biochem. Physiol.* 37, 911–917.

Blume, H.-P., and Felix-Henningsen, P. (2009). Reductosols: Natural soils and Technosols under reducing conditions without an aquic moisture regime. *J. Plant Nutr. Soil Sci.* 172, 808–820.

Blume, H.-P., Stahr, K., and Leinweber, P. (2011). *Bodenkundliches Praktikum: Eine Einführung in pedologisches Arbeiten für Ökologen, Land-und Forstwirte, Geo-und Umweltwissenschaftler*. Springer-Verlag.

Bolger, A. M., Lohse, M., and Usadel, B. (2014). Trimmomatic: a flexible trimmer for Illumina sequence data. *Bioinformatics (Oxford, England)* 30, 2114–2120.

Borgonie, G., García-Moyano, A., Litthauer, D., Bert, W., Bester, A., van Heerden, E., et al. (2011). Nematoda from the terrestrial deep subsurface of South Africa. *Nature* 474, 79–82.

Brandariz-Fontes, C., Camacho-Sanchez, M., Vilà, C., Vega-Pla, J. L., Rico, C., and Leonard, J. A. (2015). Effect of the enzyme and PCR conditions on the quality of high-throughput DNA sequencing results. *Scientific reports* 5, 8056.

Bräuer, K., Kämpf, H., Faber, E., Koch, U., Nitzsche, H.-M., and Strauch, G. (2005). Seismically triggered microbial methane production relating to the Vogtland NW Bohemia earthquake swarm period 2000, Central Europe. *Geochem. J.* 39, 441–450.

Bräuer, K., Kämpf, H., Koch, U., Niedermann, S., and Strauch, G. (2007). Seismically induced changes of the fluid signature detected by a multi-isotope approach (He, CO 2, CH 4, N 2) at the Wettinquelle, Bad Brambach (central Europe). *J. Geophys. Res.* 112, 301.

Bräuer, K., Kämpf, H., Koch, U., and Strauch, G. (2011). Monthly monitoring of gas and isotope compositions in the free gas phase at degassing locations close to the Nový Kostel focal zone in the western Eger Rift¸ Czech Republic. *Chemical Geology* 290, 163–176.

Bräuer, K., Kämpf, H., Niedermann, S., and Strauch, G. (2018). Monitoring of helium and carbon isotopes in the western Eger Rift area (Czech Republic): Relationships with the 2014 seismic activity and indications for recent (2000–2016) magmatic unrest. *Chem. Geol.* 482, 131–145.

Bräuer, K., Kämpf, H., Niedermann, S., Strauch, G., and Tesař, J. (2008). Natural laboratory NW Bohemia: Comprehensive fluid studies between 1992 and 2005 used to trace geodynamic processes. *Geochem. Geophys. Geosyst.* 9, n/a-n/a.

Bräuer, K., Kämpf, H., Strauch, G., and Weise, S. M. (2003). Isotopic evidence (3 He/ 4 He, of fluid-triggered intraplate seismicity. *J. Geophys. Res.* 108, 238.

Bräuer, S. L., Cadillo-Quiroz, H., Ward, R. J., Yavitt, J. B., and Zinder, S. H. (2011). Methanoregula boonei gen. nov., sp. nov., an acidiphilic methanogen isolated from an acidic peat bog. *International journal of systematic and evolutionary microbiology* 61, 45–52.

Breuker, A., Köweker, G., Blazejak, A., and Schippers, A. (2011). The deep biosphere in terrestrial sediments in the chesapeake bay area, virginia, USA. *Frontiers in microbiology* 2, 156.

Breuker, A., Stadler, S., and Schippers, A. (2013). Microbial community analysis of deeply buried marine sediments of the New Jersey shallow shelf (IODP Expedition 313). *FEMS microbiology ecology* 85, 578–592.

Bucha, V., Horáček, J., and Malkovský, M. (1990). Palaeomagnetic stratigraphy of the Tertiary of the Cheb Basin (W Bohemia). *Věstník Ústředního ústavu geologického 65 (5)*, 267–278.

Bussert, R., Kämpf, H., Flechsig, C., Hesse, K., Nickschick, T., Liu, Q., et al. (2017). Drilling into an active mofette: pilot-hole study of the impact of CO2-rich mantle-derived fluids on the geo–bio interaction in the western Eger Rift (Czech Republic). *Sci. Dril.* 23, 13–27.

Cadillo-Quiroz, H., Yavitt, J. B., and Zinder, S. H. (2009). Methanosphaerula palustris gen. nov., sp. nov., a hydrogenotrophic methanogen isolated from a minerotrophic fen peatland. *International journal of systematic and evolutionary microbiology* 59, 928–935.

Caporaso, J. G., Kuczynski, J., Stombaugh, J., Bittinger, K., Bushman, F. D., Costello, E. K., et al. (2010). QIIME allows analysis of high-throughput community sequencing data. *Nature methods* 7, 335–336.

Caporaso, J. G., Lauber, C. L., Walters, W. A., Berg-Lyons, D., Lozupone, C. A., Turnbaugh, P. J., et al. (2011). Global patterns of 16S rRNA diversity at a depth of millions of sequences per sample. *PNAS* 108 Suppl 1, 4516–4522.

Chapelle, F. H., O'Neill, K., Bradley, P. M., Methé, B. A., Ciufo, S. A., Knobel, L. L., et al. (2002). A hydrogen-based subsurface microbial community dominated by methanogens. *Nature* 415, 312.

Chiodini, G., Caliro, S., Cardellini, C., Avino, R., Granieri, D., and Schmidt, A. (2008). Carbon isotopic composition of soil CO2 efflux, a powerful method to discriminate different sources feeding soil CO2 degassing in volcanic-hydrothermal areas. *Earth Planet. Sci. Lett.* 274, 372–379.

Chyba, C. F. (1993). The violent environment of the origin of life: Progress and uncertainties. *Geochimica et Cosmochimica Acta* 57, 3351–3358.

Claeys, P., and Morbidelli, A. (2011). "Late Heavy Bombardment," in *Encyclopedia of astrobiology*, eds. M. Gargaud, and R. Amils (Heidelberg: Springer), 909–912.

Dahm, T., Hrubcová, P., Fischer, T., Horálek, J., Korn, M., Buske, S., et al. (2013). Eger Rift ICDP: an observatory for study of non-volcanic, mid-crustal earthquake swarms and accompanying phenomena. *Sci. Dril.* 16, 93–99.

Deflaun, M. F., Fredrickson, J. K., Dong, H., Pfiffner, S. M., Onstott, T. C., Balkwill, D. L., et al. (2007). Isolation and characterization of a Geobacillus thermoleovorans strain from an ultra-deep South African gold mine. *Systematic and applied microbiology* 30, 152–164.

Degelmann, D. M., Borken, W., Drake, H. L., and Kolb, S. (2010). Different atmospheric methane-oxidizing communities in European beech and Norway spruce soils. *Applied and environmental microbiology* 76, 3228–3235.

DeSantis, T. Z., Hugenholtz, P., Larsen, N., Rojas, M., Brodie, E. L., Keller, K., et al. (2006). Greengenes, a chimera-checked 16S rRNA gene database and workbench compatible with ARB. *Applied and environmental microbiology* 72, 5069–5072.

D'Hondt, S., Rutherford, S., and Spivack, A. J. (2002). Metabolic activity of subsurface life in deep-sea sediments. *Science (New York, N.Y.)* 295, 2067–2070.

Dobeš, M., Hercog, F., and Mazáč, F. (1986). Die geophysikalische Untersuchung der hydrogeologischen Strukturen im Cheb-Becken. *Sbor geol věd, Užitá geofyz* 21, 117–158.

Dodd, M. S., Papineau, D., Grenne, T., Slack, J. F., Rittner, M., Pirajno, F., et al. (2017). Evidence for early life in Earth's oldest hydrothermal vent precipitates. *nature* 543, 60–64.

Edgar, R. C. (2010). Search and clustering orders of magnitude faster than BLAST. *Bioinformatics (Oxford, England)* 26, 2460–2461.

Emerson, D., and Moyer, C. (1997). Isolation and characterization of novel iron-oxidizing bacteria that grow at circumneutral pH. *Applied and environmental microbiology* 63, 4784–4792.

Emiliani, C. (1992). *Planet earth: Cosmology, geology, and the evolution of life and environment / Cesare Emiliani*. Cambridge: Cambridge University Press.

Evans, P. N., Parks, D. H., Chadwick, G. L., Robbins, S. J., Orphan, V. J., Golding, S. D., et al. (2015). Methane metabolism in the archaeal phylum Bathyarchaeota revealed by genome-centric metagenomics. *Science (New York, N.Y.)* 350, 434–438.

Fernández-Montiel, I., Pedescoll, A., and Bécares, E. (2016a). Microbial communities in a range of carbon dioxide fluxes from a natural volcanic vent in Campo de Calatrava, Spain. *Int. J. Greenhouse Gas Control* 50, 70–79.

Fernández-Montiel, I., Sidrach-Cardona, R., Gabilondo, R., Pedescoll, A., Scheu, S., and Bécares, E. (2016b). Soil communities are affected by CO2 belowground emissions at a natural vent in Spain. *Soil Biol. Biochem.* 97, 92–98.

Fischer, C., and Luttge, A. (2017). Beyond the conventional understanding of water–rock reactivity. *Earth and Planetary Science Letters* 457, 100–105.

Fischer, T. (2003). Space-time distribution of earthquake swarms in the principal focal zone of the NW Bohemia/Vogtland seismoactive region: period 1985–2001. *Journal of Geodynamics* 35, 125–144.

Fischer, T., Horálek, J., Hrubcová, P., Vavryčuk, V., Bräuer, K., and Kämpf, H. (2014). Intra-continental earthquake swarms in West-Bohemia and Vogtland: A review. *Tectonophysics* 611, 1–27.

Fischer, T., Matyska, C., and Heinicke, J. (2017). Earthquake-enhanced permeability – evidence from carbon dioxide release following the M L 3.5 earthquake in West Bohemia. *Earth and Planetary Science Letters* 460, 60–67.

Flechsig, C., Bussert, R., Rechner, J., Schütze, C., and Kämpf, H. (2008). The Hartoušov Mofette field in the Cheb Basin, Western Eger Rift (Czech Republic): a comperative geoelectric, sedimentologic and soil gas study of a magmatic diffuse CO 2-degassing structure. *Z. Geol. Wiss.* 36, 177–193.

Frerichs, J., Oppermann, B. I., Gwosdz, S., Möller, I., Herrmann, M., and Krüger, M. (2013). Microbial community changes at a terrestrial volcanic CO2 vent induced by soil acidification and anaerobic microhabitats within the soil column. *FEMS microbiology ecology* 84, 60–74.

Froelich, P. N., Klinkhammer, G. P., Bender, M. L., Luedtke, N. A., Heath, G. R., Cullen, D., et al. (1979). Early oxidation of organic matter in pelagic sediments of the eastern equatorial Atlantic: suboxic diagenesis. *Geochimica et Cosmochimica Acta* 43, 1075–1090.

Geissler, W. H., Kämpf, H., Bankwitz, P., and Bankwitz, E. (2004). The Quaternary tephra-tuff deposit of Mýtina (southern rim of the western Eger Graben/Czech Republic): Indications for eruption and deformation processes. *Zeitschrift für Geologische Wissenschaften* 32, 31–54.

Girault, F., and Perrier, F. (2014). The Syabru-Bensi hydrothermal system in central Nepal: 2. Modeling and significance of the radon signature. *J. Geophys. Res. Solid Earth* 119, 4056–4089.

Girault, F., Perrier, F., Crockett, R., Bhattarai, M., Koirala, B. P., France-Lanord, C., et al. (2014). The Syabru-Bensi hydrothermal system in central Nepal: 1. Characterization of carbon dioxide and radon fluxes. *J. Geophys. Res. Solid Earth* 119, 4017–4055.

Gold, T. (1992). The deep, hot biosphere. *Proceedings of the National Academy of Sciences* 89, 6045–6049.

Goldscheider, N., Meiman, J., Pronk, M., and Smart, C. (2008). Tracer tests in karst hydrogeology and speleology. *IJS* 37, 27–40.

Großkopf, R., Stubner, S., and Liesack, W. (1998). Novel euryarchaeotal lineages detected on rice roots and in the anoxic bulk soil of flooded rice microcosms. *Applied and environmental microbiology* 64, 4983–4989.

Gulliver, D., Lipus, D., Ross, D., and Bibby, K. (2018). Insights into microbial community structure and function from a shallow, simulated CO2 -leakage aquifer demonstrate microbial selection and adaptation. *Environmental microbiology reports*. doi: 10.1111/1758-2229.12675 [Epub ahead of print].

Hainzl, S., Fischer, T., Čermáková, H., Bachura, M., and Vlček, J. (2016). Aftershocks triggered by fluid intrusion: Evidence for the aftershock sequence occurred 2014 in West Bohemia/Vogtland. *Journal of Geophysical Research: Solid Earth* 121, 2575–2590.

Hainzl, S., and Ogata, Y. (2005). Detecting fluid signals in seismicity data through statistical earthquake modeling. *Journal of Geophysical Research: Solid Earth*. 110. doi: 10.1029/2004JB003247@10.1002/(ISSN)2169-9356.STET1 [Epub ahead of print].

Hallbeck, L., and Pedersen, K. (1990). Culture parameters regulating stalk formation and growth rate of Gallionella ferruginea. *J. Gen. Microbiol.* 136, 1675–1680.

Ham, B., Choi, B.-Y., Chae, G.-T., Kirk, M. F., and Kwon, M. J. (2017). Geochemical Influence on Microbial Communities at CO2-Leakage Analog Sites. *Frontiers in microbiology* 8, 2203.

Hammer, Ø., Harper, D. A.T., and Ryan, P. D. (2001). PAST-palaeontological statistics, ver. 1.89. *Palaeontol electron* 4, 1–9.

He, Y., Li, M., Perumal, V., Feng, X., Fang, J., Xie, J., et al. (2016). Genomic and enzymatic evidence for acetogenesis among multiple lineages of the archaeal phylum Bathyarchaeota widespread in marine sediments. *Nature microbiology* 1, 16035.

Hernsdorf, A. W., Amano, Y., Miyakawa, K., Ise, K., Suzuki, Y., Anantharaman, K., et al. (2017). Potential for microbial H_2 and metal transformations associated with novel bacteria and archaea in deep terrestrial subsurface sediments. *The ISME journal* 11, 1915.

Hinrichs, K.-U., Hayes, J. M., Bach, W., Spivack, A. J., Hmelo, L. R., Holm, N. G., et al. (2006). Biological formation of ethane and propane in the deep marine subsurface. *Proceedings of the National Academy of Sciences of the United States of America* 103, 14684–14689.

Hoefs, J. (2018). *Stable isotope geochemistry*. Cham, Switzerland: Springer.

Hohberg, K., Schulz, H.-J., Balkenhol, B., Pilz, M., Thomalla, A., Russell, D. J., et al. (2015). Soil faunal communities from mofette fields: Effects of high geogenic carbon dioxide concentration. *Soil Biol. Biochem.* 88, 420–429.

Hrubcová, P., Geissler, W. H., Bräuer, K., Vavryčuk, V., Tomek, Č., and Kämpf, H. (2017). Active Magmatic Underplating in Western Eger Rift, Central Europe. *Tectonics* 36, 2846–2862.

Huang, X., Meyers, P. A., Xue, J., Gong, L., Wang, X., and Xie, S. (2015). Environmental factors affecting the low temperature isomerization of homohopanes in acidic peat deposits, central China. *Geochimica et Cosmochimica Acta* 154, 212–228.

Ibs-von Seht, M., Plenefisch, T., and Klinge, K. (2008). Earthquake swarms in continental rifts — A comparison of selected cases in America, Africa and Europe. *Tectonophysics* 452, 66–77.

Inagaki, F., Hinrichs, K.-U., Kubo, Y., Bowles, M. W., Heuer, V. B., Hong, W.-L., et al. (2015). DEEP BIOSPHERE. Exploring deep microbial life in coal-bearing sediment down to ~2.5 km below the ocean floor. *Science (New York, N.Y.)* 349, 420–424.

Inagaki, F., Takai, K., Nealson, K. H., and Horikoshi, K. (2004). Sulfurovum lithotrophicum gen. nov., sp. nov., a novel sulfur-oxidizing chemolithoautotroph within the epsilon-Proteobacteria isolated from Okinawa Trough hydrothermal sediments. *International journal of systematic and evolutionary microbiology* 54, 1477–1482.

Inglis, G. N., Naafs, B. D. A., Zheng, Y., McClymont, E. L., Evershed, R. P., and Pancost, R. D. (2018). Distributions of geohopanoids in peat: Implications for the use of hopanoid-based proxies in natural archives. *Geochimica et Cosmochimica Acta* 224, 249–261.

Inguaggiato, S., Cardellini, C., Taran, Y., and Kalacheva, E. (2017). The CO 2 flux from hydrothermal systems of the Karymsky volcanic Centre, Kamchatka. *J. Volcanol. Geotherm. Res.* 346, 1–9.

Ivanov, B. A. (2005). Numerical Modeling of the Largest Terrestrial Meteorite Craters. *Solar System Research* 39, 381–409.

Johnson, D. B., Bacelar-Nicolau, P., Okibe, N., Thomas, A., and Hallberg, K. B. (2009). Ferrimicrobium acidiphilum gen. nov., sp. nov. and Ferrithrix thermotolerans gen. nov., sp. nov. heterotrophic, iron-oxidizing, extremely acidophilic actinobacteria. *International journal of systematic and evolutionary microbiology* 59, 1082–1089.

Johnson, D. B., Hallberg, K. B., and Hedrich, S. (2014). Uncovering a microbial enigma: isolation and characterization of the streamer-generating, iron-oxidizing, acidophilic bacterium "Ferrovum myxofaciens". *Applied and environmental microbiology* 80, 672–680.

Jorgensen, S. L., Hannisdal, B., Lanzén, A., Baumberger, T., Flesland, K., Fonseca, R., et al. (2012). Correlating microbial community profiles with geochemical data in highly stratified sediments from the Arctic Mid-Ocean Ridge. *Proceedings of the National Academy of Sciences of the United States of America* 109, E2846-55.

Jørgensen BoBarker (1978). A comparison of methods for the quantification of bacterial sulfate reduction in coastal marine sediments. *Geomicrobiology Journal* 1, 29–47.

Kallmeyer, J., Pockalny, R., Adhikari, R. R., Smith, D. C., and D'Hondt, S. (2012). Global distribution of microbial abundance and biomass in subseafloor sediment. *Proceedings of the National Academy of Sciences of the United States of America* 109, 16213–16216.

Kallmeyer, J., and Wagner, D. (2014). *Microbial life of the deep biosphere*. Berlin, Boston: De Gruyter.

Kämpf, H., Bräuer, K., Schumann, J., Hahne, K., and Strauch, G. (2013). CO2 discharge in an active, non-volcanic continental rift area (Czech Republic): Characterisation (δ13C, 3He/4He) and quantification of diffuse and vent CO2 emissions. *Chem. Geol.* 339, 71–83.

Kämpf, H., Broge, A. S., Marzban, P., Allahbakhshi, M., and Nickschick, T. (2019). Nonvolcanic Carbon Dioxide Emission at Continental Rifts: The Bublak Mofette Area, Western Eger Rift, Czech Republic. *Geofluids*. 2019. doi: 10.1155/2019/4852706 [Epub ahead of print].

Kämpf, H., Geissler, W. H., and Bräuer, K. (2007). “Combined Gas-geochemical and Receiver Function Studies of the Vogtland/NW Bohemia Intraplate Mantle Degassing Field, Central Europe,” in *Mantle Plumes: A Multidisciplinary Approach*, eds. J. R. R. Ritter, and U. R. Christensen (Berlin, Heidelberg: Springer Berlin Heidelberg), 127–158.

Kämpf, H., Peterek, A., Rohrmüller, J., Kümpel, H. J., and Geissler, W. (2005). The KTB deep crustal laboratory and the western Eger Graben. *In: GeoErlangen 2005: Exkursionsführer, Ed. Koch, R.; Röhling, H.-G., GeoErlangen 2005: System Earth-Biosphere Coupling/Regional Geology of Central Europe (Erlangen 2005), 2005. 37-107 p., Schriftenreihe der Deutschen Gesellschaft für Geowissenschaften*.

Kelly, D. P., and Wood, A. P. (2000). Reclassification of some species of Thiobacillus to the newly designated genera Acidithiobacillus gen. nov., Halothiobacillus gen. nov. and Thermithiobacillus gen. nov. *International journal of systematic and evolutionary microbiology* 50 Pt 2, 511–516.

Kies, A., Hengesch, O., Tosheva, Z., Raschi, A., and Pfanz, H. (2015). Diurnal CO 2 - cycles and temperature regimes in a natural CO 2 gas lake. *International Journal of Greenhouse Gas Control* 37, 142–145.

Kita, I., Matsuo, S., and Wakita, H. (1982). H 2 generation by reaction between H 2 O and crushed rock: An experimental study on H 2 degassing from the active fault zone. *J. Geophys. Res. Solid Earth* 87, 10789–10795.

Kopecký, L. (1979). Magmatism of the Ohre rift in the Bohemian Massif, its relationship to the deep fault tectonics and to the geologic evolution, and its ore mineralisation. *Czechoslovak geology and global tectonics. Veda, Bratislava*, 167–181.

Krauze, P., Kämpf, H., Horn, F., Liu, Q., Voropaev, A., Wagner, D., et al. (2017). Microbiological and Geochemical Survey of CO2-Dominated Mofette and Mineral Waters of the Cheb Basin, Czech Republic. *Frontiers in microbiology* 8, 2446.

Kristjansson, J. K., Schönheit, P., and Thauer, R. K. (1982). Different Ks values for hydrogen of methanogenic bacteria and sulfate reducing bacteria: An explanation for the apparent inhibition of methanogenesis by sulfate. *Archives of Microbiology* 131, 278–282.

Krüger, M., Jones, D., Frerichs, J., Oppermann, B. I., West, J., Coombs, P., et al. (2011). Effects of elevated CO2 concentrations on the vegetation and microbial populations at a terrestrial CO2 vent at Laacher See, Germany. *Int. J. Greenhouse Gas Control* 5, 1093–1098.

Krüger, M., West, J., Frerichs, J., Oppermann, B., Dictor, M.-C., Jouliand, C., et al. (2009). Ecosystem effects of elevated CO2 concentrations on microbial populations at a terrestrial CO2 vent at Laacher See, Germany. *Energy Procedia* 1, 1933–1939.

Kubo, K., Lloyd, K. G., F Biddle, J., Amann, R., Teske, A., and Knittel, K. (2012). Archaea of the Miscellaneous Crenarchaeotal Group are abundant, diverse and widespread in marine sediments. *The ISME journal* 6, 1949–1965.

Kysela, D. T., Palacios, C., and Sogin, M. L. (2005). Serial analysis of V6 ribosomal sequence tags (SARST-V6): a method for efficient, high-throughput analysis of microbial community composition. *Environmental microbiology* 7, 356–364.

Lane, D. J. (1991). 16S/23S rRNA sequencing. In 'Nucleic acid techniques in bacterial systematics'.(Eds E Stackebrandt, M Goodfellow) pp. 115–175. John Wiley and Sons: Chichester, UK.

Lerm, S., Westphal, A., Miethling-Graff, R., Alawi, M., Seibt, A., Wolfgramm, M., et al. (2013). Thermal effects on microbial composition and microbiologically induced corrosion and mineral precipitation affecting operation of a geothermal plant in a deep saline aquifer. *Extremophiles* 17, 311–327.

Lin, L.-H., Hall, J., Lippmann-Pipke, J., Ward, J. A., Sherwood Lollar, B., DeFlaun, M., et al. (2005). Radiolytic H 2 in continental crust: Nuclear power for deep subsurface microbial communities. *Geochem. Geophys. Geosyst.* 6, n/a-n/a.

Liu, Q., Kämpf, H., Bussert, R., Krauze, P., Horn, F., Nickschick, T., et al. (2018). Influence of CO2 Degassing on the Microbial Community in a Dry Mofette Field in Hartoušov, Czech Republic (Western Eger Rift). *Front. Microbiol.* 9, 2787.

Logemann, J., Graue, J., Köster, J., Engelen, B., Rullkötter, J., and Cypionka, H. (2011). A laboratory experiment of intact polar lipid degradation in sandy sediments. *Biogeosciences* 8, 2547–2560.

Lomstein, B. A., Langerhuus, A. T., D'Hondt, S., Jørgensen, B. B., and Spivack, A. J. (2012). Endospore abundance, microbial growth and necromass turnover in deep sub-seafloor sediment. *Nature* 484, 101–104.

Losey, N. A., Stevenson, B. S., Busse, H.-J., Sinninghe Damsté, J. S., Rijpstra, W. I. C., Rudd, S., et al. (2013). Thermoanaerobaculum aquaticum gen. nov., sp. nov., the first cultivated member of Acidobacteria subdivision 23, isolated from a hot

spring. *International journal of systematic and evolutionary microbiology* 63, 4149–4157.

Lowe, D. R. (2013). Crustal fracturing and chert dike formation triggered by large meteorite impacts, ca. 3.260 Ga, Barberton greenstone belt, South Africa. *GSA Bulletin* 125, 894–912.

Luef, B., Frischkorn, K. R., Wrighton, K. C., Holman, H.-Y. N., Birarda, G., Thomas, B. C., et al. (2015). Diverse uncultivated ultra-small bacterial cells in groundwater. *Nature communications* 6, 6372.

Mannista, M. K., Tiirola, M., and Haggblom, M. M. (2007). Bacterial communities in Arctic fjelds of Finnish Lapland are stable but highly pH-dependent. *FEMS Microbiol. Ecol.* 59, 452–465.

Maher, K. A., and Stevenson, D. J. (1988). Impact frustration of the origin of life. *nature* 331, 612–614.

Mangelsdorf, K., Karger, C., and Zink, K.-G. (2019). "Phospholipids as Life Markers in Geological Habitats," in *Hydrocarbons, oils and lipids: Diversity, origin, chemistry and fate*, ed. H. Wilkes (Cham: Springer), 1–29.

Mangelsdorf, K., Zink, K.-G., Di Primio, R., and Horsfield, B. (2011). Microbial lipid markers within and adjacent to Challenger Mound in the Belgica carbonate mound province, Porcupine Basin, offshore Ireland (IODP Expedition 307). *Marine Geology* 282, 91–101.

Martin, M. (2011). Cutadapt removes adapter sequences from high-throughput sequencing reads. *EMBnet j.* 17, 10.

Martin, W., Baross, J., Kelley, D., and Russell, M. J. (2008). Hydrothermal vents and the origin of life. *Nat Rev Microbiol* 6, 805–814.

Martin, W., and Russell, M. J. (2007). On the origin of biochemistry at an alkaline hydrothermal vent. *Philosophical transactions of the Royal Society of London. Series B, Biological sciences* 362, 1887–1925.

McFarland, J. W., Waldrop, M. P., and Haw, M. (2013). Extreme CO2 disturbance and the resilience of soil microbial communities. *Soil Biology and Biochemistry* 65, 274–286.

McMahon, S., and Parnell, J. (2014). Weighing the deep continental biosphere. *FEMS microbiology ecology* 87, 113–120.

Mehlhorn, J., Besold, J., Lezama Pacheco, J. S., Gustafsson, J. P., Kretzschmar, R., and Planer-Friedrich, B. (2018). Copper Mobilization and Immobilization along an Organic Matter and Redox Gradient-Insights from a Mofette Site. *Environmental science & technology* 52, 13698–13707.

Mehlhorn, J., Beulig, F., Küsel, K., and Planer-Friedrich, B. (2014). Carbon dioxide triggered metal(loid) mobilisation in a mofette. *Chem. Geol.* 382, 54–66.

Mehlhorn, J., Byrne, J. M., Kappler, A., and Planer-Friedrich, B. (2016). Time and temperature dependency of carbon dioxide triggered metal(loid) mobilization in soil. *Appl. Geochem.* 74, 122–137.

Meyers, P. A. (1997). Organic geochemical proxies of paleoceanographic, paleolimnologic, and paleoclimatic processes. *Organic Geochemistry* 27, 213–250.

Meyers, P. A. (2003). Applications of organic geochemistry to paleolimnological reconstructions: a summary of examples from the Laurentian Great Lakes. *Organic Geochemistry* 34, 261–289.

Middelburg, J. J. (1989). A simple rate model for organic matter decomposition in marine sediments. *Geochimica et Cosmochimica Acta* 53, 1577–1581.

Morales, S. E., and Holben, W. E. (2013). Functional response of a near-surface soil microbial community to a simulated underground CO2 storage leak. *PloS one* 8, e81742.

Morono, Y., Terada, T., Nishizawa, M., Ito, M., Hillion, F., Takahata, N., et al. (2011). Carbon and nitrogen assimilation in deep subseafloor microbial cells. *Proceedings of the National Academy of Sciences of the United States of America* 108, 18295–18300.

Mrlina, J., Kämpf, H., Kroner, C., Mingram, J., Stebich, M., Brauer, A., et al. (2009). Discovery of the first Quaternary maar in the Bohemian Massif, Central Europe, based on combined geophysical and geological surveys. *J. Volcanol. Geotherm. Res.* 182, 97–112.

Mu, A., Boreham, C., Leong, H. X., Haese, R. R., and Moreau, J. W. (2014). Changes in the deep subsurface microbial biosphere resulting from a field-scale CO2 geosequestration experiment. *Frontiers in microbiology* 5, 209.

Müller, K.-D., Nalik, H. P., Schmid, E. N., Husmann, H., and Schomburg, G. (1993). Fast identification of mycobacterium species by GC analysis with trimethylsulfonium hydroxide (TMSH) for transesterification. *Journal of High Resolution Chromatography* 16, 161–165.

Naeher, S., Niemann, H., Peterse, F., Smittenberg, R. H., Zigah, P. K., and Schubert, C. J. (2014). Tracing the methane cycle with lipid biomarkers in Lake Rotsee (Switzerland). *Organic Geochemistry* 66, 174–181.

Nealson, K. H. (2005). Hydrogen and energy flow as "sensed" by molecular genetics. *Proceedings of the National Academy of Sciences of the United States of America* 102, 3889–3890.

Nealson, K. H. (1997). Microorganisms and biogeochemical cycles:What can we learn from layered microbial communities? *Reviews in mineralogy* 35, 3–34.

Nickschick, T., Flechsig, C., Meinel, C., Mrlina, J., and Kämpf, H. (2017). Architecture and temporal variations of a terrestrial CO2 degassing site using electric resistivity tomography and self-potential. *Int J Earth Sci (Geol Rundsch)* 106, 2915–2926.

Nickschick, T., Kämpf, H., Flechsig, C., Mrlina, J., and Heinicke, J. (2015). CO2 degassing in the Hartoušov mofette area, western Eger Rift, imaged by CO2 mapping and geoelectrical and gravity surveys. *Int. J. Earth Sci.* 104, 2107–2129.

Nowak, M. E., Beulig, F., Fischer, J. von, Muhr, J., Küsel, K., and Trumbore, S. E. (2015). Autotrophic fixation of geogenic CO₂ by microorganisms contributes to soil organic matter formation and alters isotope signatures in a wetland mofette. *Biogeosciences* 12, 7169–7183.

Nunoura, T., Soffientino, B., Blazejak, A., Kakuta, J., Oida, H., Schippers, A., et al. (2009). Subseafloor microbial communities associated with rapid turbidite deposition in the Gulf of Mexico continental slope (IODP Expedition 308). *FEMS microbiology ecology* 69, 410–424.

Nyyssönen, M., Hultman, J., Ahonen, L., Kukkonen, I., Paulin, L., Laine, P., et al. (2014). Taxonomically and functionally diverse microbial communities in deep crystalline rocks of the Fennoscandian shield. *The ISME journal* 8, 126.

Oberbeck, V. R., and Fogleman, G. (1989). Estimates of the maximum time required to originate life. *Origins of life and evolution of the biosphere* 19, 549–560.

Oppermann, B. I., Michaelis, W., Blumenberg, M., Frerichs, J., Schulz, H. M., Schippers, A., et al. (2010). Soil microbial community changes as a result of long-term exposure to a natural CO2 vent. *Geochim. Cosmochim. Acta* 74, 2697–2716.

Oude Elferink, S. J., Akkermans-van Vliet, W. M., Bogte, J. J., and Stams, A. J. (1999). Desulfobacca acetoxidans gen. nov., sp. nov., a novel acetate-degrading sulfate reducer isolated from sulfidogenic granular sludge. *International journal of systematic bacteriology* 49 Pt 2, 345–350.

Pankratov, T. A., Kirsanova, L. A., Kaparullina, E. N., Kevbrin, V. V., and Dedysh, S. N. (2012). Telmatobacter bradus gen. nov., sp. nov., a cellulolytic facultative anaerobe from subdivision 1 of the Acidobacteria, and emended description of Acidobacterium capsulatum Kishimoto et al. 1991. *International journal of systematic and evolutionary microbiology* 62, 430–437.

Patel, G. B., and Sprott, G. D. (1990). Methanosaeta concilii gen. nov., sp. nov. ("Methanothrix concilii") and Methanosaeta thermoacetophila nom. rev., comb. nov. *International journal of systematic bacteriology* 40, 79–82.

Peinado, M., García, J. L., González, E., and Ruiz, A. R. (2009). Itinerarios geográficos y paisajes por la provincia de Ciudad Real. Guía de salidas de campo del XXI Congreso de Geógrafos Españoles.

Pellizzari, L., Neumann, D., Alawi, M., Voigt, D., Norden, B., and Würdemann, H. (2013). The use of tracers to assess drill-mud penetration depth into sandstone cores during deep drilling: method development and application. *Environmental Earth Sciences* 70, 3727–3738.

Pereira, R. P. A., Peplies, J., Brettar, I., and Hoefle, M. G. (2018). Impact of DNA polymerase choice on assessment of bacterial communities by a Legionella genus-specific next-generation sequencing approach. *bioRxiv*, 247445.

Pfanz, H., Vodnik, D., Wittmann, C., Aschan, G., and Raschi, A. (2004). “Plants and Geothermal CO2 Exhalations — Survival in and Adaptation to a High CO2 Environment,” in *Progress in Botany: Genetics Physiology Systematics Ecology*, eds. K. Esser, U. Lüttge, W. Beyschlag, and J. Murata (Berlin, Heidelberg: Springer Berlin Heidelberg), 499–538.

Phelps, T. J., Murphy, E. M., Pfiffner, S. M., and White, D. C. (1994). Comparison between geochemical and biological estimates of subsurface microbial activities. *Microbial Ecology* 28, 335–349.

Phelps, T. J., Ringelberg, D., Hedrick, D., Davis, J., Fliermans, C. B., and White, D. C. (1988). Microbial biomass and activities associated with subsurface environments contaminated with chlorinated hydrocarbons. *Geomicrobiology Journal* 6, 157–170.

Podosokorskaya, O. A., Bonch-Osmolovskaya, E. A., Beskorovaynyy, A. V., Toshchakov, S. V., Kolganova, T. V., and Kublanov, I. V. (2014). Mobilitalea sibirica gen. nov., sp. nov., a halotolerant polysaccharide-degrading bacterium. *International journal of systematic and evolutionary microbiology* 64, 2657–2661.

Probst, A. J., Castelle, C. J., Singh, A., Brown, C. T., Anantharaman, K., Sharon, I., et al. (2017). Genomic resolution of a cold subsurface aquifer community provides metabolic insights for novel microbes adapted to high CO2 concentrations. *Environmental microbiology* 19, 459–474.

Probst, A. J., Ladd, B., Jarett, J. K., Geller-McGrath, D. E., Sieber, C. M. K., Emerson, J. B., et al. (2018). Differential depth distribution of microbial function and putative symbionts through sediment-hosted aquifers in the deep terrestrial subsurface. *Nature microbiology* 3, 328–336.

Quirk, M. M., Wardroper, A.M.K., Wheatley, R. E., and Maxwell, J. R. (1984). Extended hopanoids in peat environments. *Chemical Geology* 42, 25–43.

Radke, M., Willsch, H., and Welte, D. H. (1980). Preparative hydrocarbon group type determination by automated medium pressure liquid chromatography. *Analytical chemistry* 52, 406–411.

Raven, J. A. (1995). The early evolution of land plants: Aquatic ancestors and atmospheric interactions. *Botanical Journal of Scotland* 47, 151–175.

Rennert, T., Eusterhues, K., Pfanz, H., and Totsche, K. U. (2011). Influence of geogenic CO2 on mineral and organic soil constituents on a mofette site in the NW Czech Republic. *Eur. J. Soil Sci.* 62, 572–580.

Rennert, T., and Pfanz, H. (2016). Hypoxic and acidic — Soils on mofette fields. *Geoderma* 280, 73–81.

Rohrmüller, J., Kämpf, H., Geiß, E., Großmann, J., Grun, I., Mingram, J., et al. (2018). Reconnaissance study of an inferred Quaternary maar structure in the western part of the Bohemian Massif near Neualbenreuth, NE-Bavaria (Germany). *Int. J. Earth Sci.* 107, 1381–1405.

Ross, D. J., Tate, K. R., Newton, P. C. D., Wilde, R. H., and Clark, H. (2000). Carbon and nitrogen pools and mineralization in a grassland gley soil under elevated carbon dioxide at a natural CO2 spring. *Global Change Biol* 6, 779–790.

Rütters, H., Sass, H., Cypionka, H., and Rullkötter, J. (2001). Monoalkylether phospholipids in the sulfate-reducing bacteria Desulfosarcina variabilis and Desulforhabdus amnigenus. *Archives of Microbiology* 176, 435–442.

Sáenz, J. P., Grosser, D., Bradley, A. S., Lagny, T. J., Lavrynenko, O., Broda, M., et al. (2015). Hopanoids as functional analogues of cholesterol in bacterial membranes. *PNAS* 112, 11971–11976.

Sáenz de Miera, L. E., Arroyo, P., Luis Calabuig, E. de, Falagán, J., and Ansola, G. (2014). High-throughput sequencing of 16S RNA genes of soil bacterial communities from a naturally occurring CO 2 gas vent. *Int. J. Greenhouse Gas Control* 29, 176–184.

Sandig, C., Sauer, U., Bräuer, K., Serfling, U., and Schütze, C. (2014). Comparative study of geophysical and soil–gas investigations at the Hartoušov (Czech Republic) natural CO2 degassing site. *Environ Earth Sci* 72, 1421–1434.

Sass, H., and Cypionka, H. (2004). Isolation of sulfate-reducing bacteria from the terrestrial deep subsurface and description of Desulfovibrio cavernae sp. nov. *Systematic and applied microbiology* 27, 541.

Sato, M., Sutton, A. J., McGee, K. A., and Russell-Robinson, S. (1986). Monitoring of hydrogen along the San Andreas and Calaveras faults in central California in 1980-1984. *J. Geophys. Res. Solid Earth* 91, 12315–12326.

Sauer, U., Watanabe, N., Singh, A., Dietrich, P., Kolditz, O., and Schütze, C. (2014). Joint interpretation of geoelectrical and soil-gas measurements for monitoring CO 2 releases at a natural analogue. *Near Surface Geophysics* 12, 165–178.

Savary, V., and Pagel, M. (1997). The effects of water radiolysis on local redox conditions in the Oklo, Gabon, natural fission reactors 10 and 16. *Geochimica et Cosmochimica Acta* 61, 4479–4494.

Schippers, A., Kock, D., Höft, C., Köweker, G., and Siegert, M. (2012). Quantification of Microbial Communities in Subsurface Marine Sediments of the Black Sea and off Namibia. *Frontiers in microbiology* 3, 16.

Schönheit, P., Kristjansson, J. K., and Thauer, R. K. (1982). Kinetic mechanism for the ability of sulfate reducers to out-compete methanogens for acetate. *Archives of Microbiology* 132, 285–288.

Schopf, J. W. (1993). Microfossils of the Early Archean Apex chert: new evidence of the antiquity of life. *Science (New York, N.Y.)* 260, 640–646.

Schopf, J. W. (2006). Fossil evidence of Archaean life. *Philosophical transactions of the Royal Society of London. Series B, Biological sciences* 361, 869–885.

Schouten, S., Hopmans, E. C., and Sinninghe Damsté, J. S. (2013). The organic geochemistry of glycerol dialkyl glycerol tetraether lipids: A review. *Organic Geochemistry* 54, 19–61.

Schouten, S., Huguet, C., Hopmans, E. C., Kienhuis, M. V. M., and Damsté, J. S. S. (2007). Analytical methodology for TEX86 paleothermometry by high-performance liquid chromatography/atmospheric pressure chemical ionization-mass spectrometry. *Analytical chemistry* 79, 2940–2944.

Schreiber, U., Locker-Grütjen, O., and Mayer, C. (2012). Hypothesis: origin of life in deep-reaching tectonic faults. *Origins of life and evolution of the biosphere : the journal of the International Society for the Study of the Origin of Life* 42, 47–54.

Schuessler, J. A., Kämpf, H., Koch, U., and Alawi, M. (2016). Earthquake impact on iron isotope signatures recorded in mineral spring water. *J. Geophys. Res. Solid Earth* 121, 8548–8568.

Šibanc, N., Dumbrell, A. J., Mandić-Mulec, I., and Maček, I. (2014). Impacts of naturally elevated soil CO2 concentrations on communities of soil archaea and bacteria. *Soil Biol. Biochem.* 68, 348–356.

Sleep, N. H., Zahnle, K. J., Kasting, J. F., and Morowitz, H. J. (1989). Annihilation of ecosystems by large asteroid impacts on the early Earth. *nature* 342, 139–142.

Sleep, N. H., and Zoback, M. D. (2007). Did earthquakes keep the early crust habitable? *Astrobiology* 7, 1023–1032.

Šmilauer, P., and Lepš, J. (2014). *Multivariate analysis of ecological data using CANOCO 5*. Cambridge University Press.

Smith, D. R., Doucette-Stamm, L. A., Deloughery, C., Lee, H., Dubois, J., Aldredge, T., et al. (1997). Complete genome sequence of Methanobacterium thermoautotrophicum deltaH: functional analysis and comparative genomics. *J. Bacteriol.* 179, 7135–7155.

Sogin, M. L., Morrison, H. G., Huber, J. A., Mark Welch, D., Huse, S. M., Neal, P. R., et al. (2006). Microbial diversity in the deep sea and the underexplored "rare biosphere". *Proceedings of the National Academy of Sciences of the United States of America* 103, 12115–12120.

Spear, J. R., Walker, J. J., McCollom, T. M., and Pace, N. R. (2005). Hydrogen and bioenergetics in the Yellowstone geothermal ecosystem. *Proceedings of the National Academy of Sciences of the United States of America* 102, 2555–2560.

Špičáková, L., Uličný, D., and Koudelková, G. (2000). Tectonosedimentary Evolution of the Cheb Basin (NW Bohemia, Czech Republic) between Late Oligocene and Pliocene: A Preliminary Note. *Studia Geophysica et Geodaetica* 44, 556–580.

Stackebrandt, E., Sproer, C., Rainey, F. A., Burghardt, J., Päuker, O., and Hippe, H. (1997). Phylogenetic analysis of the genus Desulfotomaculum: evidence for the misclassification of Desulfotomaculum guttoideum and description of Desulfotomaculum orientis as Desulfosporosinus orientis gen. nov., comb. nov. *International journal of systematic bacteriology* 47, 1134–1139.

Steinberg, L. M., and Regan, J. M. (2009). mcrA-targeted real-time quantitative PCR method to examine methanogen communities. *Applied and environmental microbiology* 75, 4435–4442.

Stephens, J. C., and Hering, J. G. (2002). Comparative characterization of volcanic ash soils exposed to decade-long elevated carbon dioxide concentrations at Mammoth Mountain, California. *Chemical Geology* 186, 301–313.

Stevens, T. O., and McKinley, J. P. (1995). Lithoautotrophic Microbial Ecosystems in Deep Basalt Aquifers. *Science* 270, 450–455.

Strapoc, D., Picardal, F. W., Turich, C., Schaperdoth, I., Macalady, J. L., Lipp, J. S., et al. (2008). Methane-producing microbial community in a coal bed of the Illinois basin. *Applied and environmental microbiology* 74, 2424–2432.

Sugisaki, R., and Sugiura, T. (1985). Geochemical indicator of tectonic stress resulting in an earthquake in central Japan, 1984. *Science* 229, 1261–1262.

Takai, K., Moser, D. P., DeFlaun, M., Onstott, T. C., and Fredrickson, J. K. (2001a). Archaeal diversity in waters from deep South African gold mines. *Applied and environmental microbiology* 67, 5750–5760.

Takai, K., Moser, D. P., Onstott, T. C., Spoelstra, N., Pfiffner, S. M., Dohnalkova, A., et al. (2001b). Alkaliphilus transvaalensis gen. nov., sp. nov., an extremely alkaliphilic bacterium isolated from a deep South African gold mine. *International journal of systematic and evolutionary microbiology* 51, 1245–1256.

Tera, F., Papanastassiou, D. A., and Wasserburg, G. J. (1974). Isotopic evidence for a terminal lunar cataclysm. *Earth and Planetary Science Letters* 22, 1–21.

Thomas, C., Ionescu, D., and Ariztegui, D. (2014). Archaeal populations in two distinct sedimentary facies of the subsurface of the Dead Sea. *Marine genomics* 17, 53–62.

Trimarco, E., Balkwill, D., Davidson, M., and Onstott, T. C. (2006). In Situ Enrichment of a Diverse Community of Bacteria from a 4–5 km Deep Fault Zone in South Africa. *Geomicrobiology Journal* 23, 463–473.

Valley, J. W., Peck, W. H., King, E. M., and Wilde, S. A. (2002). A cool early Earth. *Geol* 30, 351.

Vaughan, D. J., and Lloyd, J. R. (2012). “Mineral-Organic-Microbe Interfacial Chemistry,” in *Fundamentals of geobiology*, eds. A. H. Knoll, D. E. Canfield, and K. Konhauser (Hoboken (N.J.): Wiley), 131–149.

Videmšek, U., Hagn, A., Suhadolc, M., Radl, V., Knicker, H., Schloter, M., et al. (2009). Abundance and Diversity of CO2-fixing Bacteria in Grassland Soils Close to Natural Carbon Dioxide Springs. *Microb. Ecol.* 58, 1–9.

Vodnik, D., Maček, I., Videmšek, U., and HLADNIK, J. (2007). The life of plants under extreme CO2. *Acta Biologica Slovenica* 50, 1.

Vovk, I. F. (1987). "Radiolytic salt enrichment and brines in the crystalline basement of the East European Platform," in *Saline water and gases in crystalline rocks* (Ottawa: Geological Association of Canada Special Paper), 197–210.

Vuillemin, A., and Ariztegui, D. (2013). Geomicrobiological investigations in subsaline maar lake sediments over the last 1500 years. *Quaternary Science Reviews* 71, 119–130.

Vuillemin, A., Friese, A., Alawi, M., Henny, C., Nomosatryo, S., Wagner, D., et al. (2016). Geomicrobiological Features of Ferruginous Sediments from Lake Towuti, Indonesia. *Frontiers in microbiology* 7, 1007.

Wagner, C., Mau, M., Schlömann, M., Heinicke, J., and Koch, U. (2007). Characterization of the bacterial flora in mineral waters in upstreaming fluids of deep igneous rock aquifers. *J. Geophys. Res.* 112, 1583.

Wakita, H., Nakamura, Y., Kita, I., Fujii, N., and Notsu, K. (1980). Hydrogen release: new indicator of fault activity. *Science* 210, 188–190.

Wandrey, M., Morozova, D., Zettlitzer, M., and Würdemann, H. (2010). Assessing drilling mud and technical fluid contamination in rock core and brine samples intended for microbiological monitoring at the CO2 storage site in Ketzin using fluorescent dye tracers. *International Journal of Greenhouse Gas Control* 4, 972–980.

Wang, Z. P., Lindau, C. W., Delaune, R. D., and Patrick, W. H. (1993). Methane emission and entrapment in flooded rice soils as affected by soil properties. *Biology and Fertility of Soils* 16, 163–168.

Watanabe, T., Kojima, H., and Fukui, M. (2015). Sulfuriferula multivorans gen. nov., sp. nov., isolated from a freshwater lake, reclassification of 'Thiobacillus plumbophilus' as Sulfuriferula plumbophilus sp. nov., and description of

Sulfuricellaceae fam. nov. and Sulfuricellales ord. nov. *International journal of systematic and evolutionary microbiology* 65, 1504–1508.

Webster, G., Blazejak, A., Cragg, B. A., Schippers, A., Sass, H., Rinna, J., et al. (2009). Subsurface microbiology and biogeochemistry of a deep, cold-water carbonate mound from the Porcupine Seabight (IODP Expedition 307). *Environmental microbiology* 11, 239–257.

Weijers, J. W. H., Wiesenberg, G. L. B., Bol, R., Hopmans, E. C., and Pancost, R. D. (2010). Carbon isotopic composition of branched tetraether membrane lipids in soils suggest a rapid turnover and a heterotrophic life style of their source organism(s). *Biogeosciences* 7, 2959–2973.

Weijers, J. W.H., Schouten, S., van den Donker, Jurgen C., Hopmans, E. C., and Sinninghe Damsté, J. S. (2007). Environmental controls on bacterial tetraether membrane lipid distribution in soils. *Geochimica et Cosmochimica Acta* 71, 703–713.

Weinlich, F. H., Bräuer, K., Kämpf, H., Strauch, G., Tesař, J., and Weise, S. M. (1999). An active subcontinental mantle volatile system in the western Eger rift, Central Europe: gas flux, isotopic (He, C, and N) and compositional fingerprints. *Geochim. Cosmochim. Acta* 63, 3653–3671.

Weise, S. M., Bräuer, K., Kämpf, H., Strauch, G., and Koch, U. (2001). Transport of mantle volatiles through the crust traced by seismically released fluids: a natural experiment in the earthquake swarm area Vogtland/NW Bohemia, Central Europe. *Tectonophysics* 336, 137–150.

Weiss, M. C., Sousa, F. L., Mrnjavac, N., Neukirchen, S., Roettger, M., Nelson-Sathi, S., et al. The physiology and habitat of the last universal common ancestor. *Nat Microbiol* 1, 1–8.

White, D. C., Davis, W. M., Nickels, J. S., King, J. D., and Bobbie, R. J. (1979). Determination of the sedimentary microbial biomass by extractible lipid phosphate. *Oecologia* 40, 51–62.

Whiticar, M. J. (1999). Carbon and hydrogen isotope systematics of bacterial formation and oxidation of methane. *Chemical Geology* 161, 291–314.

Willems, A. (2014). “The Family Comamonadaceae,” in *The Prokaryotes: Alphaproteobacteria and Betaproteobacteria*, eds. E. F. DeLong, S. Lory, E. Stackebrandt, F. Thompson, and E. Rosenberg (Berlin, Heidelberg: Springer Berlin / Heidelberg), 777–851.

Wu, X., Holmfeldt, K., Hubalek, V., Lundin, D., Åström, M., Bertilsson, S., et al. (2016). Microbial metagenomes from three aquifers in the Fennoscandian shield terrestrial deep biosphere reveal metabolic partitioning among populations. *The ISME journal* 10, 1192–1203.

Yanagawa, K., Nunoura, T., McAllister, S. M., Hirai, M., Breuker, A., Brandt, L., et al. (2013). The first microbiological contamination assessment by deep-sea drilling and coring by the D/V Chikyu at the Iheya North hydrothermal field in the Mid-Okinawa Trough (IODP Expedition 331). *Frontiers in microbiology* 4, 327.

Yarza, P., Yilmaz, P., Pruesse, E., Glöckner, F. O., Ludwig, W., Schleifer, K.-H., et al. (2014). Uniting the classification of cultured and uncultured bacteria and archaea using 16S rRNA gene sequences. *Nature reviews. Microbiology* 12, 635–645.

Young, J. N., Rickaby, R. E. M., Kapralov, M. V., and Filatov, D. A. (2012). Adaptive signals in algal Rubisco reveal a history of ancient atmospheric carbon dioxide. *Philosophical transactions of the Royal Society of London. Series B, Biological sciences* 367, 483–492.

Youssef, N., Elshahed, M. S., and McInerney, M. J. (2009). “Chapter 6 Microbial Processes in Oil Fields,” in *Advances in applied microbiology* (London: Academic), 141–251.

Zeikus, J. G. (1977). The biology of methanogenic bacteria. *Bacteriological Reviews* 41, 514–541.

Zeikus, J. G., and Wolfe, R. S. (1972). Methanobacterium thermoautotrophicus sp. n., an Anaerobic, Autotrophic, Extreme Thermophile. *Journal of Bacteriology* 109, 707–713.

Zhang, G., Dong, H., Xu, Z., Zhao, D., and Zhang, C. (2005). Microbial diversity in ultra-high-pressure rocks and fluids from the Chinese Continental Scientific Drilling Project in China. *Applied and environmental microbiology* 71, 3213–3227.

Zhang, J., Kobert, K., Flouri, T., and Stamatakis, A. (2014). PEAR: a fast and accurate Illumina Paired-End reAd mergeR. *Bioinformatics (Oxford, England)* 30, 614–620.

Zinder, S. H., Sowers, K. R., and Ferry, J. G. (1985). NOTES: Methanosarcina thermophila sp. nov., a Thermophilic, Acetotrophic, Methane-Producing Bacterium. *International journal of systematic bacteriology* 35, 522–523.

Zink, K.-G., and Mangelsdorf, K. (2004). Efficient and rapid method for extraction of intact phospholipids from sediments combined with molecular structure elucidation using LC–ESI-MS–MS analysis. *Analytical and Bioanalytical Chemistry* 380, 798–812.

Zink, K.-G., Wilkes, H., Disko, U., Elvert, M., and Horsfield, B. (2003). Intact phospholipids—microbial “life markers” in marine deep subsurface sediments. *Organic Geochemistry* 34, 755–769.

7 Supplementary

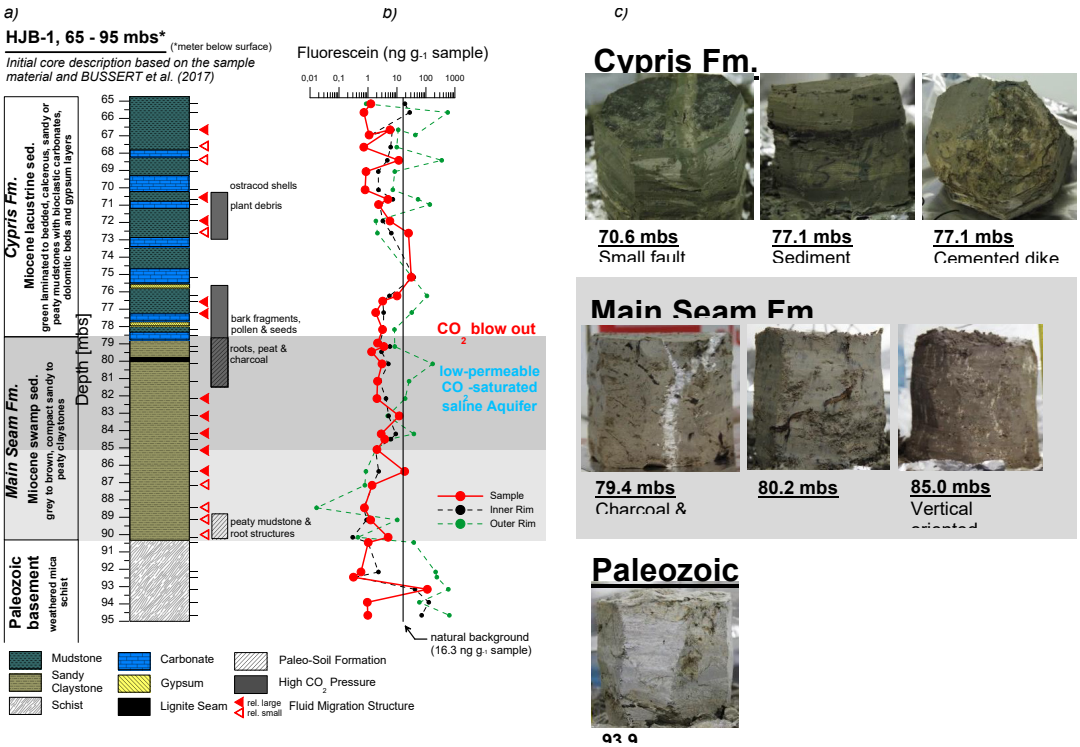

Figure S1. a) Stratigraphical and lithological description of the Hartoušov mofette core HJB-1 (2016) between 65 and 95 mbs (meter below surface) based on the sample material and Bussert et al. (2017). b) Determined fluorescein contents for the outer rim material, the outside of the inner rim and the sample material. c) Exemplarily pictures of core sections from the different lithological units partly showing CO2-fluid migration structures.

Table S1 Anion/cation concentrations, TOC, $\delta^{13}C_{org}$, pH, conductivity, water content, qPCR results, Shannon H index and Shannon Evenness index of the mofette.

Depth (cm)	sulfate (mg/L)	Na (mg/L)	NH4 (mg/L)	K (mg/L)	Mg (mg/L)	Ca (mg/L)	TOC (%)	‰13C (TOC)	pH	conductivity (mg/L)	water content (%)	16s rRNA copies/g	dsrB copies/g	mcrA copies/g	Shannon H index	Shannon EH index
2	30.7	2.5	2.9	4.4	1	2.1	3.7	-26.7	3.6	114	0.3	5.62E+08	2.49E+05	1.96E+04	7.08	0.64
7	47.6	2.8	3	4	1.2	3.4	3.9	-27	3.6	114	0.3	6.29E+08	2.58E+05	0.00E+00	7.36	0.66
12	69.4	3.1	3.6	3.5	1.2	5.8	5.6	-27.6	3.8	79	0.3	1.21E+09	1.49E+07	7.16E+05	7.74	0.69
17	76.2	2.9	2.6	2.6	1	3.2	2	-26.6	3.8	79	0.3	7.52E+08	9.52E+05	6.12E+02	7.72	0.68
22	86.7	2.8	2.7	2.4	1	6.5	6.4	-26.4	3.9	93	0.3	1.18E+09	3.36E+06	8.04E+05	7.89	0.71
27	124	2.6	3.3	2.7	1.3	6.8	4.6	-26.6	3.9	93	0.3	3.51E+08	1.48E+06	1.15E+05	7.80	0.69
32	148.1	2.9	6.9	3.9	2.8	11.2	1.4	-26.9	3.7	128	0.3	3.16E+08	2.50E+06	1.33E+05	7.98	0.71
37	125.3	2.4	6.7	6.5	2.7	13.6	1.5	-26.9	3.7	128	0.3	4.90E+08	1.29E+06	7.41E+04	7.87	0.70
42	92.2	3.8	3.1	5.7	1.5	6.8	3.2	-27.6	4	185	0.3	5.19E+08	7.71E+05	2.27E+04	7.18	0.66
47	140.8	3.2	4.1	5	1.8	9.7	4.2	-27	4	185	0.3	1.18E+08	1.35E+06	3.08E+05	8.14	0.71
52	127.5	3.4	3.8	5.3	2.4	8.3	3.6	-27.1	4	148	0.2	4.11E+07	6.69E+05	1.11E+05	8.31	0.72
57	105.2	2.8	3.2	4.7	2.1	9.4	4.2	-27.1	4	148	0.2	6.61E+07	1.37E+06	4.68E+04	7.66	0.67
75	136.8	2.7	4.8	8.5	7.3	22.4	7.1	-26.9	4	192	0.3	2.45E+07	3.32E+05	8.21E+03	7.83	0.69
85	177.9	2.9	5.6	8	9.6	37.3	9.6	-26.5	3.9	199	0.3	1.32E+07	1.81E+04	0.00E+00	8.95	0.78
95	122.3	2.9	4.6	4.9	4.6	18.2	5.2	-26.9	4.1	147	0.4	1.64E+07	3.53E+05	4.07E+03	9.09	0.79
105	10.5	2.6	2	3.9	1	3.4	4.4	-26.8	4.5	83	0.4	4.89E+07	1.04E+06	3.90E+04	9.34	0.77
125	22.2	2.8	1.5	5.6	1.5	4.7	1.8	-25.3	4.7	43	0.4	5.05E+07	3.27E+06	5.69E+04	8.84	0.75
145	69.6	2.8	1.8	7.9	3.7	15.7	6.3	-26.9	4.4	126	0.4	3.70E+07	1.64E+06	4.71E+04	8.91	0.76
175	7.1	2.8	1.1	5.2	1.3	5.2	4.9	-26.7	4.6	24	0.5	3.40E+07	2.92E+06	4.00E+04	8.69	0.75
215	49.7	2.8	1.2	4.4	2.3	12	10.5	-25.9	4.3	39	0.4	2.53E+07	8.13E+05	7.64E+04	8.04	0.71
245	34.7	3.6	1.1	4.3	2.5	9.6	20.1	-27.1	4.5	16	0.5	1.15E+08	1.21E+06	7.80E+04	7.80	0.71
275	13.4	3.6	1.2	3.7	2.1	5.9	6.1	-27.1	4.5	16	0.4	2.50E+07	9.05E+05	9.28E+04	7.73	0.70

Table S2 Anion/cation concentrations, TOC, $\delta^{13}C_{org}$, pH, conductivity, water content, qPCR results, Shannon H index and Shannon Evenness index of the reference site.

Depth (cm)	sulfate (mg/L)	Na (mg/L)	NH4 (mg/L)	K (mg/L)	Mg (mg/L)	Ca (mg/L)	TOC (%)	‰13C (TOC)	pH	conductivity (mg/L)	water content (%)	16s rRNA copies/g	dsrB copies/g	mcrA copies/g	Shannon H index	Shannon EH index
2	21.9	3.5	1.6	11.1	2.8	13.9	11.1	-28.5	4.1	78	0.2	1.16E+10	1.91E+06	0.00E+00	9.95	0.85
7	25.7	3.1	1	6	2.3	11.2	5.6	-28	4.1	78	0.2	2.91E+10	1.67E+07	1.20E+04	9.73	0.83
12	21.6	2.7	0.4	3.9	2.6	9.1	4.4	-27.8	4.2	41	0.2	2.04E+10	1.85E+07	8.61E+03	9.85	0.83
17	20.1	2.4		3.8	2	6.9	2.9	-28.3	4.2	41	0.2	1.76E+10	1.76E+07	4.44E+04	9.83	0.83
22	13.4	2.4		3.8	1.4	3.3	2.7	-28.4	4.6	56	0.2	5.83E+10	4.17E+06	4.59E+03	9.69	0.82
27	19.2	2.8	0.3	4.2	1.9	5.2	2.8	-28.5	4.6	56	0.2	4.33E+10	2.68E+06	3.63E+04	9.56	0.81
32	12.1	2.7		3.5	1.6	2.8	1.4	-27.7	4.5	36	0.1	3.35E+10	5.80E+06	7.78E+05	9.41	0.81
37	20.9	3		5	1.4	2.4	1.2	-27.6	4.5	36	0.1	1.44E+10	5.73E+06	2.40E+05	9.22	0.79
42	10.2	2.9		3.2		2.4	1.3	-27.7	4.5	30	0.2	5.73E+09	7.66E+06	8.48E+05	9.31	0.80
47	24.9	3.3		4.7	1.4	3.1	1	-27.2	4.5	30	0.2	4.17E+09	9.40E+06	1.67E+05	8.86	0.77
52	25.2	3.2		6.9	1.5	2.9	1.1	-27.2	4.3	47	0.2	1.72E+09	6.36E+06	2.48E+05	8.91	0.77
57	24.9	3.1		6.4	1.4	2.8	0.9	-26.8	4.2	32	0.2	2.31E+09	3.33E+06	1.62E+05	9.35	0.79
75	8.3	2.8		2.4			0.7	-25.9	4.2	29	0.2	2.70E+08	1.18E+06	4.82E+04	9.10	0.78
85	11.4	2.9		3.6		1.8	0.5	-27.2	4	24	0.2	7.44E+08	1.75E+06	8.42E+04	9.82	0.83
95	4.7	2.4		1.7			0.8	-26.9	4.1	32	0.2	4.59E+09	4.11E+05	7.24E+04	9.79	0.82
105	2	2.4		2.7			0.4	-27.3	4.1	9	0.2	1.73E+07	4.62E+03	0.00E+00	10.10	0.86
125	2.2	2.7		0.8			0.3	-26.7	3.6	5	0.2	9.57E+05	1.58E+02	0.00E+00	9.24	0.81
145	2.8	2.7		1.1			0.3	-26.5	3.9	8	0.2	5.44E+05	2.56E+03	0.00E+00	8.55	0.76
175	3.4	2.7		1.9			0.2	-26.8	4	11	0.2	5.91E+06	2.58E+03	0.00E+00	9.86	0.84
215	4.7	2.7		1.7			0.2	-27	4.1	11	0.2	2.84E+07	1.53E+04	0.00E+00	10.07	0.85
245	4	2.7		2.1			0.2	-26.7	4.2	12	0.2	1.19E+07	8.58E+04	0.00E+00	9.48	0.81
275	4	3.3		2.7			0.2	-26.5	4.2	12	0.2	1.75E+07	3.49E+04	0.00E+00	9.82	0.83

Table S3 Matrix of the correlation results of the mofette. The *p* values are in the upper-right and the *R* values are in the lower-left of the table.

	Shannon EH	Shannon H	sulfate (mg/L)	Na (mg/L)	NH4 (mg/L)	K (mg/L)	Mg (mg/L)	Ca (mg/L)	TOC	pH	conductivity (mg/L)	water content	16s rRNA copies/g	*dsrB* copies/g	*mcrA* copies/g
Shannon EH		1.30E-14	7.30E-01	5.80E-01	9.70E-01	1.20E-01	3.90E-02	2.20E-02	5.60E-01	8.00E-03	9.10E-01	8.00E-03	1.30E-02	1.30E-02	1.30E-02
Shannon H	9.80E-01		9.60E-01	3.70E-01	8.30E-01	1.40E-01	1.10E-01	8.00E-02	8.70E-01	4.50E-03	9.10E-01	1.90E-02	1.30E-02	1.30E-02	1.30E-02
sulfate (mg/L)	7.70E-02	1.10E-02		9.10E-01	1.00E-06	1.30E-01	3.90E-03	8.80E-04	5.20E-01	1.90E-02	7.20E-06	1.20E-02	9.10E-01	9.10E-01	9.10E-01
Na (mg/L)	-1.30E-01	-2.00E-01	-2.70E-02		2.80E-01	8.00E-01	8.70E-01	8.10E-01	1.30E-01	2.70E-01	8.70E-01	3.10E-01	6.50E-01	6.50E-01	6.50E-01
NH4 (mg/L)	8.10E-03	-4.80E-02	8.40E-01	-2.40E-01		2.00E-01	2.90E-02	1.70E-02	1.10E-01	1.40E-03	2.50E-04	2.60E-03	5.90E-01	5.90E-01	5.90E-01
K (mg/L)	3.40E-01	3.30E-01	3.40E-01	-5.60E-02	2.90E-01		6.10E-05	1.90E-04	7.10E-01	3.80E-01	1.30E-02	1.00E+00	1.40E-02	1.40E-02	1.40E-02
Mg (mg/L)	4.40E-01	3.50E-01	5.90E-01	-3.70E-02	4.70E-01	7.50E-01		9.40E-14	1.90E-01	9.10E-01	1.10E-02	9.80E-01	4.90E-02	4.90E-02	4.90E-02
Ca (mg/L)	4.90E-01	3.80E-01	6.60E-01	-5.40E-02	5.00E-01	7.10E-01	9.70E-01		1.70E-01	8.20E-01	9.10E-03	9.50E-01	7.80E-02	7.80E-02	7.80E-02
TOC	1.30E-01	3.80E-02	-1.40E-01	3.40E-01	-3.50E-01	8.50E-02	2.90E-01	3.10E-01		2.40E-01	1.90E-01	8.10E-03	3.40E-01	3.40E-01	3.40E-01
pH	5.50E-01	5.80E-01	-4.90E-01	2.40E-01	-6.40E-01	2.00E-01	-2.50E-02	-5.30E-02	2.60E-01		3.00E-02	9.90E-06	2.00E-03	2.00E-03	2.00E-03
conductivity (mg/L)	-2.60E-02	-2.60E-02	8.00E-01	-3.60E-02	7.00E-01	5.20E-01	5.30E-01	5.40E-01	-2.90E-01	-4.60E-01		3.00E-03	8.30E-01	8.30E-01	8.30E-01
water content	5.50E-01	5.00E-01	-5.20E-01	2.30E-01	-6.10E-01	1.30E-03	5.90E-03	1.40E-02	5.50E-01	7.90E-01	-6.00E-01		3.90E-02	3.90E-02	3.90E-02
16s rRNA copies/g	-5.20E-01	-5.20E-01	-2.60E-02	-1.00E-01	1.20E-01	-5.20E-01	-4.20E-01	-3.80E-01	-2.10E-01	-6.20E-01	-4.80E-02	-4.40E-01		1.80E-98	1.80E-98
***dsrB* copies/g**	-5.20E-01	-5.20E-01	-2.60E-02	-1.00E-01	1.20E-01	-5.20E-01	-4.20E-01	-3.80E-01	-2.10E-01	-6.20E-01	-4.80E-02	-4.40E-01	1.00E+00		1.80E-98
***mcrA* copies/g**	-5.20E-01	-5.20E-01	-2.60E-02	-1.00E-01	1.20E-01	-5.20E-01	-4.20E-01	-3.80E-01	-2.10E-01	-6.20E-01	-4.80E-02	-4.40E-01	1.00E+00	1.00E+00	

Table S4 Matrix of the correlation results of the reference site. The *p* values are in the upper-right and the *R* values are in the lower-left of the table.

	Shannon EH	Shannon H	sulfate (mg/L)	Na (mg/L)	NH4 (mg/L)	K (mg/L)	Mg (mg/L)	Ca (mg/L)	TOC	pH	conductivity (mg/L)	water content	16s rRNA copies/g	*dsrB* copies/g	*mcrA* copies/g
Shannon EH		6.10E-13	3.10E-01	2.90E-01	8.70E-02	8.80E-01	8.00E-01	2.30E-01	1.30E-01	2.70E-01	7.80E-01	8.80E-01	7.20E-01	1.00E+00	1.40E-01
Shannon H	9.60E-01		5.10E-01	2.20E-01	1.70E-01	8.00E-01	7.10E-01	2.50E-01	1.70E-01	7.10E-01	5.70E-01	7.20E-01	4.90E-01	8.70E-01	2.00E-01
sulfate (mg/L)	-2.30E-01	-1.50E-01		1.00E-02	4.20E-02	9.90E-06	2.30E-07	1.40E-04	9.60E-03	2.90E-02	3.00E-05	6.40E-01	7.80E-02	4.70E-04	5.90E-01
Na (mg/L)	-2.40E-01	-2.70E-01	5.40E-01		3.10E-02	5.30E-04	1.30E-01	8.80E-02	9.60E-02	6.20E-01	1.20E-01	9.10E-01	3.30E-01	7.80E-01	7.20E-01
NH4 (mg/L)	3.70E-01	3.00E-01	4.40E-01	4.60E-01		1.50E-04	1.20E-03	1.30E-07	2.90E-11	7.10E-01	1.10E-04	9.20E-01	2.90E-01	2.20E-01	3.80E-01
K (mg/L)	3.50E-02	5.90E-02	8.00E-01	6.80E-01	7.20E-01		3.30E-05	2.20E-05	2.00E-05	1.80E-01	1.20E-05	8.50E-01	3.00E-01	1.60E-01	7.90E-01
Mg (mg/L)	5.60E-02	8.50E-02	8.60E-01	3.40E-01	6.50E-01	7.70E-01		2.30E-08	2.40E-05	6.50E-02	8.80E-07	3.80E-01	3.30E-03	3.60E-04	9.60E-01
Ca (mg/L)	2.70E-01	2.60E-01	7.20E-01	3.70E-01	8.70E-01	7.80E-01	8.90E-01		1.30E-10	4.60E-01	2.60E-07	5.90E-01	3.30E-02	1.00E-03	8.00E-01
TOC	3.40E-01	3.00E-01	5.40E-01	3.60E-01	9.50E-01	7.80E-01	7.70E-01	9.40E-01		7.30E-01	3.10E-06	7.50E-01	7.10E-02	7.30E-02	5.90E-01
pH	-2.50E-01	-8.40E-02	4.70E-01	1.10E-01	-8.50E-02	3.00E-01	4.00E-01	1.70E-01	7.80E-02		6.10E-02	3.60E-03	3.80E-03	1.90E-01	1.80E-02
conductivity (mg/L)	6.30E-02	1.30E-01	7.70E-01	3.40E-01	7.30E-01	7.90E-01	8.40E-01	8.60E-01	8.20E-01	4.10E-01		5.90E-01	1.00E-03	1.20E-02	8.10E-01
water content	-3.30E-02	-8.00E-02	-1.00E-01	-2.60E-02	2.30E-02	4.30E-02	-2.00E-01	-1.20E-01	-7.20E-02	-5.90E-01	-1.20E-01		5.90E-02	2.40E-01	8.60E-02
16s rRNA copies/g	8.00E-02	1.50E-01	3.80E-01	-2.20E-01	2.40E-01	2.30E-01	6.00E-01	4.60E-01	3.90E-01	5.90E-01	6.50E-01	-4.10E-01		8.20E-02	6.40E-01
***dsrB* copies/g**	-2.40E-04	3.80E-02	6.80E-01	6.40E-02	2.70E-01	3.10E-01	6.90E-01	6.50E-01	3.90E-01	2.90E-01	5.20E-01	-2.60E-01	3.80E-01		4.90E-01
***mcrA* copies/g**	-3.30E-01	-2.80E-01	1.20E-01	8.10E-02	-2.00E-01	6.00E-02	1.10E-02	-5.70E-02	-1.20E-01	5.00E-01	5.40E-02	-3.70E-01	1.00E-01	1.60E-01	

Table S5 Number of OTUs (relative abundances) occurring either only at the mofette or the reference site, or are present at both sites.

	OTUs specific for the mofette	**OTUs shared between both sites**	**OTUs specific for the reference site**
OTU count (0- 275 cm)	138 (0.015 %)	1626 (99.97 %)	128 (0.014 %)
OTU count (100-275 cm)	184 (0.09 %)	1336 (99.81 %)	198 (0.10 %)
OTU count (200-275 cm)	124 (0.22 %)	1045 (99.34 %)	330 (0.44 %)

Table S6 Comparison of bacterial communities at 10-20 cm between HMF and La Sima (Sáenz de Miera et al., 2014)

Phylum/class/order	Mofettes (10-20 cm)		Reference sites (10-20 cm)	
	HMF	La Sima[1]	HMF	La Sima[1]
Chloroflexi	**8.7**	**76.7**	**11.7**	**14.6**
Ktedonobacteria	0.6	**51.6**	**5.5**	**13.7**
Anaerolineae	0.5	-	1.8	-
JG37-AG-4	**4.4**	-	1.5	-
JG30-KF-CM66	0.7	-	0.3	-
KD4-96	2.1	-	1.7	-
TK10	0.1	-	0.4	-
Acidobacteria	**27.9**	1.6	**34.5**	**18.4**
Acidobacteria Gp4	-	-	-	**9.9**
Acidobacteria Gp3	-	0.9	-	1.8
Acidobacteria Gp1	**24.7**	0.7	**13.7**	0.6
Acidobacteria Gp6	0.1	-	1.8	**4.7**
Acidobacteria Gp2	0.6	-	**7.7**	-
Holophagae	1.6	-	**4.4**	-
Solibacteres	0.6	-	**6**	-
Proteobacteria	**25.6**	**6.9**	**23.2**	**14.1**
Alphaproteobacteria	3.9	**6.6**	**10.1**	**11.7**
Rhizobiales	0.7	**4.6**	**8.2**	**7.8**
Rhodospirillales	3.1	-	1.8	-
Betaproteobacteria	3.2	0.1	**6.1**	1.1

Burkholderiales	0.3	0.1	0.3	0.7
Ferrovales	1.4	-	0.1	-
Hydrogenophilales	0.9	-	0.3	-
Nitrosomonadales	0.5	-	3	-
SC-I-84	0.1	-	2.1	-
Gammaproteobacteria	**8.6**	0.1	2.8	0.4
Acidithiobacillales	**8**	-	0.6	-
Xanthomonadales	0.7	-	1.9	-
Deltaproteobacteria	**8.6**	-	**4.2**	-
Bdellovibrionales	0.5	-	0.1	-
Desulfurellales	1.2	-	1.8	-
Myxococcales	**5**	-	1.1	-
Syntrophobacterales	1.7	-	0.6	-
Desulfuromonadales	< 0.1	-	0.5	-
Verrucomicrobia	0.8	0.3	**5.2**	**13.3**
OPB35 soil group	0.7	-	2.4	-
Spartobacteria	0.2	0.2	2.7	**10.3**
Gemmatimonadetes	0.2	0.1	2.4	**10**
Actinobacteria	**8.4**	0.6	**10.1**	4
Acidimicrobiales	**4.8**	-	1.5	-
Frankiales	1.1	-	2.9	-
Actinomycetales	-	0.2	-	1.6
Gaiellales	0.7	-	3.3	-
Solirubrobacterales	1.6	0.4	1.3	1.4
Planctomycetes	3.4	0.3	2.5	3.6
Planctomycetacia	2.3	0.2	2.3	2.7
Phycisphaerae	1.1	-	0.2	-
Firmicutes	**15.3**	1.3	**4.6**	1.9
Bacillales	**4.3**	0.1	2.4	1
Clostridiales	**10.6**	-	1.9	-
Halanaerobiales	0.1	-	0.3	-
Armatimonadetes	-	0.6	-	0.7
Chthonomonadales	-	0.3	-	0.4
Bacteroidetes	0.6	0.1	0.9	0.6
vadinHA17	0.4	-	0.3	-
Chitinophagales	-	0.1	-	0.5
Sphingobacteriales	0.1	-	0.6	-